

Real time PCR as a versatile tool for virus detection and transgenic plant analysis

by

Stefanie Malan

*Dissertation presented for the degree of Master of Science
At Stellenbosch University*



Department of Genetics
Natural Sciences

Promoter: Professor JT Burger
Co-Promoter: Dr MJ Freeborough

December 2009

Declaration

By submitting this dissertation electronically, I declare that the entirety of the work contained therein is my own, original work, that I am the owner of the copyright thereof (unless to the extent explicitly otherwise stated) and that I have not previously in its entirety or in part submitted it for obtaining any qualification.

December 2009

Copyright © 2009 Stellenbosch University

All rights reserved

Abstract

South Africa is regarded as one of the top wine producing countries in the world. One of the threats to the sustainability of the wine industry is viral diseases of which *Grapevine leafroll-associated virus 3* (GLRaV-3) and *Grapevine virus A* (GVA) are considered to be the most important and wide spread. Scion material is regularly tested for viruses; however scion material is often grafted onto rootstocks that have questionable phytosanitary status. Virus detection in rootstocks is challenging due to low and varying titres, but is imperative as a viral control mechanism. An additional viral control mechanism is the use of transgenic grapevine material which offers resistance to grapevine infection.

The objective of this project was to establish a detection system using real time PCR (qPCR) techniques, to accurately and routinely detect GLRaV-3 and GVA in rootstock propagation material. qPCR would furthermore be used to perform molecular characterisation of transgenic plants containing a GLRaV-3 antiviral Δ HSP-Mut construct.

A severely infected vineyard (Nietvoorbij farm) in the Stellenbosch area was screened throughout the grapevine growing season to investigate virus prevalence throughout the season and to determine the optimal time for sensitive virus detection. A large scale screening of nursery propagation material for GLRaV-3 infection was also conducted. The qRT-PCR results were compared to DAS-ELISA results to compare the efficacy and sensitivity of the two techniques. For the severely infected vineyard, the ability to detect GLRaV-3 increased as the season progressed towards winter. qRT-PCR was more sensitive and accurate in detecting GLRaV-3 than DAS-ELISA, as the latter technique delivered numerous false positive results later in the season. The best time to screen for GLRaV-3 in the Western Cape region was from the end of July to September. For the nursery screenings, our qRT-PCR results were compared to the results of the DAS-ELISA performed by the specific nurseries. No GLRaV-3 infection was detected in the specific samples received from the two different nurseries. The results for all the samples correlated between the two

techniques. This confirms that the propagation material of these nurseries has a healthy phytosanitary status with regards to GLRaV-3.

However, the detection of GVA in the severely infected vineyard yielded inconsistent results. Detection ability fluctuated throughout the season and no specific trend in seasonal variation and virus titre fluctuation could be established. The highest percentage of GVA infected samples were detected during September, April and the end of July. Previously published universal primers were used for the detection of GVA, but further investigation indicated that they might not be suitable for sensitive detection of specific GVA variants present in South Africa.

Vitis vinifera was transformed with a GLRaV-3 antiviral construct, Δ HSP-Mut. SYBR Green Real time PCR (qPCR) and qRT-PCR were utilised as alternative methods for molecular characterisation of transgenic plants. The qPCR and Southern blot results correlated for 76.5% of the samples. This illustrated the ability of qPCR to accurately estimate transgene copy numbers. Various samples were identified during qRT-PCR amplification that exhibited high mRNA expression levels of the transgene. These samples are ideal for further viral resistance studies.

This study illustrated that the versatility of real time PCR renders it a valuable tool for accurate virus detection as well as copy number determination.

Opsomming

Suid Afrika word geag as een van die top wyn produserende lande ter wereld. Die volhoubaarheid van die wynbedryf word onder andere bedreig deur virus-infeksies. *Grapevine leafroll associated virus 3* (GLRaV-3) en *Grapevine virus A* (GVA) is van die mees belangrike virusse wat siektes veroorsaak in Suid-Afrikaanse wingerde. Wingerd bo-stok materiaal word gereeld getoets vir hierdie virusse, maar hierdie materiaal word meestal geënt op onderstokmateriaal waarvan die virus status onbekend is. Virus opsporing in onderstokke word egter gekompliseer deur baie lae en variërende virus konsentrasies, maar opsporing in voortplantingsmateriaal is 'n noodsaaklike beheermeganisme vir virus-infeksie.

Die doel van die projek was om 'n opsporingsstelsel te ontwikkel via kwantitatiewe PCR (qPCR) tegnieke vir akkurate en gereelde toetsing van GLRaV-3 en GVA in onderstokmateriaal. qPCR sal ook verder gebruik word vir molekulêre karakterisering van transgeniese plante wat 'n GLRaV-3 antivirale Δ HSP-Mut konstruksie bevat.

'n Hoogs geïnfecteerde wingerd was regdeur die seisoen getoets om seisoenale fluktuasies in viruskonsentrasie te ondersoek en om die optimale tydstip vir sensitiewe virus opsporing te bepaal. 'n Groot skaalse toetsing van kwekery voortplantingsmateriaal vir GLRaV-3 infeksie was ook uitgevoer. Die qRT-PCR resultate is met die DAS-ELISA resultate vergelyk om die effektiwiteit en sensitiwiteit van die twee tegnieke te vergelyk. Vir die hoogs geïnfecteerde wingerd het die GLRaV-3 opsporing toegeneem met die verloop van die seisoen tot en met winter. qRT-PCR was meer sensitief en akkuraat as DAS-ELISA in die opsporing van GLRaV-3, weens verskeie vals positiewe resultate wat later in die seisoen deur die laasgenoemde tegniek verkry is. Die beste tyd om vir GLRaV-3 te toets is vanaf einde Julie tot September. Tydens die kwekery toetsings was qRT-PCR resultate met die DAS-ELISA resultate van die spesifieke kwekerye vergelyk. Geen GLRaV-3 infeksie was waargeneem in die spesifieke monsters wat vanaf die kwekerye ontvang is nie. Die resultate van die twee tegnieke het ooreengestem vir al die monsters wat

getoets is. Dit het bevestig dat die voortplantingsmateriaal van hierdie kwekerye gesonde fitosanitêre status met betrekking tot GLRaV-3 gehad het.

Die opsporing van GVA in die geïnfekteerde wingerd het egter wisselvallige resultate gelewer. Opsporing van die virus het ook regdeur die seisoen gefluktueer en geen spesifieke neiging in seisoenale opsporingsvermoë kon gemaak word nie. Die hoogste persentasie GVA geïnfekteerde monsters was waargeneem tydens September, April en die einde van Julie. Voorheen gepubliseerde universele inleiers was gebruik vir die opsporing van GVA, maar verdere ondersoek het getoon dat hierdie inleiers nie noodwendig geskik is vir sensitiewe opsporing van GVA variante wat teenwoordig is in Suid-Afrika nie.

Vitis vinifera was getransformeer met 'n GLRaV-3 antivirale konstrukt, Δ HSP-Mut. SYBR Green Real time PCR (qPCR) en qRT-PCR was ingespan as alternatiewe metodes vir molekulêre karakterisering van transgeniese plante. Die qPCR en Southern-klad resultate het ooreengestem vir 76.5% van die monsters. Dit illustreer die vermoë van qPCR om akkurate kopie-getalle van transgene te bepaal. Verskeie plante is geïdentifiseer tydens qRT-PCR amplifisering wat hoë vlakke van transgeen mRNA uitdrukking getoon het. Hierdie monsters is ideaal vir verdere virus weerstandbiedendheids studies.

Hierdie studie het die veelsydigheid van real time PCR bewys en getoon dat dit 'n kosbare tegniek is vir akkurate virus opsporing sowel as kopie-getal bepaling.

Acknowledgements

I would like to extend my sincere gratitude to the following people:

My supervisors, Prof JT Burger and Dr MJ Freeborough, for giving me the opportunity to be a part of an outstanding research group and for their great supervision and guidance throughout this study.

My fellow scientists in the Vitis lab for all their help throughout the study and especially in the writing of this thesis and all the fun moments together.

Winetech, THRIP and Stellenbosch University for financial support

My family, friends and Cobus for all the support, help and encouragement.

A special thanks to my parents for giving me the great gift of a tertiary education, all their love, support, encouragement and for always believing in me.

Abbreviations

µg	Microgram(s)
µl	Microlitre(s)
3'NC	3' Non-coding
5'UTR	5' Untranslated region
Amp	Ampicillin
bp	base pairs
BLAST	Basic Local Alignment Search Tool
CP	Coat Protein
Ct	Threshold cycle
dCP	Divergent coat protein
dH ₂ O	Deionised water
DNA	Deoxyribonucleic Acid
dNTPs	Deoxynucleoside triphosphate(s)
DTT	1,4-Dithiothreitol
DAS-ELISA	Double Antibody Sandwich - Enzyme-Linked Immunosorbent Assay
e	Sampling error
EDTA	Ethylene Diamine Tetra-acetic Acid di-sodium Salt
ELISA	Enzyme-Linked Immunosorbent Assay
GLR	Grapevine leafroll
GLRaV's	Grapevine leafroll associated viruses
GLRaV-3	<i>Grapevine leafroll associated virus-3</i>
GLRaV-2	<i>Grapevine leafroll associated virus-2</i>
GRW	Grapevine rugose wood
GVA	<i>Grapevine virus A</i>
GVB	<i>Grapevine virus B</i>
GVD	<i>Grapevine virus D</i>
GVE	<i>Grapevine virus E</i>
HLV	Heracleum latent virus
HSP-70h	Heat shock protein-70 homologue
HSP-90	Heat shock protein-90
IDT	Integrated DNA Technologies
IPTG	Isopropyl-β-D-thiogalactoside
kb	kilobase
kDa	kiloDalton
LB	Luria Bertani broth
M	Molar
mM	Millimolar
MP	Movement protein
Mr	Molecular weight
MV	Mint virus 2
n	Sample size
ng	Nanograms
nm	Nanometer(s)
nt	Nucleotides
OD600	Absorption value at 600 nm
ORF	Open reading frame

PCR	Polymerase Chain Reaction
PEG	Polyethylene Glycol
qPCR	Quantitative Polymerase Chain Reaction / Real Time PCR
qRT-PCR	Quantitative Reverse Transcription - Polymerase Chain Reaction
RdRp	RNA-dependant RNA polymerase
REST	Relative Expression Software Tool
RFLP	Restriction Fragment Length Polymorphism
RNA	Ribonucleic Acid
RT-PCR	Reverse Transcription - Polymerase Chain Reaction
RW	Rugose wood
SAWIS	South African Wine Industry Information and Systems
SDS	Sodium Dodecyl Sulphate
SG	SYBR Green
SSCP	Single-strand DNA conformational polymorphisms
TAE	Tris Acetic Acid
TBS-T	Tris buffered saline with Tween
U	Units
V	Volt
v/v	Volume per volume
w/v	Weight per volume
β-ME	β-mercaptoethanol

Chemical Compounds

Acetic Acid	HOAc
Calcium Chloride	CaCl ₂
Ethanol	EtOH
Hydrogen Chloride	HCl
Isopropanol	C ₃ H ₇ O
Lithium Chloride	LiCl
Magnesium	Mg
Magnesium Chloride	MgCl ₂
p-nitrophenyl phosphate (pNPP)	C ₆ H ₆ NO ₆ P
PVP-40 (Polyvinylpyrrolidone)	(C ₆ H ₉ NO) ₄₀
Sodium Acetate	NaOAc
Sodium Hydrogen Carbonate	NaHCO ₃
Sodium Carbonate	Na ₂ CO ₃
Sodium Chloride	NaCl
Sodium Hydroxide	NaOH
Sodium Metabisulfite	Na ₂ S ₂ O ₅
Tris	(HOCH ₂) ₃ CNH ₂

Table of Contents

Declaration	ii
Abstract	ii
Opsomming	iv
Acknowledgements	vi
Abbreviations	vii
Chemical Compounds	ix
Table of Figures	xiii
List of Tables	xvi
1. Introduction	1
1.1 <i>Background</i>	1
1.2 <i>Motivation</i>	2
1.3 <i>Objectives</i>	2
2. Real time PCR for sensitive virus detection	4
2.1 <i>Literature Review</i>	4
2.1.1 South African grapevine industry.....	4
2.1.1.1 Current situation.....	4
2.1.2 <i>Grapevine leafroll associated virus-3 (GLRaV-3)</i>	5
2.1.2.1 Viral classification, genome organisation and morphology	5
2.1.2.2 Molecular diversity	6
2.1.2.3 Geographical distribution, transmission and spread	7
2.1.2.4 Symptoms of GLRaV-3 infection.....	8
2.1.2.5 GLRaV-3 control	8
2.1.3 <i>Grapevine virus A (GVA)</i>	9
2.1.3.1 Viral classification, genome organisation and morphology	9
2.1.3.2 Molecular Diversity	10
2.1.3.3 GVA associated diseases	10
2.1.3.4 Transmission and spread.....	11
2.1.3.5 GVA control.....	11
2.1.4 <i>Diagnostic tests for grapevine viruses</i>	12
2.1.4.1 Current context.....	12
2.1.4.2 Enzyme-linked immunosorbent assay (ELISA).....	13
2.1.4.3 RT-PCR.....	14
2.1.4.4 Real time RT-PCR (qRT-PCR) introduction	14
2.1.4.5 qRT-PCR for virus detection	15
2.2. <i>Materials and Methods</i>	18
2.2.1 Plant Material.....	18
2.2.2 Primer design	18
2.2.3 Sample preparation for virus detection	18
2.2.4 Virus detection via RT-PCR.....	21
2.2.5 Virus detection via qRT-PCR.....	21
2.2.6 Cloning and transformation of the 332 bp GLRaV-3 CP region	22
2.2.7 Sequencing and sequence analysis of the GLRaV-3 CP region	22
2.2.8 Statistical analysis for determining minimum replicate samples.....	22
2.2.9 Virus detection via DAS-ELISA	24
2.2.10 PCR Amplification of potentially false ELISA positives	24

2.2.11 Cloning and transformation of the unknown sequence amplified from sample 15.2 with HSP-70h primers.....	25
2.2.12 Sequencing and sequence analysis of the unknown sequence amplified from sample 15.2 with HSP-70h primers.....	25
2.3 Results	26
2.3.1 RT-PCR detection of GLRaV-3	26
2.3.2 RT-PCR detection of GVA.....	26
2.3.3 qRT-PCR detection of GLRaV-3	27
2.3.4 qRT-PCR detection of GVA.....	28
2.3.5 Rootstock screening for GLRaV-3 and GVA	29
2.3.5.1 Nietvoorbij rootstock screening for GLRaV-3 with qRT-PCR and ELISA.....	29
2.3.5.2 Rootstock screening for GVA with qRT-PCR.....	37
2.3.6 Nursery rootstock screening for GLRaV-3	39
2.4 Discussion.....	40
3. Investigation of real time PCR for application in transgenic plant analysis	45
3.1 Literature Review.....	45
3.1.1 Introduction	45
3.1.2 Pathogen derived resistance.....	45
3.1.3 Analysis of transgenic plants.....	46
3.1.4 Transgene copy number determination	46
3.1.4.1 Southern Blot Analysis	46
3.1.4.2 PCR based techniques.....	47
3.1.5 Transgene expression level determination	49
3.1.5.1 Northern Blot Analyses	49
3.1.5.2 PCR based techniques.....	50
3.2 Materials and Methods	52
3.2.1 Transgenic grapevine material.....	52
3.2.2 Primer design	52
3.2.3 DNA extraction	53
3.2.4 DNA Clean-up	54
3.2.5 Detection and quantification of the transgene.....	54
3.2.5.1 Initial PCR optimisation	54
3.2.5.2 Transgene detection with qPCR	54
3.2.5.3 Southern Blot Analyses	55
3.2.6 RNA extraction	57
3.2.7 Estimation of relative transgene mRNA expression levels.....	58
3.2.7.1 Real time RT-PCR (qRT-PCR)	58
3.3 Results	59
3.3.1 DNA extraction from transgenic grapevine	59
3.3.2 Detection and quantification of the transgene.....	59
3.3.2.1 Amplification of a fragment of the transgene	59
3.3.2.2 qPCR detection of the Δ HSP-Mut transgene construct.....	60
3.3.2.3 qPCR amplification of reference genes.....	62
3.3.2.4 Estimation of transgene copy numbers with qPCR using REST.....	69
3.3.2.5 Southern Blot Analyses for transgene copy number estimation.....	69
3.3.3 Estimation of relative transgene mRNA expression levels with qRT-PCR and REST	70
3.4 Discussion.....	76
4. Conclusion	79
References.....	82
Appendix A.....	I
<i>PCR and real time PCR constituents and cycles</i>	<i>I</i>
Standard 25 μ l PCR reaction mix	I

Standard 25µl RT-PCR reaction mix.....	I
Standard 25µl qPCR reaction mix	I
Standard 25µl qRT-PCR reaction mix.....	I
Standard PCR amplification cycle.....	I
Standard RT-PCR amplification cycle	I
Standard qPCR amplification cycle.....	I
Standard qRT-PCR amplification cycle	II
Appendix B	III
<i>Protocols</i>	<i>III</i>
Chemically competent cells	III
Transformation with the pDrive cloning vector.....	III
Virus detection via DAS-ELISA	IV
Appendix C	V
<i>Sequence Alignments</i>	<i>V</i>
GLRaV-3 variants for CP primer design.....	V
GVA variants and published universal primers	VII
Appendix D	VIII
<i>Amplification curves for all 34 Nietvoorbij samples</i>	<i>VIII</i>
GLRaV-3 screening in January 2009	VIII
GLRaV-3 screening in July 2009	IX
GVA screening in July 2009.....	X

Table of Figures

Figure 1: Schematic representation of GLRaV-3 (drawn to scale). Boxes represent different genes: methionine, helicase, RNA dependant RNA polymerase, HSP-70 homologue region, HSP90 homologue region, coat protein, divergent coat protein and replication-enhancing proteins respectively. Putative proteins indicated as p6, p5, p21, p19.6, p19.7, p7 and p4 respectively (Adapted from Maree et al. 2008).....	5
Figure 2: (A) GLRaV-3 infection in a red variety with typical downward rolling of the leaves and the interveinal reddening (http://entopl.okstate.edu/ddd/diseases/leafroll.htm). (B) GLRaV-3 infection in a white variety, with typical rolling of the leaves as well as chlorosis (http://www.edenwines.co.uk/images/leafroll.jpg)	8
Figure 3: Schematic representation of the GVA genome. Boxes represent open reading frames and functions of ORFs are indicated (supplied by Jaques de Preez).....	9
Figure 4: (A) Leaves showing clear Shiraz disease symptoms (http://www.wynboer.co.za/recentarticles/200612shiraz.php3). (B) Typical stem grooving patterns on an infected grapevine cane (http://www.fao.org/docrep/t0675e/T0675E09.htm)	11
Figure 5: Required sample size n_2 as a function of sampling error e_2	24
Figure 6: Agarose gel electrophoresis showing amplified GLRaV-3 coat protein region from grapevine scion material. Lane 1: 1kb DNA ladder, lane 2: GLRaV-3 negative sample, lanes 3-8: samples from our greenhouse displaying visual symptoms of GLRaV-3	26
Figure 7: Agarose gel electrophoresis showing amplified product of GVA from grapevine scion material. Lane 1: 1kb DNA ladder. Lanes 2-3: Samples collected from the Stellenbosch area that tested negative for GVA infection; lanes 4-9: samples tested positive for GVA infection and lane 10: negative control.....	27
Figure 8: (A) Amplification curves for grapevine scion samples (indicated in the legend) tested via qRT-PCR for GLRaV-3 infection. (B) Melting curves (change of fluorescence vs temperature increase) for the qRT-PCR amplified samples. Samples infected with the virus had melting temperatures ranging from 82.5°C – 83.8°C. The no template control had a melting temperature of 79.5°C.....	28
Figure 9: (A) Amplification curves for grapevine scion samples (as indicated in the legend) tested via qRT-PCR for GVA infection. (B) Melting curves for the qRT-PCR amplified samples. Samples infected with the virus had melting temperatures ranging from 82.2°C – 82.7°C. The no template control had a melting temperature of 77.2°C	29
Figure 10: (A) Amplification curves for Nietvoorbij rootstock samples tested positive via qRT-PCR for GLRaV-3 infection during January. (B) Melting curves for the amplified samples to identify samples infected with GLRaV-3. Samples 1.2, 2.2, 2.3, 3.2, 3.3, 4.2, 4.3, .2, 6.3, 7.2, 7.3, 8.2, 9.2, 9.3, 10.2, 10.3, 11.2, 11.3, 12.2, 12.3, 13.2, 13.3, 14.2, 14.3, 15.2, 15.3, 17.2, 17.3 is not indicated on the graph as they did not test positive for GLRaV-3 infection (see Appendix D for graphs with all samples indicated).....	31
Figure 11: (A) Amplification curves for Nietvoorbij rootstock samples tested positive via qRT-PCR for GLRaV-3 infection at the end of July. (B) Melting curves for the amplified samples to identify samples infected with GLRaV-3. Samples 1.2, 2.2, 2.3, 3.2, 3.3, 4.2, 4.3, .2, 6.3, 7.2, 7.3, 9.3, 10.2, 10.3, 11.3, 12.2, 13.2, 13.3, 14.2, 14.3, 15.2, 15.3, 17.3 is not indicated on the graph as they did not test positive for GLRaV-3 infection (see Appendix D for graphs with all samples indicated).....	32
Figure 12: Percentage GLRaV-3 infected samples tested via qRT-PCR and ELISA from January 2009 – July 2009 in Nietvoorbij rootstock samples (ELISA false positives included). Numbers 1, 2 and 3 followed by the month indicate the first, second or third sampling dates for that month.....	34
Figure 13: ELISA false positive samples tested with various GLRaV-3 primers. Negative (neg) and positive (pos) controls were included	34
Figure 14: ELISA false positive samples tested with GLRaV-1 and 2 primers. Negative (neg) no template controls were included. LQV1-H47 and LEV1-C447 primers were used for GRaV-1 detection and LR2 forward and reverse primers were used for GLRaV-2 amplification	35
Figure 15: Percentage GLRaV-3 infected samples tested via qRT-PCR and ELISA from January 2009 – July 2009 in Nietvoorbij rootstock samples (ELISA false positives excluded).....	35

Figure 16: Percentage GLRaV-3 infected samples tested via qRT-PCR from January 2009 – July 2009 in Nietvoorbij rootstock samples (degraded April samples excluded)	36
Figure 17: ELISA positive sample (15.2) tested with different GLRaV primers.....	36
Figure 18: Percentage GVA infected samples tested via qRT-PCR from January 2009 – May 2009 in Nietvoorbij rootstock samples.....	37
Figure 19: (A) Amplification curves for Nietvoorbij rootstock samples tested positive via qRT-PCR for GVA infection at the end of July. (B) Melting curves for the amplified samples to identify samples infected with GVA. Samples 2.3, 3.2, 3.3, 4.2, 4.3, 6.2, 6.3, 7.3, 8.2, 9.3, 13.2, 13.3, 14.2, 14.3, 15.2, 16.2, 16.3, 17.2, 17.3, 17.4 are not indicated in the graph as these samples tested negative (see Appendix D for graphs with all samples indicated).....	39
Figure 20: Graphical representation of the dysfunctional HSP-70h transgene (Δ HSP-Mut)	52
Figure 21: DNA extracted from transgenic plants visualised on a 1.2% agarose gel. Lane 1: untransformed control, lane 2: Transgenic Grapevine plant line Δ HSP-Mut1, lane 3: Δ HSP-Mut2, lane 4: Δ HSP-Mut3, lane 5: Δ HSP-Mut4, lane 6: Δ HSP-Mut 4, lane 7: Δ HSP-Mut5, lane 8: Δ HSP-Mut6, lane 9: Δ HSP-Mut7, lane 10: Δ HSP-Mut8, lane 11: Δ HSP-Mut9, lane 12: Δ HSP-Mut11	59
Figure 22: DNA from transgenic plants amplified with HSP primers visualised on a 1.2% agarose gel to confirm transformation with the antiviral construct. At the top lane 1: 1kb DNA ladder, lane 2: untransformed control, lane 3: Δ HSP-Mut1, lane 4: Δ HSP-Mut2, lane 5: Δ HSP-Mut3, lane 6: Δ HSP-Mut4, lane 7: Δ HSP-Mut4, lane 8: Δ HSP-Mut5, lane 9: Δ HSP-Mut6, lane 10: Δ HSP-Mut7. At the bottom row lane 1: 1kb DNA ladder, lane 2: Δ HSP-Mut8, lane 3: Δ HSP-Mut9, lane 4: Δ HSP-Mut11, lane 5: no template control.....	60
Figure 23: (A) Amplification curves of five fold DNA serial dilutions from sample 9 (from 250ng/reaction to 0.4ng/reaction as indicated in the legend) of a specific transgenic plant, amplified with HSP-70h primers to produce (B) a standard curve (Ct vs log of concentration) for the gene of interest (Δ HSP-Mut). R: square root of correlation coefficient, R ² : correlation coefficient, M: slope of the standard curve, B: intercept of the standard curve and efficiency (effective doubling of PCR product during each PCR cycle) as indicated on the standard curve	61
Figure 24: (A) Amplification curves for transgenic Δ HSP-Mut grapevine samples amplified via qPCR with HSP-70h primers (see different Δ HSP-Mut samples in legend). (B) Melting curve analysis to confirm amplification of correct amplicon. Samples containing the HSP fragment had a melting peak between 83.5°C and 83.8°C. (C) Ct values of amplified samples imported onto HSP-70h standard curve.....	62
Figure 25: (A) Amplification curves of five fold DNA serial dilutions from sample 9 (from 250ng/reaction to 0.4ng/reaction as indicated in the legend) of a specific transgenic plant, amplified with β -tubulin primers to produce (B) a standard curve (Ct vs log of concentration) for the β -tubulin reference gene. R, R ² , M, B and efficiency values as indicated on the standard curve (as explained in Figure 23).....	63
Figure 26: (A) Amplification curves for transgenic Δ HSP-Mut grapevine samples amplified via qPCR with β -tubulin primers (see different Δ HSP-Mut samples in legend). (B) Melting curve analysis to confirm amplification of correct amplicon, shown as melting peaks between 86.5°C and 87°C. (C) Ct values of amplified samples imported onto β -tubulin standard curve.....	64
Figure 27: (A) Amplification curves of five fold DNA serial dilutions from sample 9 (from 250ng/reaction to 0.4ng/reaction as indicated in the legend) of a specific transgenic plant, amplified with cyclophilin primers to produce (B) a standard curve (Ct vs log of concentration) for the cyclophilin reference gene. R, R ² , M, B and efficiency values as indicated on the standard curve (as explained in Figure 23).....	65
Figure 28: (A) Amplification curves for transgenic Δ HSP-Mut grapevine samples amplified via qPCR with cyclophilin primers (see different Δ HSP-Mut samples in legend). (B) Melting curve analysis to confirm amplification of correct amplicon, shown as melting peaks between 88.5 °C-89°C. (C) Ct values of amplified samples imported onto Cyclophilin standard curve.....	66
Figure 29: (A) Amplification curves of five fold DNA serial dilutions from sample 9 (from 250ng/reaction to 0.4ng/reaction as indicated in the legend) of a specific transgenic plant, amplified with GAPDH primers to produce (B) a standard curve (Ct vs log of concentration) for the GAPDH reference gene. R, R ² , M, B and efficiency values as indicated on the standard curve (as explained in Figure 23).....	67

Figure 30: (A) Amplification curves for transgenic Δ HSP-Mut grapevine samples amplified via qPCR with GAPDH primers (see different Δ HSP-Mut samples in legend). (B) Melting curve analysis to confirm amplification of correct amplicon, shown as melting peaks between 82.0°C and 82.3°C. (C) Ct values of amplified samples imported onto GAPDH standard curve..... 68

Figure 31: Southern blot of transgenic samples containing the Δ HSP-Mut construct (approximately 1500bp). Lane 1: DIG molecular weight marker VII, lane 2: untransformed, undigested genomic DNA control, lane 3: Δ HSP-Mut1, lane 4: Δ HSP-Mut2, lane 5: Δ HSP-Mut4, lane 6: Δ HSP-Mut6, lane 7: Δ HSP-Mut7, lane 8: Δ HSP-Mut8, lane 9: Δ HSP-Mut9, lane 10: Δ HSP-Mut10, lane 11: DIG molecular weight marker VII, lane 12: Δ HSP-Mut11, lane 13: Δ HSP-Mut12, lane 14: Δ HSP-Mut13, lane 15: Δ HSP-Mut14, lane 16: Δ HSP-Mut15, lane 17: Δ HSP-Mut16, lane 18: Δ HSP-Mut17, lane 19: Δ HSP-Mut18, lane 20: Δ HSP-Mut20, lane 23: plasmid, containing Δ HSP-Mut construct, digested with *Hind*III, lane 24: undigested plasmid (containing Δ HSP-Mut construct)..... 70

Figure 32: (A) Amplification curves of five fold RNA serial dilutions from sample 8 (from 500ng/reaction to 0.2ng/reaction as indicated in the legend) of a transgenic plant, amplified with HSP-70h primers to produce (B) a standard curve (Ct vs log of concentration) for the gene of interest. R, R², M, B and efficiency values as indicated on the standard curve (as explained in Figure 23). 71

Figure 33: (A) Amplification curves for transgenic Δ HSP-Mut grapevine samples (as indicated in the legend) amplified via qRT-PCR with HSP-70h primers for transgene expression level determination (see different Δ HSP-Mut samples in legend). (B) Melting curve analysis to verify amplification of correct amplicon, shown as melting peaks between 82.5°C and 83.0°C. (C) Ct values of the amplified samples imported onto the gene of interest (HSP) standard curve..... 72

Figure 34: (A) Amplification curves of five fold RNA serial dilutions from sample 8 (from 500ng/reaction to 0.2ng/reaction as indicated in the legend) of a transgenic plant, amplified with GAPDH primers to produce (B) a standard curve (Ct vs log of concentration) for the gene of interest. R, R², M, B and efficiency values as indicated on the standard curve (as explained in Figure 23) 73

Figure 35: (A) Amplification curves for transgenic grapevine samples amplified via qRT-PCR with GAPDH primers for transgene expression level determination. (B) Melting curve analysis to verify amplification of correct amplicon, as shown in melting peaks between 80.7°C and 81.0°C. (C) Ct values of the amplified samples imported onto the reference gene (GAPDH) standard curve..... 74

Figure 36: (A) Amplification curves for all 34 Nietvoorbij rootstock samples tested via qRT-PCR for GLRaV-3 infection during January 2009. (B) Melting curves for the amplified samples to identify samples infected with GLRaV-3.....VIII

Figure 37: (A) Amplification curves for all 34 Nietvoorbij rootstock samples tested via qRT-PCR for GLRaV-3 infection during July 2009. (B) Melting curves for the amplified samples to identify samples infected with GLRaV-3.IX

Figure 38: (A) Amplification curves for all 34 Nietvoorbij rootstock samples tested via qRT-PCR for GVA infection during July 2009. (B) Melting curves for the amplified samples to identify samples infected with GLRaV-3. X

List of Tables

Table 1: Diagnostic and plasmid sequencing primer sequences and fragment sizes of their products.....	20
Table 2: Results for 34 Nietvoorbij rootstock samples tested for GLRaV-3 infection TESTED VIA Qrt-pcr (✓) and DAS-ELISA (X) in September 2008 (initial screening) and throughout the growing season in 2009 from January to July. Marks indicate samples that tested positive during that screening period (April 2 was excluded as positives and negatives were indistinguishable).	33
Table 3: Results for 34 Nietvoorbij rootstock samples tested for GVA infection via qRT-PCR in September 2008 (initial screening) and throughout the growing season in 2009 from January to July. Marks indicate samples that tested positive during that screening period	38
Table 4: Primer names, sequences, product fragment sizes and optimal annealing temperatures (Ta).....	53
Table 5: ΔHSP-Mut copy numbers for the transgenic samples relatively quantified to each of the reference genes as well as determined by the Southern blot analysis. ΔHSP-Mut expression levels for the transgenic samples relatively quantified to GAPDH.....	75

Chapter 1

1. Introduction

1.1 Background

The versatility of real time PCR within the field of Molecular Biology has become more evident in recent years. Due to its high specificity, sensitivity, reliability, reproducibility and quantitative ability, it has proved to be a relevant application in various plant studies (Gachon et al. 2004). The applications of real time PCR include measuring mRNA expression levels, DNA copy number, transgene copy number and expression levels, allelic discrimination, and measuring viral titres (Ginzinger 2002). The focus of this study was directed towards virus detection and transgenic plant analysis within *Vitis -vinifera* by employing real time PCR.

Grapevine scion material is routinely tested for various grapevine viruses. However, virus detection in rootstocks is problematic due to low and varying virus titres. Certified virus-free scion material could thus be grafted on rootstock material of unknown viral status and could lead to further spread of the disease. The high variability of certain viruses further hampers sensitive virus detection. For these reasons real time reverse transcription PCR (qRT-PCR) could be an ideal method for virus diagnostics. qRT-PCR has been shown to be 125 times more sensitive in detecting *Grapevine leafroll associated virus-2* than conventional RT-PCR methods (Beuve et al. 2006). Sensitive diagnostic tools could therefore help to enable large scale screening and improve sanitary selection of grapevine rootstock in nurseries.

An additional approach for virus eradication includes the introduction of transgenic resistance to the virus by means of genetic engineering of various viral genes into rootstocks. It is important that these plants are accurately characterised in order to identify specific lines suitable for further use; plants identified as expressing the transgenic insert. Real time PCR has also proven to be a powerful tool in accurately determining transgene copy numbers and expression within transgenic plants. Because of its high level of accuracy and sensitivity it is the most reliable tool for

quantifying exogenous gene integration and expression (Savazzini et al. 2005) and was employed in this study for transgenic plant screening.

1.2 Motivation

Grapevine leafroll associated virus-3 (GLRaV-3) is an economically important virus in South Africa as well as other parts of the world. Detection of the virus in rootstocks is problematic due to very low titres. Previous studies have obtained sensitive, reproducible results with the use of SYBR Green qRT-PCR in the detection of plant viruses. The wine industry utilizes DAS-ELISA for the detection of GLRaV-3 in grapevine rootstock material. This study investigated the efficacy of qRT-PCR to detect GLRaV-3 and *Grapevine virus A* (GVA) in grapevine rootstock material. The sensitivity and accuracy of qRT-PCR and DAS-ELISA were also compared for GLRaV-3 detection in grapevine rootstocks.

Genetic engineering of crop plants serves as a mechanism to control fungal, bacterial, viral and insect pathogens (Vivier and Pretorius et al. 2000). This approach was also implemented for the control of GLRaV-3 infection and spread. Molecular characterisation of transgenic plants is essential, as the number of transgene copies influence the expression level and genetic stability of the transgene (Weng et al. 2004). Southern and northern blot analyses are routinely used to determine copy number and expression levels in transgenic plants. These procedures are however laborious, time-consuming, requires large amounts of plant material and may also involve the use of harmful radioisotopes. This project investigated the effectiveness of real time PCR (qPCR) and qRT-PCR for the relative quantification of copy numbers and expression levels in transgenic grapevine.

1.3 Objectives

Virus diagnostics

- Optimise a sensitive qRT-PCR detection system for GLRaV-3 and GVA in grapevine rootstock material
- Determine optimum sampling time for sensitive and accurate detection of GLRaV-3 and GVA

- Compare efficacy, sensitivity and accuracy of qRT-PCR and DAS-ELISA for GLRaV-3 detection in both a severely infected vineyard and propagation material from nurseries

Transgenic plant analysis

- Construct standard curves for the transgene and reference genes with DNA and RNA extracted from transgenic plant lines
- Utilise standard curves and amplification information of the transgenic samples to estimate the relative copy numbers and expression levels of the transgene in each of the transgenic plants using the relative expression software tool (REST)
- Perform Southern blot analysis for copy number determination
- Investigate whether qPCR is an effective and accurate system for transgene copy number estimation
- Investigate correlations between transgene copy number and transgene expression levels

Chapter 2

2. Real time PCR for sensitive virus detection

2.1 Literature Review

Grapevine leafroll associated virus-3 (GLRaV-3) and *Grapevine virus A* (GVA) both pose a threat to the South African grapevine industry. In this chapter a brief description of the South African grapevine industry will be presented. This will be followed by a literature review of GLRaV-3 and GVA, their associated diseases, transmission, spread and control. The chapter will conclude with a summary of the diagnostic tests available for use in grapevine virus detection.

2.1.1 South African grapevine industry

2.1.1.1 Current situation

Approximately 257 000 people are employed in the wine industry and it contributes R16,3 billion to the regional economy and 8,2% to the Western Cape's gross geographic product (according to SA Wine Industry Information & Systems (SAWIS) based on 2003 figures). South Africa ranks as number nine globally in terms of wine volume production and produces 3,3% of the world's wine (2003 figures). (http://www.wine.co.za/Misc/Page_Detail.aspx?PAGEID=304).

The sustainability of the grapevine industry is however threatened by various infectious agents. These include viruses, viroids, phytoplasma and insect-transmitted xylematic bacteria (Martelli and Boudon-Padieu, 2006). Grapevine leafroll (GLR) and grapevine rugose wood complex (GRW) are two of the most significant and widely distributed graft-transmittable grapevine diseases throughout the world (Martelli 1993). GLRaV-3 is the main aetiological agent causing GLR disease (Martelli et al. 2002). There is a lack of recent studies reporting on the prevalence of GLRaV-3, but a study conducted in 1972 in the Western Cape indicated a high prevalence of GLRaV-3 infection which was mainly attributed to infected rootstock material (Nel and Engelbrecht, 1972). Anecdotal evidence indicates that this would still be the case seeing as the main agent spreading the disease are scale insects which

are very hard to control, leaving the only other option for disease control, to rogue infected material. One of the main viruses involved in the aetiology of grapevine rugose wood (RW) complex is *Grapevine virus A* (GVA) (Dovas and Katis, 2003) and it is one of the most common viruses infecting grapevine worldwide (Goszczynski and Jooste, 2003).

In South Africa all grapevine scion material are required to be grafted onto phylloxera resistant rootstocks in order to prevent the detrimental effect of phylloxera infestations. However, low and varying virus titres in the rootstocks hamper accurate virus detection and more sensitive detection methods than ELISA and conventional PCR may be required.

2.1.2 *Grapevine leafroll associated virus-3 (GLRaV-3)*

2.1.2.1 Viral classification, genome organisation and morphology

There are currently 9 identified GLRaVs all belonging to the *Closteroviridae* family (Martelli and Boudon-Padieu, 2006). GLRaV-2 is a member of the *Closterovirus* genus and GLRaV-7 is presently classified as an unassigned species to the family (Martelli and Boudon-Padieu, 2006). The rest of the GLRaVs are all members of the *Ampelovirus* genus (Alkowni et al. 2004), however reclassification is being discussed. GLRaV-3 is a positive-sense ssRNA virus (Martelli et al. 2002) encompassing 13 open reading frames (ORFs) which encode various genes as seen in Figure 1 (Maree et al. 2008).

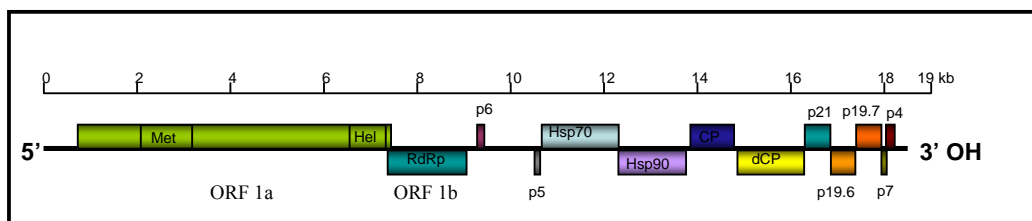


Figure 1: Schematic representation of GLRaV-3 (drawn to scale). Boxes represent different genes: methionine, helicase, RNA dependant RNA polymerase, HSP-70 homologue region, HSP90 homologue region, coat protein, divergent coat protein and replication-enhancing proteins respectively. Putative proteins indicated as p6, p5, p21, p19.6, p19.7, p7 and p4 respectively (Adapted from Maree et al. 2008)

2.1.2.2 Molecular diversity

The first complete nucleotide sequence of GLRaV-3 was published in 2004 by Ling et al. (isolate NY-1, AF037268). This sequence encompassed a 5' untranslated region (UTR) of 158 nucleotides (nt) long. Thereafter various studies investigated the molecular variability within the GLRaV-3 genome. Upon further investigation into the 5'UTR, Maree et al. (2008) discovered a larger 5' UTR of 737 nt in the GP18 (EU259806) isolate. An additional 82-nt overlap between ORF1a and ORF1b in the GP18 sequence was also discovered, with ORF1b still being expressed as a +1 frameshift in the GP18 sequence (Maree et al. 2008).

Fajardo et al. (2005) studied the variability within the GLRaV-3 genome in Brazilian isolates via single-strand DNA conformational polymorphisms (SSCP), these researchers obtained two different electrophoretic profiles that showed 75,1% and 81,8% homology with that of the NY-1 sequence. In 2008 Engel et al. compared their complete GLRaV-3 genome sequence of the Chilean isolate (CI-766) with the NY-1 sequence and found 97.6% nucleotide identity between them and most of the genetic diversity was found in the ORF1a region.

Variability within conserved regions of GLRaV-3, such as RNA-dependant RNA polymerase (RdRp), CP and heat shock protein (HSP) regions, was also a subject of interest. In these regions, the Czech isolate showed more than 99% nucleotide and amino acid identity with the NY-1 sequence and similarly high identity with other partial GLRaV-3 sequences of isolates from around the world (Engel et al. 2004). Turturo et al. (2005) found that 10% of RdRp and HSP genes and 15% of CP genes consisted of a combination of two or more variants in their samples. Genetic diversity and phylogenetic analysis suggested the possible existence of vines that have a mixed infection with diverse sequence variants and in some cases showing possible recombination events. Their results also indicated a higher variability in the CP gene (Turturo et al. 2005). A study by Fajardo et al. (2007) confirmed these results when they detected a total of seventeen amino acid substitutions in their four characterized isolates in comparison to the NY1, Dawanhong No.2 and SL10 sequences. The RdRp gene was found to be more conserved than that of the CP, suggesting a higher selective pressure existing on the RdRp gene (Turturo et al. 2005). The 3' terminal region of the RdRp of three Brazilian GLRaV-3 isolates

showed amino acid differences of only 4% to 6% when compared with that of other isolates found in the GenBank database as well as isolates from North American and southern Brazil (Dianese et al. 2005).

These results indicate that a degree of variation does exist among different GLRaV-3 isolates; with more variability in certain regions than others. This should be taken into account in the design of sensitive diagnostic detection systems to ensure that all variants will be detected.

2.1.2.3 Geographical distribution, transmission and spread

GLRaV-3 is transmitted during vegetative propagation (Martelli and Boudon-Padiou 2006) and by insect vectors (Sforza et al. 2003). In a study by Pietersen (2002) between 0% and 29.3% leafroll infection was detected in mother blocks containing propagation material, with an average rate of infection of 1.58%.

Insect vectors for leafroll viruses are known within two hemipteran insect families, Pseudococcidae (mealybugs) and Coccidae (soft scales). At least eight mealybugs (*Pseudococcus longispinus*, *Pseudococcus viburni*, *Pseudococcus calceolariae*, *Pseudococcus maritimus*, *Planococcus citri*, *Planococcus ficus*, *H. bohemicus*, and *Phenacoccus aceris*) and one soft scale insect (*Pulvinaria vitis*) have been reported as vectors of GLRaV-3 (Tsai et al. 2008).

GLRaV-3 is the most important virus associated with leafroll locally. A survey conducted in 1970 on Stellenbosch vineyards showed that 68.4% of vineyards displayed leafroll symptoms (Nel and Engelbrecht, 1972); this high prevalence was attributed to infected rootstock. Stellenbosch vineyards have the highest incidence of leafroll infection, compared to the Paarl, Robertson and Worcester regions (Pietersen personal communication as referenced in Freeborough and Burger 2008). Although the exact percentage of leafroll infection in the different wine producing regions is presently unknown, Ferdi Van Zyl (SAPO Trust) conducted a survey in 2005 and found that table grapes had a 44% incidence of leafroll infection which provides the nearest estimation of the current situation (Van Zyl personal communication as referenced in Freeborough and Burger 2008).

2.1.2.4 Symptoms of GLRaV-3 infection

The effects associated with GLRaV-3 infection include delayed ripening of fruit, lower fruit quality, diminishing sugar content and a reduction of fruit colour in red cultivars (Borgo and Angelini 2002). Additional symptoms also include downward rolling of basal leaves with subsequent rolling of leaves near the shoot tips, chlorosis in some white cultivars and interveinal reddening in red cultivars (Figure 2) (Osman et al. 2007). Visual symptoms of GLRaV-3 infection can be best observed in late summer (Pietersen 2004). Leafroll decreases grapevine yield (15%-20% average) and decreases rooting ability, graft take and plant vigour.

Visual symptoms are most severe in red cultivars. Symptoms appear to be less severe on some white varieties and most rootstock and certain hybrid varieties may be infected and yet show no foliar symptoms. One explanation for these observations is the genetic tolerance of certain varieties to GLRaV-3 (Charles et al. 2006).

A



B



Figure 2: (A) GLRaV-3 infection in a red variety with typical downward rolling of the leaves and the interveinal reddening (<http://entopl.okstate.edu/ddd/diseases/leafroll.htm>). (B) GLRaV-3 infection in a white variety, with typical rolling of the leaves as well as chlorosis (<http://www.edenwines.co.uk/images/leafroll.jpg>)

2.1.2.5 GLRaV-3 control

Because grapevine has no active resistance response against viral disease, these viral diseases could have a more severe effect than pathogens like fungi and bacteria (Espinoza et al. 2007). In South Africa nuclear-blocks of the two main plant improvement organizations supplies more than 90% of the certified material. Vines from these nuclear blocks are used for mass production of propagation material; this

is firstly done in Foundation-blocks and then in Mother-blocks. Commercial nurseries can purchase certified material from the Mother-blocks. In order to gain sufficient amounts of planting material, some of the phases are conducted in the field. Since the majority of Mother-blocks and Nurseries are currently situated within commercial production areas, certified vines often become infected with viruses, in spite of requirements such as isolation distances and virus indexing (Pietersen 2004). Foundation-block material is screened for the presence of GLRaV-3 via sensitive detection methods, such as ELISA or PCR, whereas Mother-blocks and Nurseries are visually screened by experienced industry inspectors for leafroll symptoms. Due to a lag period between the time of virus infection and when the virus becomes detectable by conventional virus detection techniques, a number of infected plants might escape detection. It is therefore not guaranteed that all material from the Certification Scheme is virus-free; nonetheless it does ensure that the planting material is significantly healthier, and delivers the best planting material available (Pietersen 2004).

2.1.3 Grapevine virus A (GVA)

2.1.3.1 Viral classification, genome organisation and morphology

Grapevine virus A (GVA) is one of the emerging grapevine viruses in South Africa (Goszczynski and Jooste, 2003) and is a member of the family *Flexiviridae* and *Vitivirus* genus. Other viruses in this genus includes *Grapevine virus B* (GVB), *Grapevine virus D* (GVD), and *Heracleum latent virus* (HLV) (Saldarelli et al.1996; Minafra et al. 1997) as well as the recently discovered members, *Mint virus 2* (MV2) (Tzanetakis et al. 2007) and *Grapevine virus E* (GVE) (Nakaune et al. 2008). GVA has a positive-sense ssRNA genome (Martelli and Boudon-Padieu, 2006) organised into five ORFs consisting of 7351 nucleotides (Figure 3) (Minafra et al. 1997).

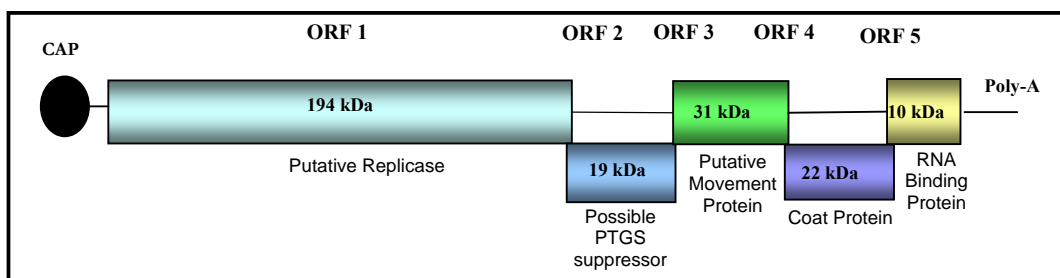


Figure 3: Schematic representation of the GVA genome. Boxes represent open reading frames and functions of ORFs are indicated (supplied by Jaques de Preez).

2.1.3.2 Molecular Diversity

Divergent variants of this virus were identified and clustered into three groups (I, II, III) on the basis of nucleotide similarity (Goszczynski and Jooste, 2003). Chimaeric sequences of GVA exist and are most likely due to recombination between divergent variants of the virus. An RT-PCR assay was developed by Goszczynski and Jooste (2003) to detect these divergent variants which share between 78.1% - 79.4% nucleotide similarity in the 3' terminal end of the genome (comprising of part of ORF3, complete ORF4 and ORF5 and part of the 3'UTR). Their results suggest that it is common for South African grapevine infected with GVA to have a mixed infection with divergent variants of GVA and it is thus important to design a sensitive diagnostic test to ensure accurate detection of the different variants (Goszczynski and Jooste, 2003).

Murolo et al. (2008) investigated the genetic variability of the CP gene of GVA in infected Italian vines. The genetic and population diversity was studied by RT-PCR-RFLP analysis. Their analysis showed some of the plants to be infected with more than one variant of GVA. All the isolates belonged to groups I and II (according to the groups described by Goszczynski and Jooste, 2003). Several full length sequences of GVA variants were also generated by Goszczynski et al (2008). Of the few differences found when compared to the Italian sequence (Is151), the most significant was the presence of a 119 nt insert downstream of the start codon of ORF 2 as well as a shifted ORF 2 start codon in all variants of this group (group II) (Goszczynski et al. 2008).

2.1.3.3 GVA associated diseases

GVA is one of the most common viruses infecting grapevine worldwide (Goszczynski and Jooste, 2003). It is one of five phloem limited viruses involved in the aetiology of grapevine rugose wood (GRW) complex (Dovas and Katis, 2003) and was also found to be closely associated with Kober stem grooving disease (Chevalier et al. 1995) and Shiraz disease (Goszczynski and Jooste, 2003). Shiraz disease mainly infects Shiraz, Merlot, Gamay, Malbec and Viognier cultivars in South Africa (Goszczynski et al. 2008). Symptoms of Shiraz disease include stunted growth, delayed budburst, canes that do not mature and canes that do not lignify (Figure 4) (Nicholas 2006). Goszczynski (2007) found that GVA variants of group II

are closely associated with Shiraz disease and those of group III are usually present in Shiraz disease susceptible vines, but they don't show symptoms of the disease. Isolates of the different groups also show drastically different symptoms in the herbaceous host *Nicotiana Benthamiana* (Goszczyński et al. 2008).

Kober stem grooving is one of several diseases that are part of the rugose wood complex. These diseases usually develop in grafted vines, but appear latent in ungrafted *V. vinifera*, American *Vitis* species and rootstock hybrids. Grapevines displaying Kober stem grooving disease have typical marked grooving on the stems (Martelli and Boudon-Padieu, 2006) and affected vines may also show swelling at the graft union and failure to thrive (Figure 4) (<http://www.agf.gov.bc.ca/cropprot/grapeipm/virus.htm>).

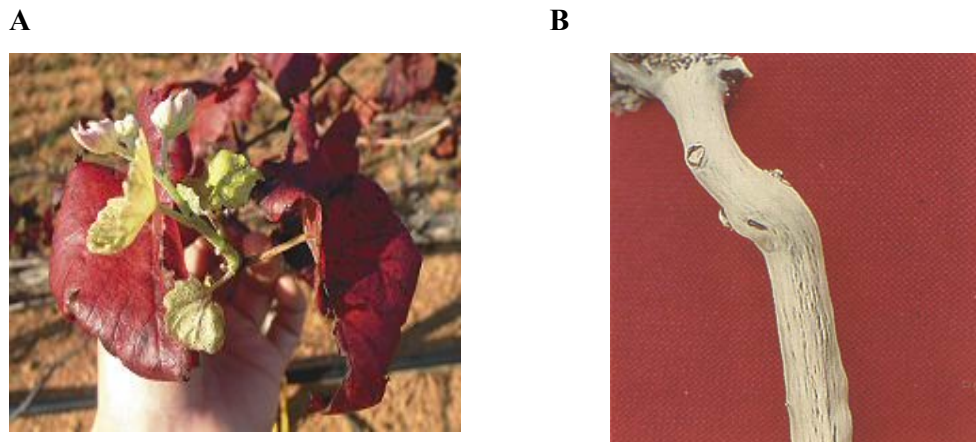


Figure 4: (A) Leaves showing clear Shiraz disease symptoms (<http://www.wynboer.co.za/recentarticles/200612shiraz.php3>). (B) Typical stem grooving patterns on an infected grapevine cane (<http://www.fao.org/docrep/t0675e/T0675E09.htm>)

2.1.3.4 Transmission and spread

GVA is transmitted by various species of pseudococcid mealybugs (*Pseudococcus* spp., and *Planococcus* spp.) (Goszczyński and Jooste, 2003) as well as through vegetative propagation (Dovas and Katis, 2003). GVA can also be transmitted to herbaceous plants by the above insects or via mechanical inoculation (Goszczyński et al. 1996).

2.1.3.5 GVA control

Correlations between virus presence and crop performance or symptom expression have only recently been established through experimental trials which are incorporated for the elimination of RW-associated viruses. The main difficulty is the

assessment of the current situation; this is due to the presence of mixed infections by uncharacterized virus isolates and uncertain sanitary status of donor vines (Bottalico et al. 2000). The control of grapevine viruses is achieved through the production of healthy plants. Thermotherapy and meristem culture are the most frequently used methods for the production of virus-free grapevine plants. However, thermotherapy is laborious and often has a low success rate. Regeneration ability is proportional to the size of the meristem tissue cultured; the frequency of successful virus eradication is inversely proportional to the size of excised meristems (about 0.2 - 0.5 mm).

Cryopreservation has been extensively employed for numerous plant species ranging from temperate to tropical regions (Wang et al. 2003). Wang et al. (2003) achieved up to 97% elimination of GVA by cryopreservation of shoot explants, regardless of the explant size (which only influenced the survival), while standard meristem culture resulted in only 12% of GVA elimination.

2.1.4 Diagnostic tests for grapevine viruses

2.1.4.1 Current context

As previously mentioned, GLRaV-3 and GVA are two of the most important grapevine viruses threatening the sustainability of the grapevine industry. Scion material is routinely tested by ELISA or RT-PCR. However, low and varying virus titres present in grapevine rootstocks are problematic for vegetative propagation as routine detection systems are not always sensitive enough to detect the virus. This could result in certified virus free scion material being grafted onto rootstock with unknown virus status consequently leading to high concentrations of virus accumulating in scion material. It is thus important that the virus detection systems used are sensitive enough to detect low virus titres which could be due to the uneven distribution of the virus in rootstock material. This will enable large scale screening and consequently improve sanitary selection of grapevine stock nurseries and thus help to control virus infection and spread (Beuve et al. 2007).

Currently, sanitary selection and the use of clean propagating material are the best preventative measure against grapevine viruses; it is thus necessary to have efficient methods to identify healthy source material in order to limit detrimental viral effects (Murolo et al. 2008). Heat therapy and meristem tip culture or somatic

embryogenesis can however be employed in order to eliminate various viruses (Pietersen 2004). Supplementary approaches also include the introduction of transgenic resistance to GLRaV-3 by means of genetic engineering of various viral genes into rootstocks or European grape cultivars (Martelli and Boudon-Padieu, 2006).

2.1.4.2 Enzyme-linked immunosorbent assay (ELISA)

Currently, enzyme-linked immunosorbent assay (ELISA) is the method routinely used to screen for most grapevine viruses in South Africa. Pathogen detection via ELISA relies on the interaction between the viral antigen and viral specific antibodies. Different variations of the ELISA have been developed, with the indirect DAS-ELISA being the most commonly used test. In the DAS-ELISA the plate is first coated with antibody followed by incubation with the sample to be tested. If the sample contains the specific antigen, it will interact with the antibodies fixed on the microtiter plate. Thereafter a detecting antibody is added followed by an enzyme-linked secondary antibody which binds to the detecting antibody. Attached to this secondary antibody is a reporter molecule that allows for indirect detection of the virus. The reporter molecule, usually an enzyme, acts on a substrate causing a change in colour, which can be measured by a spectrophotometer (O'Donnell, 1999; Ward et al., 2004). The colour intensity can be correlated to the amount of bound antibodies and thus the amount of antigen present in the sample (Gugerli and Gehringer, 1980).

Advantages of DAS-ELISA include higher specificity and a reduction of non-specific binding with respect to the direct ELISA. Therefore DAS-ELISA is commonly employed in plant pathogen detection in plant sap without prior purification of the pathogen (Gugerli and Gehringer, 1980). Some of the disadvantages of ELISA are that the polyclonal antibodies are generated in limited amounts and the specificity could vary between different batches; the antibodies recognize multiple epitopes and could bind to similar viruses and plant protein extracts which could lead to false positive results. The development of monoclonal antibodies increased the specificity of these serological tests. Monoclonal antibodies recognize a single epitope, are highly specific and are more readily available which makes them ideal for specific virus detection. However, small changes in the epitope, due to the rapid mutation rate

of especially RNA viruses, could lead to false negatives. Additionally, monoclonal antibody production is laborious and expensive (Köhler and Milstein 1975).

Detection of viruses associated with Rugose wood complex (such as GVA) by ELISA is difficult and unreliable at times due to the low virus concentration in grapevine, uneven distribution in the host plant and seasonal variation in virus titre. Furthermore, reliable antibody sources for all these viruses are not available (Osman and Rowhani et al. 2008).

2.1.4.3 RT-PCR

PCR-based technologies have recently gained popularity for virus detection because of their higher sensitivity and the fact that RT-PCR can facilitate assays of closteroviruses for which antisera are not available or suitable (Ling et al. 2001). Waite Diagnostics (University of Adelaide in Australia) was established to provide the Australian viticulture industry a service to detect numerous viruses. They currently test for more than 12 grapevine viruses (including GLRaV-3 and GVA) via RT-PCR methods which give them the competitive advantage of a highly sensitive and rapid diagnostic assay (<http://www.agwine.adelaide.edu.au/facilities/wdiag.html>). There is no such service provider currently in South Africa and certain samples are sent to Waite Diagnostics for testing. RT-PCR is capable of detecting very low viral titres, and proved to be between 10-1000 times more sensitive than ELISA (Charles et al. 2006). Numerous viral sequences of GLRaV are currently available, enabling the design of specific RT-PCR primers (Osman et al. 2007). Due to noticeable sequence variation within certain regions of GLRaV-3, it is essential to design primers that will be able to detect all known variants.

2.1.4.4 Real time RT-PCR (qRT-PCR) introduction

Real-time PCR (qPCR) has become a powerful technology for the detection and quantification of small amounts of nucleic acids due to its high sensitivity and large dynamic range. qPCR has played a significant role in biological research, including virology (Feng et al. 2008). qPCR has the ability to accurately quantify the initial amount of template contrary to other PCR systems that quantify the final end point product. The qPCR detection system is based on the detection of a fluorescent reporter dye. The fluorescent signal increases in direct proportion to the amount of PCR product in the reaction. The amount of fluorescence is recorded which enables

the monitoring of PCR product in exponential phase during real time. Here the first significant increase in fluorescence (threshold cycle or Ct value) correlates to the initial amount of starting material; the higher the initial concentration of starting material the lower the Ct value (Dorak 2006).

Various fluorescent probes have been designed for use in qPCR reactions. TaqMan is an example of a hydrolysis probe. These probes are oligonucleotides that are longer than the primers (20-30 bp) and contain a fluorescent dye on the 5' end and a quencher molecule on the 3' end. When the probe is unbound and intact, it emits no fluorescent signal, but once bound to a specific internal region of the PCR product, the 5' exonuclease activity of the polymerase cleaves the 5' end that contains the fluorescent dye. Fluorescence is thus emitted as the quencher is not attached to the 5' end any more and fluorescence increases during each cycle as the amplified PCR product accumulates (Dorak 2006). The advantage of TaqMan probes is that primer-dimers and any non-specific amplification have no influence on the results as it detects specific amplification only. However, the cost of these probes makes it an expensive diagnostic test.

A more economic alternative for qPCR is the use of a double stranded DNA binding dye, such as SYBR Green. SYBR Green is a minor groove binding dye that does not emit fluorescence when in solution but emits a strong fluorescent signal when bound to double-stranded DNA. It quantifies the amplicon product, which also includes non-specific amplification and primer-dimers. With adequate optimization non-specific amplification and primer-dimers can be eliminated. After amplification is complete, dissociation or melting curve analysis can be performed on the PCR product. Samples containing the specific amplicon will show a clear peak (on the first derivative plot) at the specific melting temperature of the amplicon (Dorak 2006).

2.1.4.5 qRT-PCR for virus detection

Real-time RT-PCR (qRT-PCR) using a TaqMan probe has successfully been utilised in the detection of various plant viruses, including GLRaV-3 (Osman et al. 2007). The advantage of TaqMan probes is that primer-dimers have no influence on the results. PCR product accumulation is measured by the increase of fluorescence of the

reporter dye and the detected fluorescence is of specific amplification only (Dorak 2006).

Real-time PCR with SYBR Green melting curve analysis is a simple and reliable technique which has been effectively employed for the detection and identification of various pathogens including RNA plant viruses. Melting curve analysis is performed for specific identification at the species level, or even identification of different strains of a virus pathogen (Varga et al. 2005).

SYBR Green based detection methods proved to be reliable for the detection of nucleic acid targets characterized by sequence variability. Papin et al. (2004) studied single nucleotide variants of the West Nile virus and found that the use of a probe based assay, such as TaqMan, was unable to detect 47% of single nucleotide variants, while a SYBR Green assay was equally sensitive, and more notably, it detected 100% of possible variants. In the case where broad spectrum detection is required, as with the Noroviruses, degenerate primers with a SYBR Green assay proved to work effectively but that probe systems, such as TaqMan, require high complementarity (Richards et al. 2004). This may result in false negatives due to the presence of viruses with high sequence variability in the probe-binding region.

Osman and Rowhani et al. (2008) compared the efficiency of virus detection by RT-PCR to that of a TaqMan qRT-PCR method. When using crude extracts, the TaqMan qRT-PCR system was 32-fold more sensitive than RT-PCR and with RNA extracts 256-fold more sensitive. They also investigated how these two starting templates compared in TaqMan qRT-PCR detection of viruses associated with Rugose wood complex. The crude extracts contain more RT-PCR enzyme inhibitors and this was evident in higher Ct values compared to Ct values of RNA samples. They further investigated the lowest concentration detectable with the qRT-PCR; serial dilutions were performed on the two different starting materials. Virus was still detectable in crude extracts at a 1:40,960 fold dilution and the RNA extracts at 1:81,920 fold dilutions (Osman and Rowhani, 2008). However, due to the laborious nature of most RNA extraction protocols, it is not feasible for the industry to use RNA as starting template for large scale virus detection. Where high throughput is of the essence, it would be adequate to use crude extracts as starting material, but where questionable

samples are present, RNA extractions can be employed for absolute certainty. Thus where high throughput is essential, crude virus extractions are preferred, and coupled with qRT-PCR, could thus lead to even higher throughput capacity.

Another study that used crude virus extracts as starting template investigated the sensitivity of a SYBR Green real-time RT-PCR method to detect and quantify Norwalk virus in stool samples. These researchers used the sample with the highest virus titre to establish a standard curve by performing ten-fold dilutions on the samples to 10^{-8} . They were able to detect the virus successfully at a 10^{-7} dilution. They further described a relatively straightforward approach for the construction of standard curves for virtually any virus (granted the virus is present at a high enough titre) that can be used to semi-quantify minimum virus levels (Richards et al. 2004).

A qRT-PCR method using SYBR Green has been developed to detect GLRaV-2 in grapevine. This method was proven to be 125 times more sensitive than conventional RT-PCR and has the advantage of not requiring TaqMan hybridization probes thus making the assay more affordable and enabling a simple transfer of conventional RT-PCR procedure to qRT-PCR (Beuve et al. 2007). As real-time PCR also eliminates post PCR processing (such as gel electrophoresis and ethidium bromide staining), it markedly decreases the reaction time which increases the PCR throughput and makes it ideal for large scale screening (Scheda et al. 2004).

2.2. Materials and Methods

2.2.1 Plant Material

For initial optimisation of RT-PCR detection of GLRaV-3 and GVA, symptomatic plants from our plant collection and field collected samples were used. Petioles as well as phloem scrapings from scion bark material were used. Thereafter we proceeded to test asymptomatic rootstock material from various sources, including Nietvoorbij, Ernita nursery and the KWV mother block. For both instances the time of sample collection as well as the type of sample material was validated to ensure optimal amplification and sensitive detection. The samples from Nietvoorbij were screened from January 2009 to July 2009. The grapevines were arranged in a series of four plants per segment, for labelling of the samples, the first number refers to the segment and the second to the number in series (as indicated in the results section). For each segment the second and third plants were selected and for segment 17 the fourth plant was also included as his segment had an extra plant.

2.2.2 Primer design

Diagnostic primers specific for GLRaV-3 detection were designed to detect all known variants of the virus. Primers were designed based on multiple sequence alignments of all known sequences of the coat protein (CP) region of GLRaV-3 (Appendix C). The CP region of the virus was chosen as it was believed that this region would be expressed by the virus at a higher level due to the positions of sub-genomic promoters. This would then lead to better amplification and thus better detection of the virus. These primers were designed and analysed on the Integrated DNA Technologies (IDT) website (<http://www.idtdna.com/Home/Home.aspx>). Diagnostic GVA primers, (specific for the region between the CP and ORF 5) designed by MacKenzie (1997) to detect all GVA variants were used for GVA detection (Table 1).

2.2.3 Sample preparation for virus detection

Initial sample preparation consisted of extractions performed on petioles or phloem scrapings from grapevine canes. Ling et al. (2001) found that bark phloem scrapings were the most reliable sample to use for diagnostic testing. But due to the specific protocol followed (for leaf lamina samples), these researchers used petiole samples

and reported high levels of virus in the petioles. For the 34 Nietvoorbij samples that were tested at 2 week intervals (as annotated in Figures 12 and 15 as Feb1 and Feb2 etc), we used petiole material, for as long as it was available, which proved to be more time efficient than bark phloem scrapings. The samples we received from the nurseries were from bark phloem scrapings already macerated in buffer in extraction bags.

Table 1: Diagnostic and plasmid sequencing primer sequences and fragment sizes of their products

Primer name	Sequence	T _A	Fragment size	Virus	Position	Primers deigned by
Coat protein F	ACATCGTCTTCGACGGAGTT	56°C	332 bp	GLRaV-3	13814	This study
Coat protein R	CTAAACGCCTGCTGTCTAGC				14146	
GP18 18034 F	AGGCGATGAGGCACTTAGAA	52°C	414 bp	GLRaV-3	18034	Maree (not published)
GP18 18448 R	CCAAACTTTGATTGGATTTTGGC				18448	
GVA F	AGGTCCACGTTTGCTAAG	56°C	238 bp	GVA	7037	MacKenzie (1997)
GVA R	CATCGTCTGAGGTTTCTACTA				7275	
HSP-70 F	GGGGGTCAAGTGCTCTAGTT	56°C	470 bp	GLRaV-3	11052	This study
HSP-70 R	TGTCCCGGGTACCAGATTAT				11521	
LC 1	CGCTAGGGCTGTGGAAGTATT	58°C	546 bp	GLRaV-3	11557	Osman and Rowhani (2006)
LC 2	GTTGTCCCGGGTACCAGATAT				12103	
LQV1-H47	GTTACGGCCCTTTGTTTATTATGG	58°C	397 bp	GLRaV-1	9622	Osman and Rowhani (2006)
LEV1-C447	CGACCCCTTTATTGTTTGAGTATG				9996	
GLRaV-2 CP F	TATGAGTTCCAACACAAGCGTGC	58°C	681 bp	GLRaV-2	13835	Engelbrecht (not published)
GLRaV-2 CP R	ACACCGTGCTTAGTACCTCC				14497	
T7	TAATACGACTCACTATAGGG	53°C	Used for sequencing	Not applicable	Not applicable	
SP6	TACGATTTAGGTGACACTATAG		Dependant on insert size	Not applicable	Not applicable	

We performed crude virus extractions on the petiole samples by macerating these tissues in extraction buffer as described by Osman et al. 2007 (1.59g/l Na₂CO₃, 2.93g/l NaHCO₃, pH9.6 containing 2% (w/v) PVP-40, 0.2% (w/v) bovine serum albumin, 0.05% (v/v) Tween 20 and 1% (w/v) Na₂S₂O₅) at 1:20 (w/v). Final optimisation of extraction procedures however consisted of a different extraction buffer (60.5g/l Tris-HCl pH 8.2, 8g/l NaCl, 20g/l PVP 40 000, 10g/l PEG 6000, 2g/l MgCl₂·H₂O, 50ml HCl to set pH to 8.2. 0.5ml/l Tween 20 made up to 1l). Ten microlitres of this plant extract were added to 100µl of GES denaturing buffer (0.1M glycine, 0.05M NaCl, 1mM EDTA and 0.5% (v/v) Triton X-100) and incubated at 95°C for 10min to release the viral RNA from the capsid. Two microlitres of the GES homogenate was used in the final 25µl RT-PCR and quantitative real-time reverse-transcription PCR (qRT-PCR) reactions.

2.2.4 Virus detection via RT-PCR

Detection of GLRaV-3 and GVA was initially optimised with the use of conventional one-step RT-PCR methods. The GLRaV-3 coat protein primers (Table 1) were used for amplification and GLRaV-3 detection. The standard 25µl RT-PCR reaction mix was prepared (Appendix A) and the standard RT-PCR amplification cycle was used (Appendix A). Specific annealing temperatures for the GLRaV-3 coat protein primers and GVA primers are listed in Table 1.

To visualize the amplified product, agarose gel electrophoresis was performed. DNA fragment separation was performed on a 1.2% (w/v) agarose gel in 1 x TAE buffer (40mM Tris, 0.114% (v/v) acetic acid (HOAc), 1mM EDTA pH 8.0) at 120V for 30min. Ethidium bromide (0.5µg/ml) was added to the agarose gel to a final concentration of 0.01% (v/v) for ultra violet visualisation (SynGene, Multigenius Bio Imaging gel documentation system). Gene Ruler 1 kb DNA ladder (Fermentas) was used to determine the molecular size of the DNA fragments.

2.2.5 Virus detection via qRT-PCR

Initially optimised RT-PCR conditions were used to further optimise virus detection with qRT-PCR. A SensiMix™ One-Step Kit (Quantace QT205-02) was used for the one step qRT-PCR reaction. The standard 25µl qRT-PCR reaction mix was prepared (Appendix A) and standard qRT-PCR amplification cycles (Appendix A) were used

with annealing temperatures for GLRaV-3 CP primers and GVA primers as indicated in Table 1.

2.2.6 Cloning and transformation of the 332 bp GLRaV-3 CP region

In order to verify whether the correct sequence was amplified for GLRaV-3, the amplified PCR product (of CP region) was excised from the agarose gel and purified with the Wizard® SV Gel and PCR cleanup system (Promega). The purified GLRaV-3 amplified region was ligated into the pDrive cloning vector using the Qiagen PCR cloning kit. Purification and ligation procedures were performed according to the manufacturer's specifications. Chemically competent cells were prepared according to a modified method of Sambrook et al. (1989) (Appendix B).

Transformation procedures were performed according to the protocol of Sambrook et al. (1989) (Appendix B). The plasmid DNA was purified with a GeneJet Plasmid Miniprep kit (Fermentas) according to the manufacturer's specifications. The plasmid alkaline lysis mini-prep method (Sambrook et al., 1989) was used when large quantities of plasmid DNA were purified for restriction enzyme analysis. All plasmid DNA samples were screened with restriction enzyme digestion for confirmation of the appropriate size insert before sequencing. The plasmids were digested with *EcoRI* (Fermentas) according to the manufacturer's specifications.

2.2.7 Sequencing and sequence analysis of the GLRaV-3 CP region

Plasmid DNA templates were sequenced with the Applied Biosystems ABI PRISM BigDye Terminator v3.0 Ready Reaction Cycle Sequencing Kit according to the manufacturer's instructions. T7 and SP6 primers (Table 1) were used for the sequencing reaction. The sequencing reaction was performed by the Core DNA Sequencing Unit, Department of Genetics, Stellenbosch University. The sequences were analysed and edited with the use of BioEdit (version v7.0.4, Hall, 1999). Sequence similarity searches were performed using the BLAST algorithm (blastn) (Altschul et al., 1990) against the GenBank database of the National Centre for Biotechnology Information (www.ncbi.nlm.nih.gov).

2.2.8 Statistical analysis for determining minimum replicate samples

It is imperative that the qRT-PCR results for virus detection are consistent, thus ideally every sample would be tested in duplicate and the same result would be

expected for duplicate samples. During initial optimization screening, only 2 out of 168 samples didn't deliver reproducible results. The optimization screening consisted of 16 KWV samples, 34 Nietvoorbij samples (September 2008) and 118 Ernita samples. The results for the September screening are indicated in Table 2, from the nursery samples tested, only 2 samples from Ernita tested positive for GLRaV-3 infection. However, when these 2 samples were tested again, they didn't show amplification. The estimated reproducibility rate, therefore, is 98.8%. Using percentile bootstrap confidence intervals (Efron & Tibshirani 1993), it can further be stated with 95% confidence that the true rate of reproducibility lies between 97.02% and 100%, or with 99% confidence that the true rate of reproducibility lies between 96.43% and 100%.

The high levels of reproducibility are clear. However testing in duplicate is expensive. Statistical methods were used to determine the minimum number of replicate samples required in order to construct a 95% confidence interval for the reproducibility rate, subject to a less stringent sampling error than above. In symmetric confidence intervals, the sampling error is half the width of the confidence interval. For example, the confidence interval [0.2, 0.4] has a width of $0.4 - 0.2 = 0.2$ and a subsequent sampling error of $0.2/2 = 0.1$. The required sample size, n , is related to the sampling error, e , by the following equation:

$$n = \frac{(z_{(1-\frac{\alpha}{2})})^2 p_a (1 - p_a)}{e^2}$$

Equation 1

In this equation, $(z_{(1-\frac{\alpha}{2})})^2$ is a quantile from the normal distribution, where for a 95% confidence interval alpha is chosen to be 0.05 so that $(z_{(1-\frac{\alpha}{2})})^2 = 1.96$. The initial estimate of the reproducibility rate is $p_a = 166/168 = 0.988$ so that equation 1 simplifies to

$$n_2 = \frac{1.96^2 \cdot 0.988 \cdot (1 - 0.988)}{e_2^2}$$

Equation 2

As the acceptable sampling error e is made smaller, more samples n are therefore required. Figure 5 shows the relationship graphically.

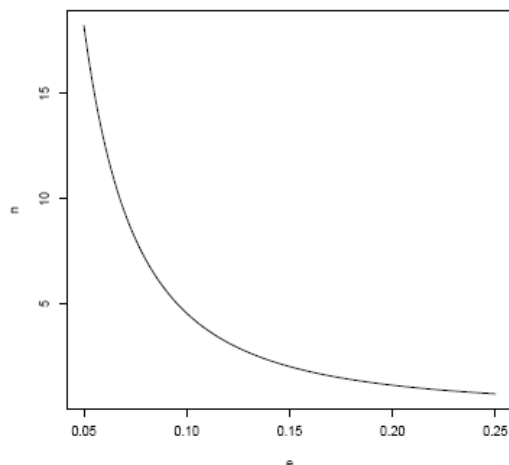


Figure 5: Required sample size n_2 as a function of sampling error e_2

It was decided that a sampling error of 0.1 was adequate. From Equation 2 this means that 5 samples should be tested in duplicate. To be prudent, however, 7 samples were tested in duplicate. This leads to the smaller sampling error of 0.08. These replicates were chosen at random to ensure reliability and repeatability. It was decided that bootstrap confidence intervals could again be calculated for the new results if necessary.

2.2.9 Virus detection via DAS-ELISA

Grapevine rootstock material from Nietvoorbij was also tested for GLRaV-3 via DAS-ELISA (GLRaV-3 DAS-ELISA kit received from Agricultural Research Council) in order to compare the results with that of the qRT-PCR with regards to sensitivity and reliability. Crude virus extraction was performed on the samples as described in 2.2.3. The DAS-ELISA protocol was performed according to the manufacturer's specifications (Appendix B).

2.2.10 PCR Amplification of potentially false ELISA positives

During the February screening date and for certain screening periods thereafter, one sample (15.2) tested positive with DAS-ELISA, but not with qRT-PCR. During the screenings in July more samples were tested positive with DAS-ELISA that did not test positive with qRT-PCR. ELISAs have the potential to yield false positive results and it was necessary to verify that these samples were not infected with GLRaV-3. We also wanted to determine if it was different grapevine leafroll associated viruses causing these results. Additional GLRaV-3 primers, HSP-70h forward and reverse,

LC1 and LC2 (Osman et al. 2007) and GP18 18034 and GP18 18448 (Table 1) were used to confirm that these samples were not infected with GLRaV-3. The particular samples (2.3, 6.2, 13.3, 15.2, and 17.3) were amplified via RT-PCR as described in 2.2.4 with the specific annealing temperatures as stated in Table 1. Sample 5.2 was included as a positive control for each of the GLRaV-3 diagnostic primer sets. No positive control material was available for GLRaV-1 and 2. The products were visualised on a 1.2 % agarose gel as previously described.

2.2.11 Cloning and transformation of the unknown sequence amplified from sample 15.2 with HSP-70h primers

The same procedures were followed as described in 2.2.7, except that the smaller than expected band (Figure 17) from sample 15.2 (amplified with LC1 and LC2 primers) was excised from the gel and purified. The transformation procedures were followed as described in Appendix B. Colony PCR was performed with the GLRaV-3 HSP-70h primers. The plasmid DNA was purified with a GeneJet Plasmid Miniprep kit (Fermentas) according to the manufacturer's specifications. The plasmids were digested with *EcoRI* (Fermentas) for confirmation of the appropriate size insert.

2.2.12 Sequencing and sequence analysis of the unknown sequence amplified from sample 15.2 with HSP-70h primers

The same procedures were followed as previously (described for the GLRaV-3 CP region) to determine the unknown origin of the potential false GLRaV-3 ELISA positive sample.

2.3 Results

2.3.1 RT-PCR detection of GLRaV-3

Initial optimisation of GLRaV-3 CP amplification was performed on grapevine scion material collected from the Stellenbosch area. Crude virus extractions were performed on the samples (petioles) and the CP region was amplified via a one step RT-PCR method. The PCR products were visualised on a 1.2% agarose gel and a band with a fragment size of 332bp was visible after UV visualization for samples infected with GLRaV-3 (Figure 6). The sequencing results were analysed on BioEdit (version v7.0.4, Hall, 1999) and submitted for BLAST analysis (blastn) that verified that the amplified product was the coat protein region of GLRaV-3.

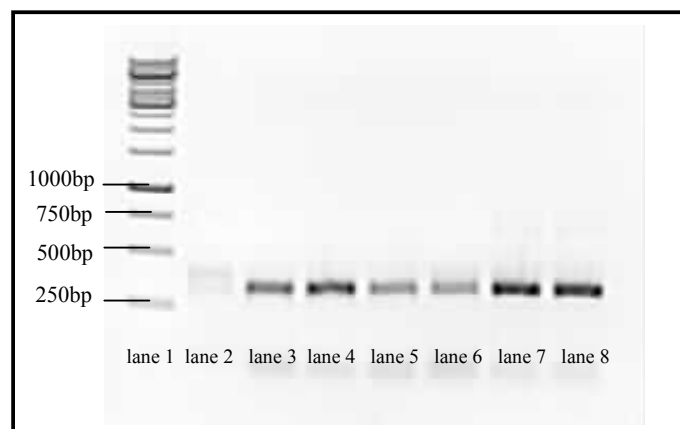


Figure 6: Agarose gel electrophoresis showing amplified GLRaV-3 coat protein region from grapevine scion material. Lane 1: 1kb DNA ladder, lane 2: GLRaV-3 negative sample, lanes 3-8: samples from our greenhouse displaying visual symptoms of GLRaV-3

2.3.2 RT-PCR detection of GVA

The procedures described in 2.3.1 were also followed for initial optimisation of GVA amplification from grapevine scion material with specific GVA primers (Table 1). A band with a fragment size of 238bp was visible after UV visualisation for samples infected with GVA (Figure 7).

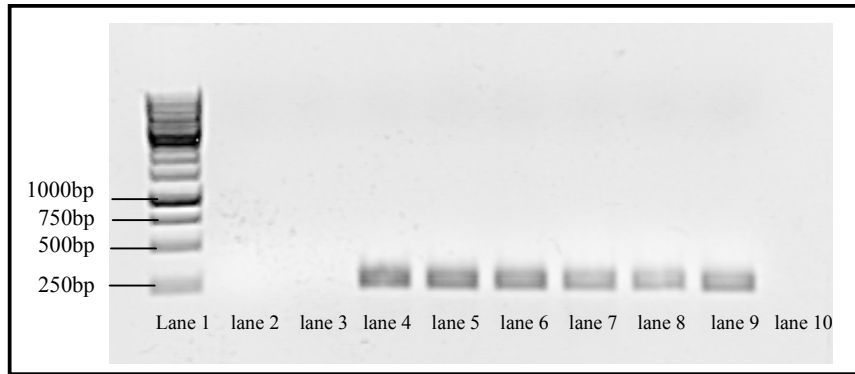


Figure 7: Agarose gel electrophoresis showing amplified product of GVA from grapevine scion material. Lane 1: 1kb DNA ladder. Lanes 2-3: Samples collected from the Stellenbosch area that tested negative for GVA infection; lanes 4-9: samples tested positive for GVA infection and lane 10: negative control

2.3.3 qRT-PCR detection of GLRaV-3

The optimised one step RT-PCR method was adapted and further optimised to enable a simple one step qRT-PCR GLRaV-3 detection protocol with the SensiMix™ One-Step qRT-PCR Kit and the RotorGene 6000 real time PCR thermal cycler. Melting curve analyses was performed to identify the amplicon and confirm virus infection (Figure 8). GLRaV-3 amplicons had a melting temperature between 82.5°C – 83.8°C. Primer dimers had a melting temperature of approximately 79°C allowing distinction between specific amplicon and primer dimers. Various aspects of the protocol were optimised, including the specific part of the plant used for extraction (leaves, petioles or phloem); the amount of crude extract added to the denaturing buffer and the amount of denatured virus extract to add to the qRT-PCR mix. These optimisation procedures were performed on scion material and applied to the rootstock material for detection of the virus.

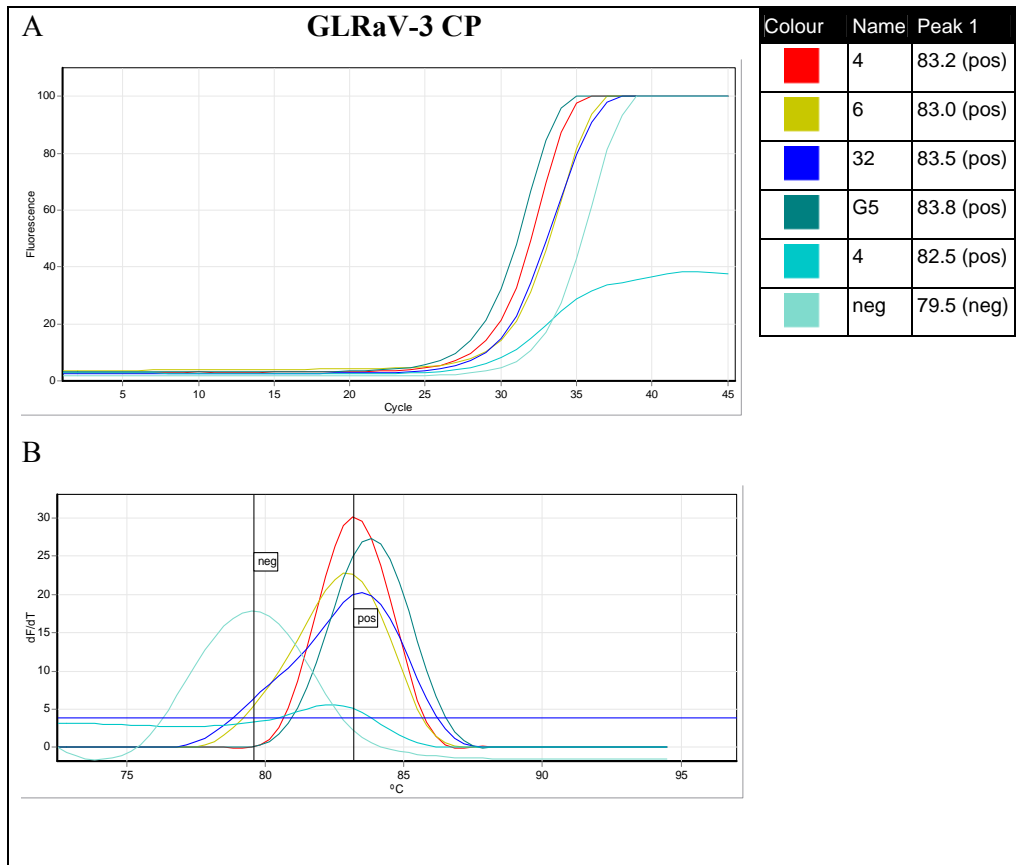


Figure 8: (A) Amplification curves for grapevine scion samples (indicated in the legend) tested via qRT-PCR for GLRaV-3 infection. (B) Melting curves (change of fluorescence vs temperature increase) for the qRT-PCR amplified samples. Samples infected with the virus had melting temperatures ranging from 82.5°C – 83.8°C. The no template control had a melting temperature of 79.5°C

2.3.4 qRT-PCR detection of GVA

The optimised one step RT-PCR method was adapted and further optimised to enable a simple one step qRT-PCR GVA detection protocol with the SensiMix™ One-Step qRT-PCR Kit as described above for GLRaV-3. Melting curve analyses were performed to identify the amplicon and confirm virus infection. GVA amplicons had a melting temperature between 82.2°C – 82.7°C. Primer dimers had a melting temperature of approximately 79°C allowing distinction between specific amplicon and primer dimers (Figure 9).

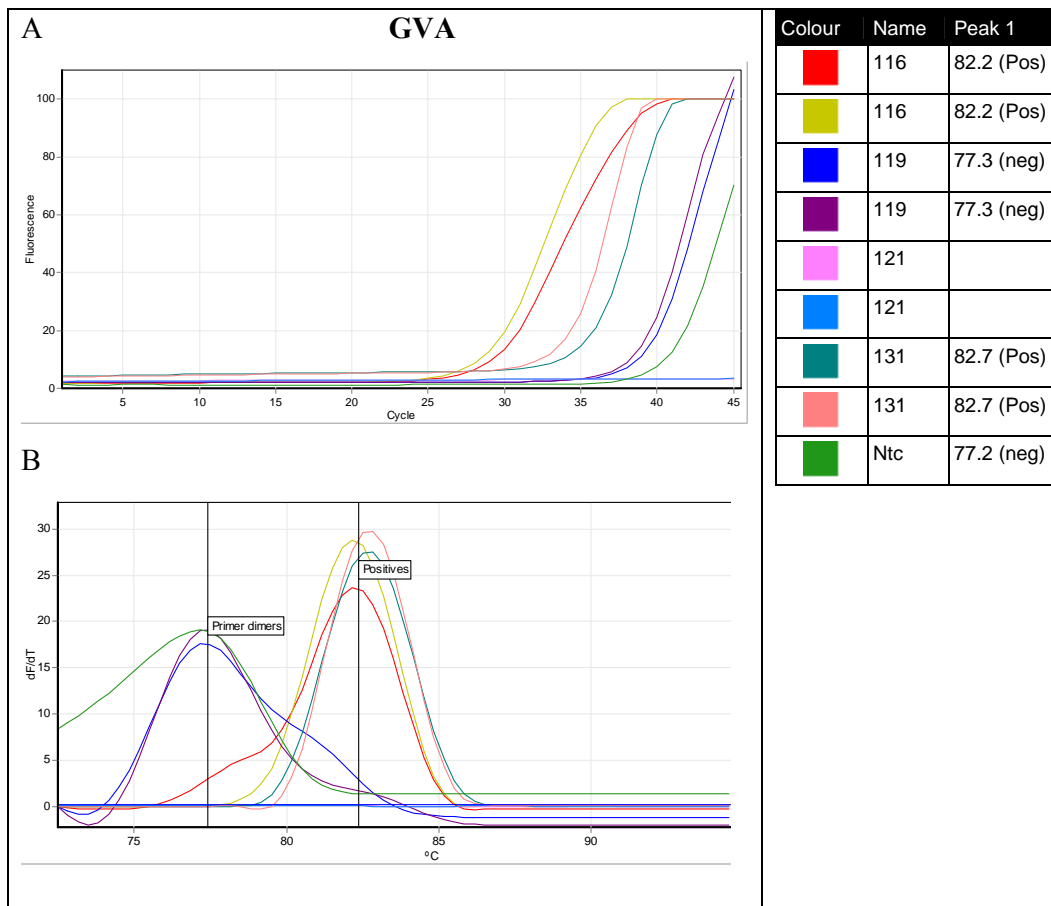


Figure 9: (A) Amplification curves for grapevine scion samples (as indicated in the legend) tested via qRT-PCR for GVA infection. (B) Melting curves for the qRT-PCR amplified samples. Samples infected with the virus had melting temperatures ranging from 82.2°C – 82.7°C. The no template control had a melting temperature of 77.2°C

2.3.5 Rootstock screening for GLRaV-3 and GVA

Two different groups of rootstock samples were used during the rootstock screening. The one group was severely infected and was screened over a period of time to observe the change in virus titre throughout the season and to compare DAS-ELISA and qRT-PCR results for these samples. These samples were collected from the Nietvoorbij farm in Stellenbosch. The other group of samples were nursery samples (KVV and Ermita nurseries) used in the industry and expected to be virus-free. These samples were used in a large scale screening to verify viral status and to compare the efficacy of the real time detection system to the ELISA results from the nurseries.

2.3.5.1 Nietvoorbij rootstock screening for GLRaV-3 with qRT-PCR and ELISA

Initial virus screening was performed in September 2008 to determine the infection status of the vines. The same samples were subsequently screened (qRT-PCR and

DAS-ELISA) from January 2009 to April 2009 at two weekly intervals, and again in July to evaluate the accumulation and ability to detect the virus in the rootstocks over time.

During the initial virus screening in September 2008, 35.3% of the samples were found to be infected with GLRaV-3. This was a relatively high incidence level and an ideal vineyard to study virus accumulation throughout the season. As the season progressed and virus prevalence increased, qRT-PCR was able to detect more GLRaV-3 infected samples (Table 2). Throughout the growing season, the percentage rootstock samples that tested positive for GLRaV-3 infection via qRT-PCR, increased from 20.6% in January (Figure 10) to 35.3% in July (Figure 11 and Figure 12). Samples collected during April were stored in a frozen state for a prolonged period. It is expected that this led to the degradation of viral nucleic acids and hence samples didn't amplify as expected as certain previously infected samples didn't amplify and most samples collected during the second screening date in April were indistinguishable on the melting curve.

During each screening, 7 samples were selected at random and were amplified in duplicate as described by the equation in 2.8.8 in order to ensure repeatability of the technique. Reproducible and repeatable results were obtained for these duplicated samples during the screening period as duplicated samples delivered identical results. The results were also consistent throughout the screening period as the same samples tested positive during consecutive screenings (excluding new additional samples that could be detected). However, during the second screening in February, sample 17.3 tested positive for GLRaV-3 infection with qRT-PCR. This sample had never tested positive previously, and did not test positive thereafter. The same samples tested positive for GLRaV-3 infection nearly a year after the initial September 2008 screening, illustrating the reproducibility of qRT-PCR.

DAS-ELISAs for these samples were only performed from the second sample date of February onwards. The percentage samples that tested positive for GLRaV-3 infection with DAS-ELISA increased from 19.11% in February to 50% in the end of July. qRT-PCR constantly detected more infected samples than DAS-ELISA throughout the screening period up to July. However, during the July screening DAS-ELISA detected more GLRaV-3 infected samples than qRT-PCR (Figure 12).

These results were further investigated with various GLRaV-3 primer sets and other GLRaV primer sets. The GLRaV-3 DAS-ELISA false positive samples and a GLRaV-3 positive control was subjected to PCR amplification with all the different GLRaV-3 primers, but no specific amplification product was visible on the agarose gels for any of the samples (Figure 13). Sample 2.3 showed amplification, but it was regarded as non specific as it was smaller than the expected amplicon. PCR with the LQV1-H47, LEV1-C447 and LR2 primers also did not show any specific amplification (Figure 13 and Figure 14). These DAS-ELISA false positive samples were then excluded and a second graph constructed to visualise the true % GLRaV-3 infection (Figure 15). A trendline was also constructed which excluded the DAS-ELISA false positive results as well as the April results to illustrate the trend of virus prevalence throughout the growing season.

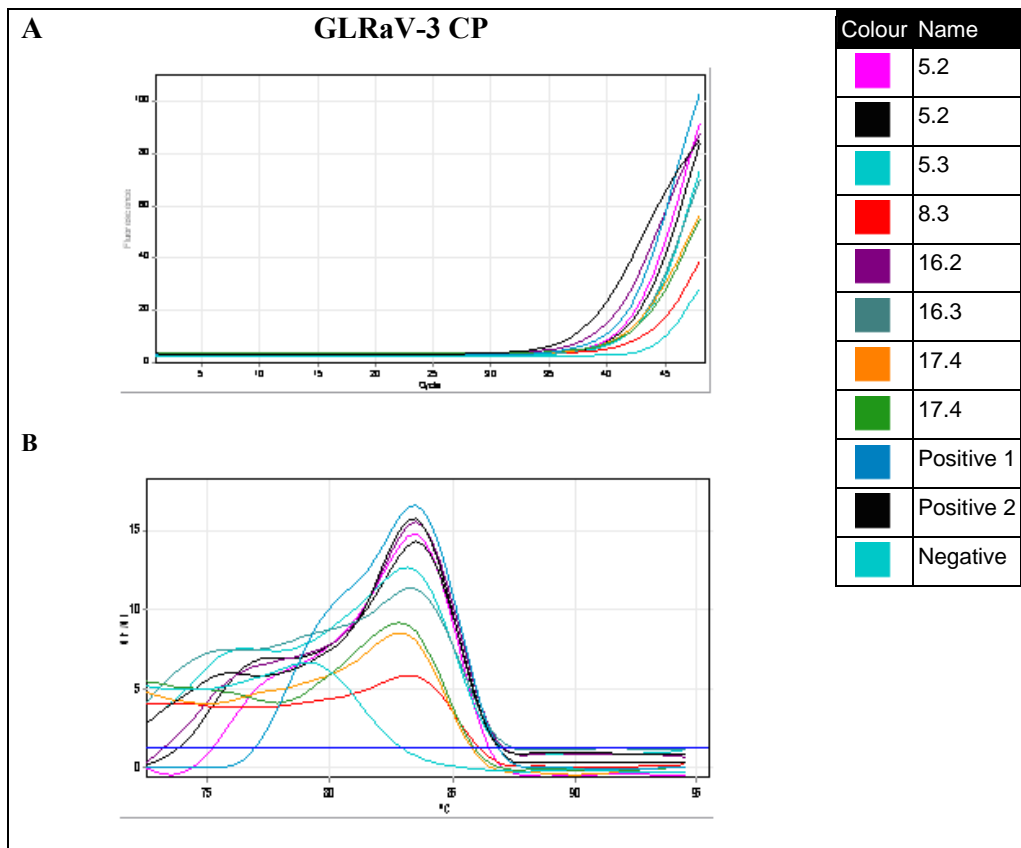


Figure 10: (A) Amplification curves for Nietvoorbij rootstock samples tested positive via qRT-PCR for GLRaV-3 infection during January. (B) Melting curves for the amplified samples to identify samples infected with GLRaV-3. Samples 1.2, 2.2, 2.3, 3.2, 3.3, 4.2, 4.3, .2, 6.3, 7.2, 7.3, 8.2, 9.2, 9.3, 10.2, 10.3, 11.2, 11.3, 12.2, 12.3, 13.2, 13.3, 14.2, 14.3, 15.2, 15.3, 17.2, 17.3 is not indicated on the graph as they did not test positive for GLRaV-3 infection (see Appendix D for graphs with all samples indicated).

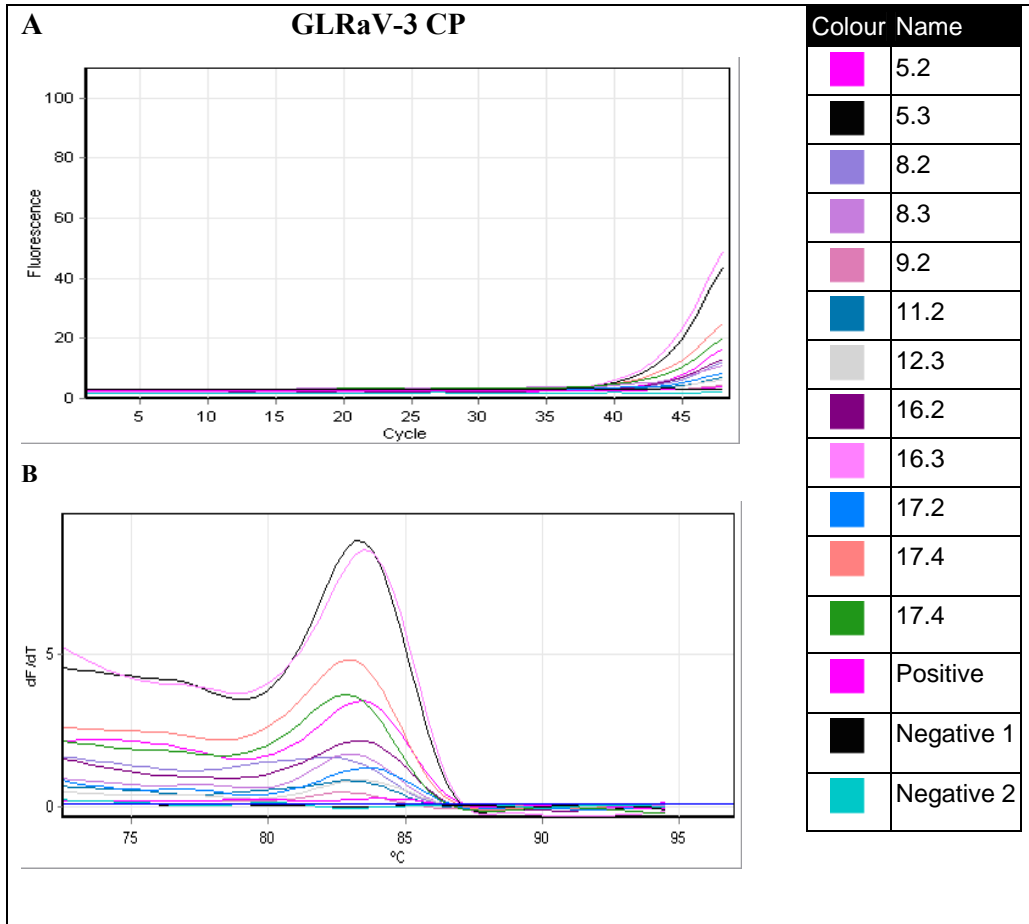


Figure 11: (A) Amplification curves for Nietvoorbij rootstock samples tested positive via qRT-PCR for GLRaV-3 infection at the end of July. (B) Melting curves for the amplified samples to identify samples infected with GLRaV-3. Samples 1.2, 2.2, 2.3, 3.2, 3.3, 4.2, 4.3, .2, 6.3, 7.2, 7.3, 9.3, 10.2, 10.3, 11.3, 12.2, 13.2, 13.3, 14.2, 14.3, 15.2, 15.3, 17.3 is not indicated on the graph as they did not test positive for GLRaV-3 infection (see Appendix D for graphs with all samples indicated).

Table 2: Results for 34 Nietvoorbij rootstock samples tested for GLRaV-3 infection TESTED VIA Qrt-pcr (√) and DAS-ELISA (X) in September 2008 (initial screening) and throughout the growing season in 2009 from January to July. Marks indicate samples that tested positive during that screening period (April 2 was excluded as positives and negatives were indistinguishable).

Sample	Sept '08	Jan	Feb 1	Feb 2	March 1	March 2	April 1	April 3	July 1	July 2
1.2										
2.2										
2.3										X
3.2										
3.3										
4.2										
4.3										
5.2	√	√	√	√ X	√ X	√ X	√ X	√ X	√ X	√ X
5.3	√	√	√	√ X	√ X	√ X	√ X	√ X	√ X	√ X
6.2									X	X
6.3										
7.2										
7.3										
8.2	√	√	√	√	√	√	√	√ X	√ X	√ X
8.3	√	√	√	√ X	√ X	√ X	√ X	√ X	√ X	√ X
9.2	√					√			√	√ X
9.3										
10.2										
10.3										
11.2	√		√		√	√	√		√ X	√ X
11.3										
12.2	√									√ X
12.3	√								√ X	√ X
13.2										
13.3										X
14.2										
14.3										
15.2					X	X	X		X	X
15.3										
16.2	√	√	√	√ X	√ X	√ X	√ X	√ X	√ X	√ X
16.3	√	√	√	√ X	√ X	√ X	√ X	√ X	√ X	√ X
17.2	√			√ X	√ X	√ X	√ X	√ X	√ X	√ X
17.3				√						X
17.4	√	√	√	√ X	√ X	√ X	√ X	√ X	√ X	√ X

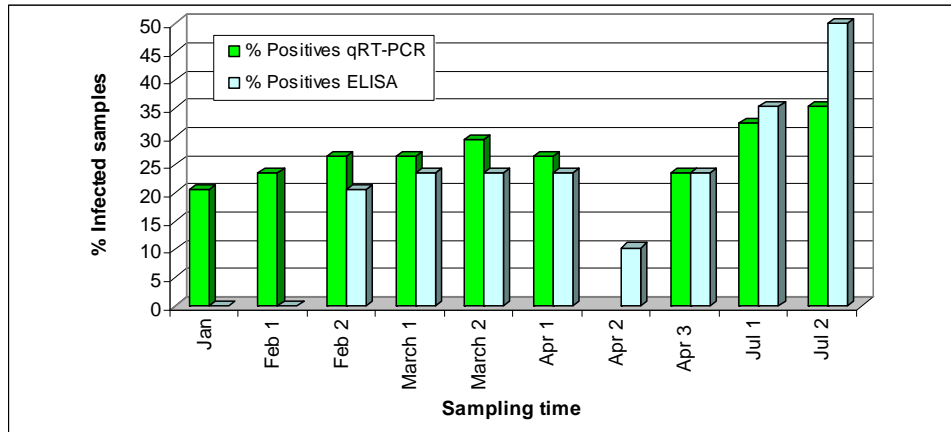


Figure 12: Percentage GLRaV-3 infected samples tested via qRT-PCR and ELISA from January 2009 – July 2009 in Nietvoorbij rootstock samples (ELISA false positives included). Numbers 1, 2 and 3 followed by the month indicate the first, second or third sampling dates for that month.

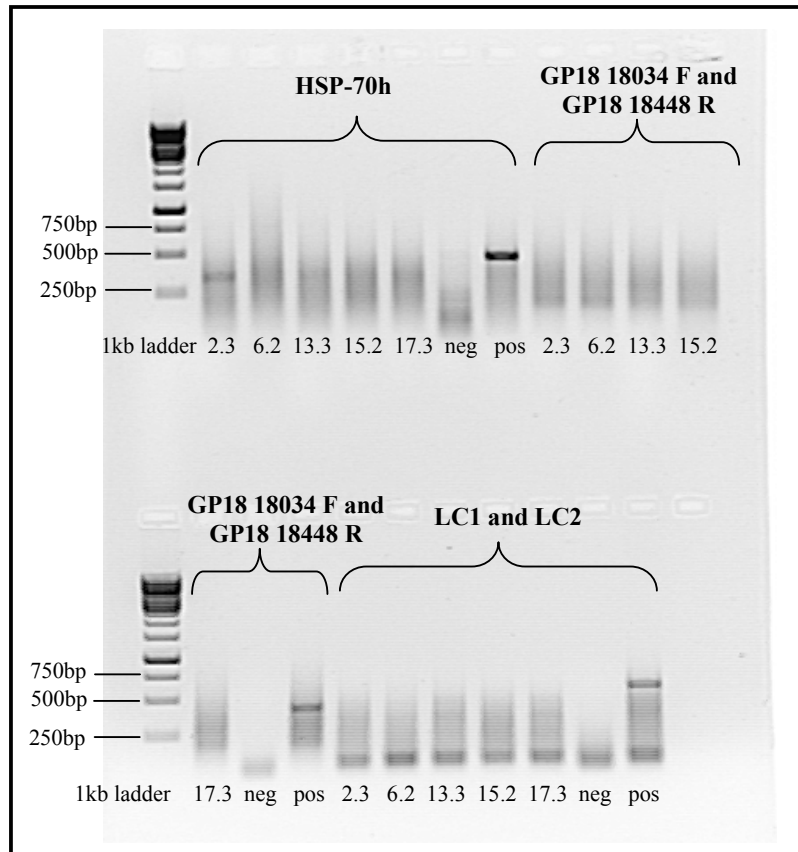


Figure 13: ELISA false positive samples tested with various GLRaV-3 primers. Negative (neg) and positive (pos) controls were included

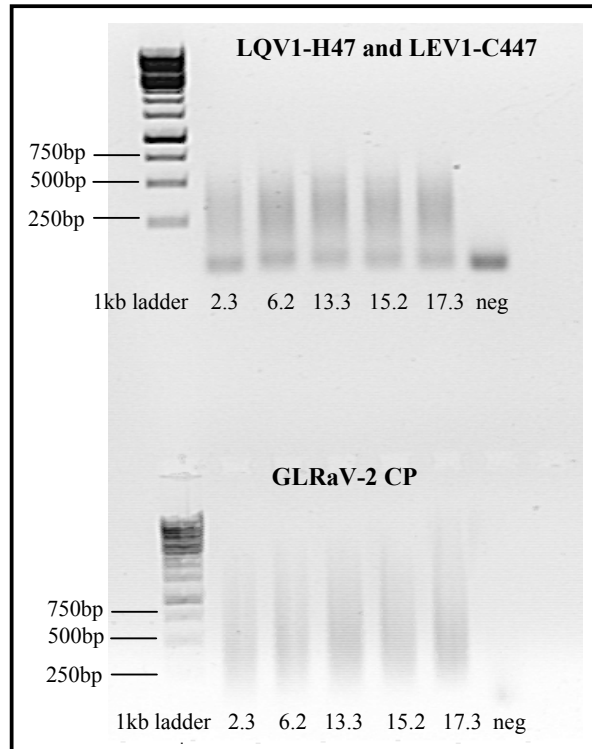


Figure 14: ELISA false positive samples tested with GLRaV-1 and 2 primers. Negative (neg) no template controls were included. LQV1-H47 and LEV1-C447 primers were used for GRaV-1 detection and LR2 forward and reverse primers were used for GLRaV-2 amplification

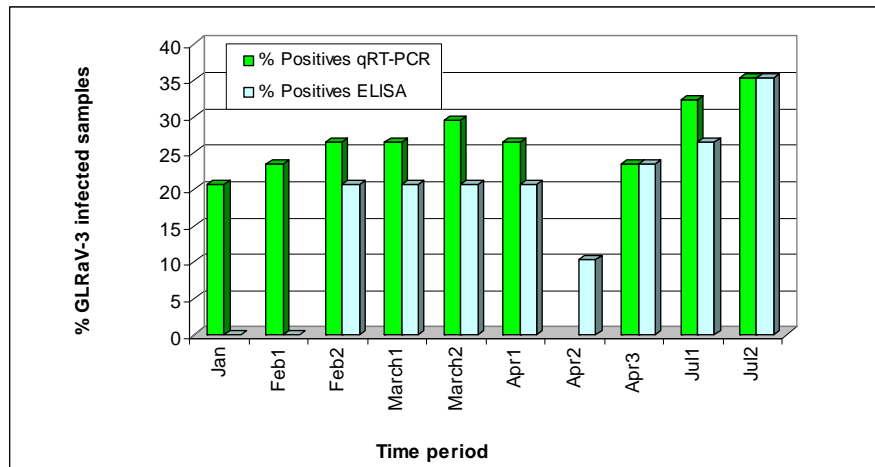


Figure 15: Percentage GLRaV-3 infected samples tested via qRT-PCR and ELISA from January 2009 – July 2009 in Nietvoorbij rootstock samples (ELISA false positives excluded)

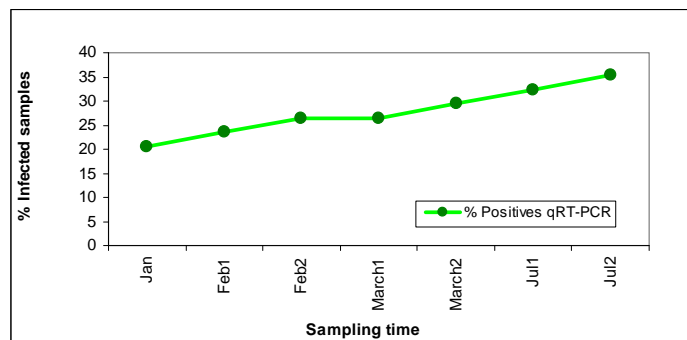


Figure 16: Percentage GLRaV-3 infected samples tested via qRT-PCR from January 2009 – July 2009 in Nietvoorbij rootstock samples (degraded April samples excluded)

Sample 15.2 consistently tested positive for GLRaV-3 with DAS-ELISA from February 2009, but not with qRT-PCR. Further PCR analyses with various GLRaV-3 diagnostic primers revealed that it was not infected with GLRaV-3. Additional PCRs were performed in order to determine if the sample was infected with another leafroll associated virus. GLRaV's -1, 2, 3, 5 and 9 were tested for in this sample (Figure 17).

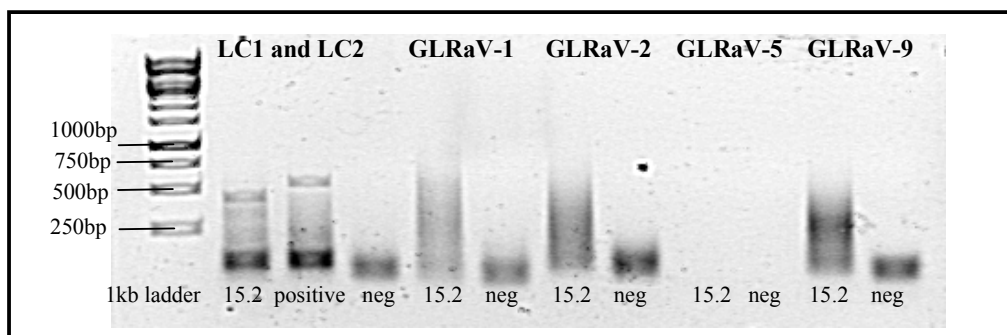


Figure 17: ELISA positive sample (15.2) tested with different GLRaV primers

From all the primer pairs tested, only the LC1 and LC2 primers (Osman et al 2007) showed clear amplification. However, the size of the amplicon for sample 15.2 was smaller than the expected size of 546bp as seen with the positive control (Figure 17). No positive controls for GLRaV-1, 2, 5 and 9 were available. The fragment was extracted from the agarose gel, purified and sequenced. The sequence was found to be of *Vitis vinifera* origin. It is important to note that this specific ELISA kit, used by the industry, could potentially pick up another virus or plant protein that could lead to false positive results.

2.3.5.2 Rootstock screening for GVA with qRT-PCR

The same Nietvoorbij samples that were tested for GLRaV-3 were also subjected to screening for GVA infection. These samples were only tested for GVA infection via qRT-PCR, partly for economic reasons and because most South African nurseries only test for GLRaV-3 via DAS-ELISA. Throughout the growing season (January 2009 – July 2009), variable percentages of GVA infection was detected in the rootstock samples (Table 3 and Figure 18) and no definite correlation could be drawn between virus detectability and the time of the growth season. The sampling periods during which the highest percentage of virus could be detected were the beginning of April and end of July (Figure 18 and Figure 19). The reproducibility of the results was also poor, as different samples would test positive for GVA at different times and little consistency was observed (Table 3).

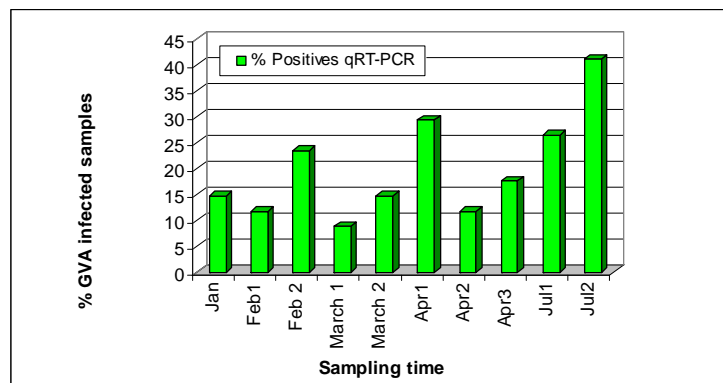
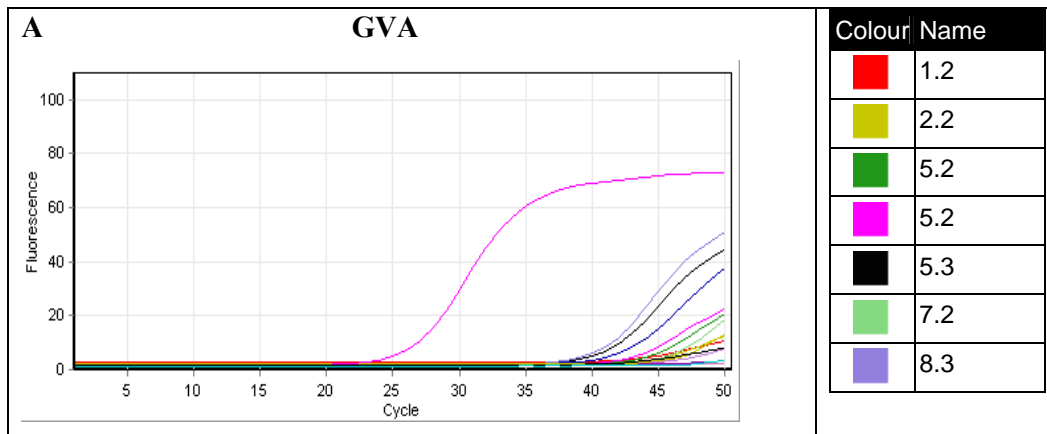


Figure 18: Percentage GVA infected samples tested via qRT-PCR from January 2009 – May 2009 in Nietvoorbij rootstock samples

Table 3: Results for 34 Nietvoorbij rootstock samples tested for GVA infection via qRT-PCR in September 2008 (initial screening) and throughout the growing season in 2009 from January to July. Marks indicate samples that tested positive during that screening period

Sample	Sept '08	Jan	Feb 1	Feb 2	March 1	March 2	April 1	April 2	April 3	July 1	July 2
1.2							√				√
2.2	√						√				
2.3											
3.2	√										√
3.3	√										
4.2	√										
4.3											
5.2	√	√	√	√	√	√	√	√	√	√	√
5.3	√	√	√	√	√	√	√	√	√	√	√
6.2											
6.3										√	
7.2	√						√				
7.3	√										
8.2	√										
8.3	√	√	√	√	√	√	√	√	√		√
9.2	√						√			√	√
9.3											√
10.2	√									√	√
10.3	√									√	√
11.2	√										
11.3	√									√	
12.2	√	√	√	√		√	√		√	√	√
12.3	√	√		√		√	√	√	√	√	√
13.2	√										√
13.3											
14.2											
14.3											√
15.2											
15.3					√		√		√		
16.2					√						
16.3											
17.2											
17.3					√						
17.4											√



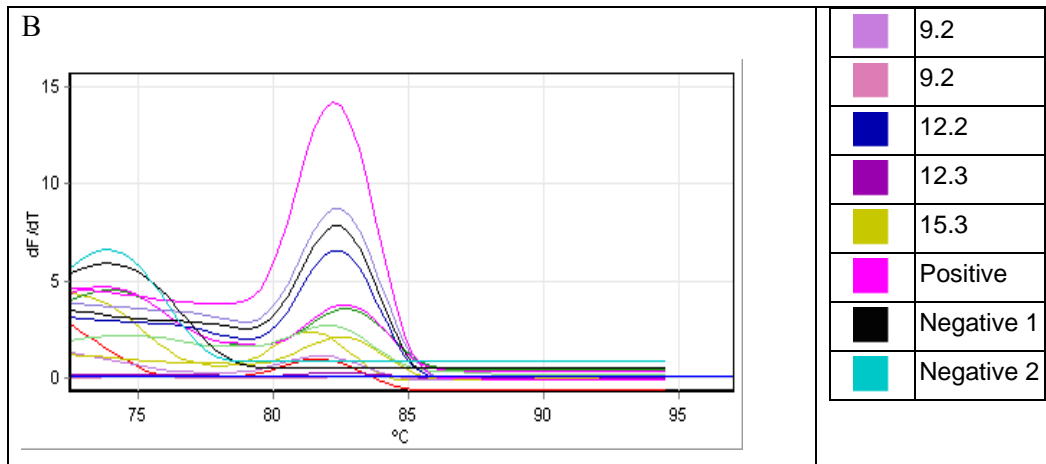


Figure 19: (A) Amplification curves for Nietvoorbij rootstock samples tested positive via qRT-PCR for GVA infection at the end of July. (B) Melting curves for the amplified samples to identify samples infected with GVA. Samples 2.3, 3.2, 3.3, 4.2, 4.3, 6.2, 6.3, 7.3, 8.2, 9.3, 13.2, 13.3, 14.2, 14.3, 15.2, 16.2, 16.3, 17.2, 17.3, 17.4 are not indicated in the graph as these samples tested negative (see Appendix D for graphs with all samples indicated)

2.3.6 Nursery rootstock screening for GLRaV-3

Rootstock samples from KWV and Ernita nurseries were tested for GLRaV-3 by qRT-PCR. As this material is propagated and distributed to wine farms around South Africa, it is expected that these samples should be virus free.

We received 18 samples from KWV in 2008. Our results showed none of the samples to be infected with GLRaV-3 using qRT-PCR. Our qRT-PCR results correlated with their ELISA results for these samples. During 2008 we also received 116 samples from Ernita nursery that we tested for GLRaV-3. Two of these samples delivered a weak positive result as seen in the high Ct values, typical of low virus titres present in the rootstock. Once again their ELISA results correlated with that of our qRT-PCR results.

In 2009 we received a further 200 samples from Ernita nursery. We detected GLRaV-3 in one of the samples, which was a sample from a neighbouring farm and included as positive control. Their ELISA test also detected this sample positive for GLRaV-3 infection. Once again their ELISA results correlated with our qRT-PCR results.

2.4 Discussion

The optimised one step RT-PCR amplification of the respective regions of GLRaV-3 and GVA was easily transformed into a one step qRT-PCR reaction, with minor alterations to the annealing temperature and the addition of a melt step at the end of the amplification. SYBR Green (SG) was used as a double stranded DNA binding dye in the qRT-PCR reaction. SG is more economical than the probe-based systems and is furthermore believed to produce fewer false negative results compared to probe-based systems (Papin et al. 2004). This is due to the fact that minor sequence changes inside the probe target sequence could prevent the binding of the probe and subsequent amplification of the amplicon (as shown for the West Nile virus by Papin et al. 2004).

After initial confirmation, with agarose gel electrophoresis, that the correct amplicon was amplified, no further post PCR processing was necessary with qRT-PCR. This reduced the risk of contamination, but also the time required before infected samples could be identified. With qRT-PCR, amplification of PCR product can be viewed in real time, which enables an operator to edit the reaction cycle at any point. The melting curve provides an effective visual means of discriminating between specific amplified product and non specific amplification. One of the main advantages of qRT-PCR is its higher sensitivity which is due to the incorporation of fluorescent dyes which are much more sensitive than ethidium bromide staining on an agarose gel. This also decreases the post PCR processing and lowers the chances of contamination.

Samples infected with GLRaV-3 could clearly be distinguished by a distinct peak on the melting curve at 82.5°C – 83.8°C. The samples collected during April were stored in a frozen state for prolonged periods. This could have resulted in the degradation of viral nucleic acid and could explain why they did not amplify as expected. Those poorly amplified results skewed the expected general trend (increase in virus detection as the season progresses) (Figure 12). Melting curve analysis of samples collected during the second sample date of April delivered melting peaks that were indistinguishable and those results could not be used. We excluded the April results in further discussions. Two extra sample dates were added at the beginning

and end of July to compensate for these results and to better distinguish the general trend in the change of virus titre with the change in season (Figure 16).

qRT-PCR results showed an increase in GLRaV-3 prevalence as the season progressed from January to July (Figure 16). This is in accordance with what has previously been shown by Charles et al. (2006). The Ct values observed were however higher for the samples collected later in the season, which was not expected, considering that the prevalence of the virus was expected to be higher later in the season. The samples tested during July were phloem material as leaf material used during the early season was not available. The possible higher level of polyphenolic compounds in the phloem material could have inhibited the qRT-PCR reaction. The optimum time for GLRaV-3 screening via qRT-PCR is thus later in the season closer to the end of July. However, extraction protocols from bark material and subsequent elimination of inhibiting factors should be explored in order to optimise the amplification of the virus.

qRT-PCR delivered reproducible results throughout the screening process. However, during the second screening in February sample 17.3 tested positive with qRT-PCR; this sample had never tested positive previously, and did not test positive thereafter. This sample grows between two infected samples and the vines grew very dense which could easily have resulted in miss-sampling and could explain this unexpected result.

qRT-PCR proved to be more sensitive than DAS-ELISA in detecting GLRaV-3 throughout the season up to July. The highest percentage of infected samples detected by both qRT-PCR and DAS-ELISA was at the end of July. During the end of July DAS-ELISA detected more GLRaV-3 infected samples than qRT-PCR. However, further analysis indicated that several of those samples were false GLRaV-3 positives (Figure 13 and Figure 14). With those false positive samples excluded, qRT-PCR and ELISA detected the same number of infected samples at the end of July. These results indicate that the best time for GLRaV-3 detection is July to September. It is also evident that qRT-PCR proved to be the better system in accurate and effective GLRaV-3 detection. It is unclear what caused the positive results in those GLRaV-3 false positive samples. It is important to note that the DAS-ELISA test is being utilized by the industry and the test could detect false GLRaV-3

positives, which could be leading to unnecessary expenses to the industry if uninfected plants are discarded.

In virus diagnostics it is essential that the detection system is reproducible, repeatable, sensitive and accurate. From the results it is apparent that qRT-PCR was reproducible as exactly the same samples were found to be infected with GLRaV-3 in September 2008 and in July 2009. With the comparable amplification plots of samples amplified in duplicate, the repeatability of the qRT-PCR technique was proven for GLRaV-3. The samples that tested positive for GLRaV-3 via qRT-PCR were amplified with primers specifically designed for all known GLRaV-3 variants (Appendix C). These primers amplified a specific GLRaV-3 CP region, which was distinguishable with definite melting temperatures with qRT-PCR. The qRT-PCR technique was consistently more sensitive in detecting GLRaV-3 infected samples, proving to be the more sensitive system (excluding the second screening date in July where they detected the same number of samples) (Figure 15). The fact that exactly the same samples tested positive for 2 consecutive years with qRT-PCR, also demonstrates the accuracy of the technique. Moreover, when compared to the DAS-ELISA's false positive results, qRT-PCR proved to be the more accurate detection system for sensitive GLRaV-3 detection in grapevine rootstock material.

During the initial screening of the Nietvoorbij vineyards during September 2008, 55.9% of the samples were infected with GVA. Throughout the screening period in 2009, no definite trend in virus detection ability was evident. The reproducibility of the results was poor as different samples tested positive for GVA at different times. There was no definite correlation between seasonal variation and virus titre, but it seems as if more samples were tested positive later in the season, from July to September (Figure 18). Only a few samples tested positive for GVA infection in the second screening date in April, however it could not be concluded if this was due to the degradation of viral nucleic acids as seen with GLRaV-3 or just the overall inconsistency of the GVA virus to be detected. PCR conditions (with regards to MgCl₂, primer concentrations and starting material) and cycles were optimised for GVA detection; however this did not improve the overall results for GVA detection. The heterogeneous nature of the GVA genome and subsequent difficulty of sensitive primer design were the main contributors of these results.

The primers used for the rootstock screening of GVA, were designed by MacKenzie (1997) to detect all GVA variants. The reported sequence variability for GVA (Dovas and Katis 2003) and the heterogenous nature of the genome, complicates the design of universal primers for the detection of all 3 variants. Goszczynski and Jooste (2003) found that it is quite common for South African grapevine to have mixed infections of the divergent variants of GVA. This could also contribute to the problem of designing sensitive primers for GVA detection.

A recent study also indicated that a high prevalence of molecular group III (GTR1-1 and P163-1 isolates) and GTG11-1 isolate of group I to be present in a severely infected vineyard in Stellenbosch. Alignment of these sequences and subsequent analysis of the primers used in this study (Appendix C), revealed that the primers were more specific for the GTG11-1 isolate than the isolates of group II. All of these factors could have contributed to the lack of reproducibility for GVA detection in grapevine. Specific GVA isolates which are more prevalent in South Africa should be studied thoroughly and any new sequence variants should be incorporated to design more sensitive and accurate primers for GVA detection in grapevine. Different regions of the GVA genome can also be studied to identify highly conserved regions for the design of more sensitive primers.

From all the samples that we received from the KWV nursery in 2008, none of the samples tested positive for GLRaV-3 infection and the qRT-PCR results correlated with their DAS-ELISA results. We also received 116 samples from Ernita nursery (2008) that was tested for GLRaV-3 by qRT-PCR. Their DAS-ELISA results correlated with the qRT-PCR results and showed no GLRaV-3 infection in their rootstock material. For the large screening in 2009, all Ernita samples were again found to be free of any GLRaV-3 infection, indicating a healthy phytosanitary status of the nursery (with regards to GLRaV-3). Once again both systems (qRT-PCR and DAS-ELISA) were able to detect the positive control.

The same crude virus extraction protocol performed at the nurseries was used for the extractions of the Nietvoorbij and nursery samples. This method is much more time effective than RNA extractions. However, using extracted RNA rather than crude virus extractions from the grapevine, leads to more sensitive qRT-PCR detection of the virus (Osman and Rowhani, 2008). More time effective RNA extraction

protocols could be investigated and utilised to increase the sensitivity of the qRT-PCR system even further. This can be used on smaller sample groups, samples at a greater risk of infection or as a spot check to verify the results from the crude extractions.

From these results we can deduce that the specific nursery samples supplied to us were propagation material is of a high phytosanitary standard, with no virus (GLRaV-3) infection. The qRT-PCR and DAS-ELISA results correlated with regards to these samples and both were able to detect the positive controls. The time of sampling for the Ernita samples was in June. From our seasonal virus screening, an increase in virus detection was observed from the beginning of January to the end of July. The sampling time of the nurseries could perhaps be rescheduled for a later date to enable optimal virus detection. Additionally, the sampling procedure, whereby about 10 rootstock samples are pooled and the combined sample is tested, might hinder the detection of the already very low virus concentrations. A different approach should be investigated whereby samples growing close to neighbouring vines or next to other material (generally samples at greater risk of infection) should be more thoroughly screened (individually). A combined approach can also be followed whereby qRT-PCR is used to test individual samples at risk and ELISA to screen the pooled masses, in order to optimise virus detection cost effectively.

The major objective of the study was to improve the sensitivity of GLRaV-3 detection in propagation material. The virus is economically important due to its disease inducing capabilities and its detection is especially important in symptomless rootstocks used as propagation material. qRT-PCR was shown to be more sensitive, accurate and time effective than DAS-ELISA for the detection of GLRaV-3 in grapevine rootstock material. qRT-PCR also proved to deliver repeatable and reproducible results for GLRaV-3 detection over a time span of about a year. The qRT-PCR system can effectively be utilized as a high throughput screening tool for sensitive virus detection in grapevine and grapevine rootstock material.

Chapter 3

3. Investigation of real time PCR for application in transgenic plant analysis

3.1 Literature Review

An additional approach for the control of viral diseases is through the genetic transformation of plants in order to confer viral resistance. This chapter gives an overview of genetic transformation and pathogen-derived resistance. The chapter concludes with a thorough discussion of the different techniques used to characterise genetically transformed plants, in terms of copy number and expression levels of the transgene.

3.1.1 Introduction

Genetic transformation of plants is an important experimental tool in many aspects of plant biology (Toplak et al. 2004). Genetic engineering of crop plants is not only exploited to study plant physiology, but is also effectively employed by industry to obtain commercial crops with improved agronomic characters (Mason et al. 2002) and serves as a mechanism to control fungal, bacterial, viral and insect pathogens (Vivier and Pretorius et al. 2000).

3.1.2 Pathogen derived resistance

As single genes can confer disease resistance to plants, the current approach is that of single gene transformations into plant genomes to bring about enhanced disease tolerance. Various approaches exist to improve disease tolerance in plants but most of them make use of some part of the natural interaction between host and pathogen. One of the main approaches of manipulated disease tolerance in grapevine relies on pathogen-derived resistance and its various applications. By using a pathogen-derived gene and expressing its encoding product at an inappropriate time or in an incorrect form or amount during the infection cycle, the pathogen is prevented from continuing its infection (Sanford and Johnston et al. 1985).

3.1.3 Analysis of transgenic plants

Molecular characterization is essential once new transgenic plants have been obtained. DNA is randomly inserted into the plant genome during *Agrobacterium* transformation procedures. This often leads to the generation of plants that can have multiple transgene copies integrated into one or more chromosomal locations. The number of transgene copies in transgenic plants can influence the level of expression and the genetic stability of the target gene (Weng et al. 2004). It is thus important to analyse primary transformants in order to determine the transgene copy number. Single or low copy transformation events confers stability over several generations of successive breeding (Assem and Hassan 2008). Due to variation that might exist between independent transgenic lines produced under identical conditions, it is imperative to also assess the mRNA expression levels of the transgene for each transgenic line as expression levels are dependant on insertion site and transgene copy numbers (Toplak et al. 2004).

3.1.4 Transgene copy number determination

3.1.4.1 Southern Blot Analysis

A classic molecular method for transgene copy number determination is Southern blot analysis. During this procedure DNA fragments are transferred from an electrophoresis gel to a membrane. This results in the immobilization of the DNA fragments, and the membrane thus carries a semi-permanent replica of the gel's banding pattern. After immobilization, the DNA can be subjected to hybridization analysis, enabling the identification of bands with sequence similarity to a labelled probe (Brown 1999). It provides an indication of the number of integrated copies; however the procedure is laborious, time-consuming, requires large amounts of plant material and may also involve the use of harmful radioisotopes (Weng et al. 2004). Furthermore, it is possible that certain lines may contain rearranged transgenes. Mason et al. (2002) showed that such rearrangements are not the exception, but happen more often than is usually recognised. Such changes could still be detected by qPCR but would not always be detected by performing a single Southern blot analysis (Mason et al. 2002). This provides difficulty for accurate Southern analysis and the copy number estimates may be inaccurate.

3.1.4.2 PCR based techniques

In the study of transgenic plants, conventional PCR has also been employed, where the analysis is performed on PCR products in a plateau phase. However this method is more qualitative than quantitative as it is only capable of end point analysis. Various approaches have been attempted to produce a PCR based method with more quantitative abilities, like the semi quantitative competitive PCR. In 1991 a PCR system was created that enabled researchers to monitor PCR product amplification and accumulation in real time. Since then the method has been improved and the chemistry and instruments have been further developed into the real time PCR systems in use today (Toplak et al. 2004).

Quantitative Real-time PCR (qPCR) has proven to be a powerful tool to accurately determine transgene copy number in transgenic organisms. Advantages of this technique include a large dynamic quantification range, no post-PCR processing (thus reducing the risk of carryover contamination), small amounts of starting material required, and high-throughput capacity (Weng et al. 2004). However, preliminary standardizing and optimization is required for this technique (Savazzini et al. 2005). Accurate qPCR and qRT-PCR reactions depend on high quality starting material and validated stable reference genes for normalization of data. These reference genes impact on the results generated for determining copy number and expression levels of the transgene and should therefore be thoroughly evaluated before use. However, few statistically validated reference genes have been reported in grapevine (Reid et al. 2006).

qPCR produces large quantities of numerical data which is generally analyzed by software tools provided with the PCR thermal cyclers. Unknown samples are quantified either relatively or absolutely by comparing them to calibrator samples. Absolute quantification quantifies the input copy number by directly relating it to a standard curve. Relative quantification relates the PCR signal of the gene of interest sequence in a transformed group to that of a reference gene (Livak and Schmittgen 2001). When performing relative quantification various methods can be followed, including the two standard curve method, comparative delta delta Ct (Ramakers et al. 2003) and Relative Expression Software Tool (REST) (Pfaffl 2001).

The two standard curve method requires standard curves for both the gene of interest and the reference gene. The copy numbers of the gene of interest and reference gene for each sample are determined from their respective standard curves. The difference in amplification efficiencies for the two genes is therefore not important in the calculation. For samples amplified in duplicate or triplicate the equation below describes the calculation. Copy number (ratio) = mean copy number of gene of interest / mean copy number of reference gene. These values can then be normalised to a chosen calibrator sample.

For the comparative quantitation or comparative delta delta Ct method the amount of gene of interest X in sample S is normalized to an endogenous reference gene R and related to a calibrator sample C and is calculated as $2^{\{-(Ct^{X,S} - Ct^{R,S}) - (Ct^{X,C} - Ct^{R,C})\}}$ = $2^{-\Delta\Delta Ct}$, resulting in the fold difference between sample and control. This method assumes amplification efficiency is equal to 1, or 100% for the gene of interest and the reference amplicon (Ramakers et al. 2003).

Some of the above methods are based on the assumption that equal amplification efficiencies exists between the target genes and standard DNA or reference genes, as well as constant amplification efficiency throughout the PCR reaction. However, this is often not the case in practical applications and it is believed to lead to biased results. However, the two standard curve method and REST doesn't require equal amplification efficiencies. To evade the amplification efficiency problem, numerous new mathematical models have also been developed for real time PCR data analyses (Feng et al. 2008).

Mason et al. (2002) developed a rapid and reliable method for the estimation of the number of integrated transgene copies in transformed tomato plants with the use of qPCR with TaqMan probes. This method is not dependent on identical amplification efficiencies and requires no preliminary information about the calibrator. The model is thus ideal for those reactions where further optimization or identical reaction efficiencies are unattainable. They also found that the quality of the information produced by the real time PCR was higher than that obtained by Southern blot analysis (Mason et al. 2002).

Savazzini et al. (2005) also effectively utilised qPCR as a tool for accurate estimation of transgene integration. They used both TaqMan probes and SYBR Green dye and compared their results to Southern blot data. Their results indicated that TaqMan probes were more specific and stable in such qPCR assays. They emphasised the importance of preliminary standardisation especially for SYBR Green.

qPCR with SYBR Green can effectively be utilised to determine copy numbers, as shown by Song et al. (2002) in transgenic maize callus and plants. Southern blot analysis was also performed to correlate the results to that of the qPCR. The results indicated a significant correlation between the two methods. Furthermore, they also established that low copy numbers can be identified very early in the transformation process, thereby enabling more focus on resources for tissue bulk-up and plant regeneration.

Hernández et al. (2004) evaluated the efficacy of Taq Man, SYBR Green and Amplifluor™ technologies for the detection and quantification of a transgenic maize event GA21. From their results it was apparent that all three methods were specific, reliable and very sensitive for identification and quantification of GA21 DNA. A similar finding was made by Andersen et al. (2006) when they compared the performance of TaqMan, MGB (minor groove binding probes), Molecular beacon and SYBR Green-based detection assays in the context of genetically modified organisms. They found that the chemistries were equally sensitive, except for molecular beacon which showed lower efficiency and also seemed to be more sensitive to alteration in experimental setup. Thus SYBR Green can be effectively used for accurate quantification of exogenous DNA.

3.1.5 Transgene expression level determination

3.1.5.1 Northern Blot Analyses

In order to broaden our understanding of how the information in the genome is utilized by the cellular machinery, it is essential to closely examine gene expression (Yun et al. 2006). Once successful integration of the transgene is confirmed, it is also important to establish whether and at what level the transgene is being expressed. Northern blot analyses are routinely used for the analyses of transgene expression. It is possible to obtain semi quantitative results by creating a dilution series and varying

the exposure time during the detection step. However, as with Southern blot analyses, these analyses takes several days to complete and could include the use of harmful radioisotopes (Toplak et al. 2004).

3.1.5.2 PCR based techniques

Northern blot analysis and semi-quantitative RT-PCR methods for determining RNA transcript levels are only semi-quantitative and therefore a more reliable and higher throughput screening method is required. This method should parallel the advancing developments for the efficient characterization and selection of appropriate transgenic lines (Toplak et al. 2004). PCR has become the standard technology for gene expression profiling for the accurate quantification of nucleic acids. For an exact quantitative measurement of low quantity mRNA, real-time quantitative reverse-transcription PCR (qRT-PCR) is the method of choice (Czechowski et al. 2004). Relative quantification determines the changes in steady-state mRNA levels of a gene across multiple samples and expresses it relative to the levels of an internal control RNA. This control RNA is often a typical reference gene, like glyceraldehyde 3-phosphate dehydrogenase (GAPDH), ribosomal RNA subunits (18S and 28S rRNA), or β -actin (Bustin and Nolan 2004). The relative quantification strategy is adequate for most purposes to investigate physiological changes in gene expression levels (Fleige et al. 2006).

Reid et al. (2006) evaluated the expression stability of numerous reference genes during berry development. These genes included actin, AP47 (clathrin-associated protein), cyclophilin, EF1- α (elongation factor 1- α), GAPDH, MDH (malate dehydrogenase), PP2A (protein phosphatase), SAND, TIP41, α -tubulin, β -tubulin, UBC (ubiquitin conjugating enzyme), UBQ-L40 (ubiquitin L40) and UBQ10 (polyubiquitin). These authors evaluated these genes from *V. vinifera* cv. Cabernet Sauvignon pericarp and employed three different statistical approaches. Some of the genes proved to be relatively stable, but no particular gene out performed any other genes in each of the three evaluation methods tested. They recommend that a combination of several genes be used for normalizing data for grape berry development. Their data support GAPDH, actin, EF1- α and SAND as the most relevant reference genes for expression studies during berry development (Reid et al. 2006).

The real-time PCR-based assay for measuring mRNA levels was introduced in 1999 by Wang and Brown and has now become the method of choice for determining gene expression levels (Fleige et al. 2006). Toplak et al. (2004) compared northern blot analysis, semi-quantitative RT-PCR, and real-time qRT-PCR methods (with TaqMan probes) for gene expression analysis in terms of precision and sensitivity. They found that all the lines that tested positive for expression of the specific mRNA on northern blots were also found to be positive by semi-quantitative RT-PCR and by real-time qRT-PCR. However, 2 lines that tested negative by northern blots were found to be positive by the other 2 methods. The relative expression level of the transgene in these 2 lines, as detected by real-time PCR, was low (line 34: 3.8% and line 35: 3.3%). These results indicated the higher sensitivity of the PCR-based methods.

When comparing the two PCR-based techniques, the real-time PCR method had more advantages than semi-quantitative RT-PCR. The main reason for this was the automated detection during the PCR amplification; it is a closed system that reduces the possibility of sample contamination and it provides higher specificity due to the use of a fluorescent probe. Furthermore, real-time PCR is highly repeatable over a wide dynamic range and therefore enables reliable quantification of very low mRNA levels, including those that can not be detected by hybridization-based methods (Toplak et al. 2004).

Although SYBR Green reactions require more extensive optimisation than TaqMan probe reactions, Assem and Hassan (2008) effectively demonstrated the utility of the SYBR Green qRT-PCR system for estimating transgene expression levels in GM maize.

3.2 Materials and Methods

3.2.1 Transgenic grapevine material

Vitis vinifera cv Richter 110 was used for the transformation of an antiviral construct, Δ HSP-Mut, (Freeborough 2003) into grapevine. The construct is a dysfunctional form of the GLRaV-3 HSP-70 homologue (GLRaV-3 HSP-70h) region. The transgenic grapevine plants analysed in this study were transformed by the Institute for Wine Biotechnology (IWBT) (Stellenbosch University) via *Agrobacterium* transformation of pre-embryogenic callus tissue. *In vitro* and hardened off plantlets were supplied for transgene copy number and mRNA expression level determination experiments.

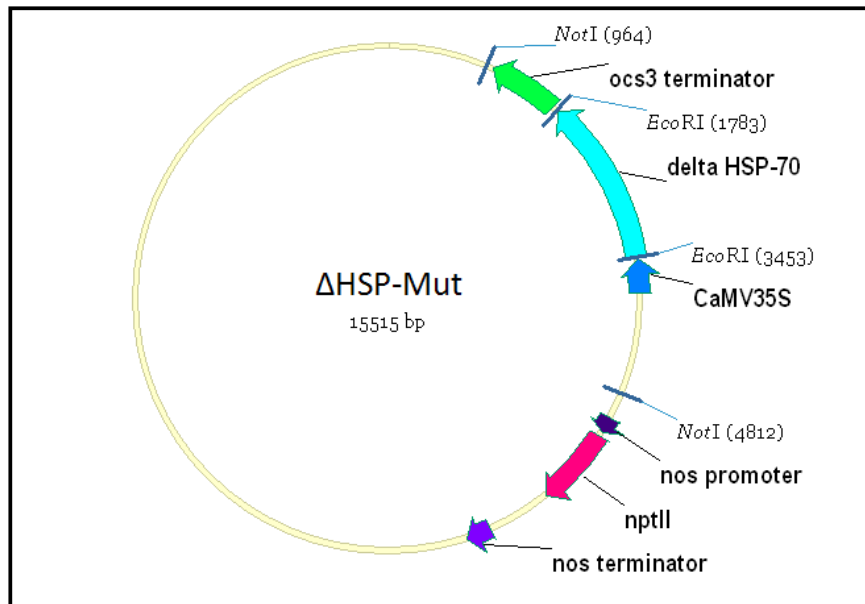


Figure 20: Graphical representation of the dysfunctional HSP-70h transgene (Δ HSP-Mut)

3.2.2 Primer design

Primers were designed to amplify a 470 bp fragment for the qPCR determination of transgene copy number and mRNA expression levels. Primers were designed to amplify a fragment of the dysfunctional HSP-70h transgene. Reference genes with stable expression levels in *Vitis vinifera* were identified namely Cyclophilin, β -Tubulin and GAPDH. The primers were designed to produce a product of the same approximate size as that amplified by the HSP-70h primers in order to simplify optimisation procedures and subsequent analyses. All primers were designed and

analysed via and ordered from Integrated DNA Technologies (IDT) (<http://www.idtdna.com/Home/Home.aspx>) (Table 4).

Table 4: Primer names, sequences, product fragment sizes and optimal annealing temperatures (Ta)

Primer name	Sequence	Fragment size	Ta*
HSP-70h F	GGGGGTCAAGTGCTCTAGTT	470 bp	56°C
HSP-70h R	TGTCCCGGGTACCAGATTAT		
Cyclophilin F	TGTGACCTGAACCACTTGA	451 bp	56°C
Cyclophilin R	CCGGTAGGATTGTGATGGAG		
β-Tubulin F	TGGTGACCTGAACCACTTGA	479 bp	56°C
β-Tubulin R	TCACCCTCCTGAACATCTCC		
GAPDH F	AGGGAGGAGTCAGAGGGAAA	455 bp	56°C
GAPDH R	GTGTGGCTGTGGCAGAGTTA		
ClosF1	CCATGGAAGTAGGTATAGATTTGG	1500 bp	55°C
ClosR2	TTATCCATTCAAATCGTGTC		

* Annealing temperatures for DNA template

3.2.3 DNA extraction

For molecular analysis of the transgenic plants, a general CTAB extraction method was followed for the extraction of DNA (Sambrook et al. 1989). Approximately 0.3g of leaf material was frozen with liquid nitrogen and finely ground in a 1.5ml eppendorf tube. Eight hundred microlitres of CTAB extraction buffer (3% CTAB, 1.4M NaCl₂, 0.02M EDTA, 1M Tris/HCl (pH 8.0)) was added and the mixture was vortexed for 10min and incubated at 60°C for 1 hour. Chloroform (600µl) was added to the mixture, followed by vortexing the sample for 5min and centrifugation at 12 000g for 8 min. The supernatant was transferred to a clean tube, 1 volume of chloroform was added and the mixture then vortexed for 3min and centrifuged at 12 000 xg for 3min. This step was repeated. The aqueous phase was transferred to a clean tube and one volume of isopropanol was added. This was followed by another centrifugation step followed by the removal of the supernatant. Two microlitres of RNase A was added to 1.2ml distilled water and mixed well. Two hundred microlitres of this RNase A mix was added to the pellet and incubated at 37°C for 30min. After incubation 20µl of 3M sodium acetate (NaOAc) and 500µl 100% ethanol was added, gently inverted and the mixture was placed at -20°C for 30min. This was followed by a centrifugation step for 10min at 12 000g. The supernatant

was discarded and the DNA pellet washed using 1ml of 70% ethanol and centrifuged at 12 000 xg for 5min. The supernatant was discarded and the pellet dried and resuspended in 40µl of dH₂O.

3.2.4 DNA Clean-up

The DNA purification protocol of Sharma et al. (2000) was used for DNA clean-up. DNA subjected to this clean-up was used for Southern blot analysis. DEAE sepharose (DFF100 SIGMA-ALDRICH USA) was used rather than the described DEAE cellulose as it was easier to work with (De Beer, Pers Comm).

3.2.5 Detection and quantification of the transgene

3.2.5.1 Initial PCR optimisation

The DNA extracted from the transgenic plants was diluted to 100ng/ul. These samples were initially amplified in a normal PCR reaction with the HSP-70h primers and the different reference gene primers (β -Tubulin, Cyclophilin and GAPDH) to evaluate the primers and PCR cycle before further optimisation with qPCR. The standard 25µl PCR reaction mix was prepared (Appendix A). The standard PCR cycles were used for amplification for the various primer pairs (Appendix A) with all annealing temperatures set at 55°C.

To visualize the amplified product, agarose gel electrophoresis was performed. DNA fragment separation was performed on a 1.2% (w/v) agarose gel in 1 x TAE buffer (40 mM Tris, 0.114% (v/v) HOAc, 1mM EDTA pH 8.0) at 120V for 30min. Ethidium bromide (0.5µg/ml) was added to the agarose gel to a final concentration of 0.01% (v/v) for ultra violet visualisation (SynGene, Multigenius Bio Imaging gel documentation system). Gene Ruler 1 kb DNA ladder (Fermentas) was used to determine the molecular size of the DNA fragments.

3.2.5.2 Transgene detection with qPCR

Detection of the transgene was further optimised with qPCR. For quantification of the transgene, the genomic DNA extracted from transgenic plants was amplified with primers for the reference gene as well as the transgene. For the construction of a standard curve, serial 5-fold dilutions of the DNA of a specific sample were made (from 250ng to 0.4ng) and amplified, in duplicate, with the primers for the gene of interest (HSP-70h) and reference genes (β -Tubulin, Cyclophilin and GAPDH). The

standard 25µl qPCR reaction was prepared (Appendix A) and the optimised qPCR cycles for the gene of interest and reference genes were followed as described in Appendix A with annealing temperature as indicated in Table 4.

For the amplification of the remainder of the samples, 50ng of DNA from each sample was also amplified in duplicate with both sets of primers (gene of interest and reference genes). One sample had to be defined as a calibrator sample. Preferably this would be a sample of which the copy number is known to which the data of the other samples can be normalised (we chose sample 9 and later verified the copy number by Southern blot). This sample is also included in every run in order to compensate for different efficiencies for the same type of reactions performed in different runs in order to make them comparable.

Different methods were compared for the determination of transgene copy number, namely the two standard curve method, delta delta Ct method and the relative expression software tool (REST). Since the efficiency of the two reactions (transgene and reference gene amplification) differed, the delta delta Ct method could not be used. Thus a model where different efficiencies for reference and transgene are taken into account, were rather used. This model, REST, was introduced for the determination of mRNA expression levels by Pfaffl et al. (2001), but has since also been employed in copy number determination (Škulj et al. 2008). The Ct values of the sample in question and the calibrator sample amplified with the two different primer sets (gene of interest and reference gene) are imported into the program, as well as the different efficiency values for these reactions (see equation 1). The program performs 50 000 mathematical iterations to generate an estimated copy number value.

$$\text{Ratio} = \frac{(E_{GOI})^{\Delta Ct_{GOI}} (\text{Control} - \text{Sample})}{(E_{REF})^{\Delta Ct_{REF}} (\text{Control} - \text{Sample})}$$

Equation 3

3.2.5.3 Southern Blot Analyses

DNA restriction digest and agarose gel electrophoresis

The purified and cleaned transgenic plant DNA was digested to completion with *Bam*HI (Fermentas). The plasmid containing the ΔHSP-Mut construct was digested

with *Hind*III (the plasmid contains two *Hind*III recognition sites either side of the Δ HSP-Mut construct) and was included on the gel as a control, together with an undigested plasmid sample. An undigested, untransformed genomic DNA sample was also included as a control. All of these samples and the DIG molecular weight marker VII were electrophoresed on a 0.8% agarose gel for several hours at 30V.

Denaturation, neutralisation and blotting

Denaturation, neutralization and blotting were performed as described in the DIG systems user's guide for filter hybridisation (1995) by Roche Molecular Biochemicals. Thereafter the DNA was UV crosslinked to the positively charged nylon membrane (Roche diagnostics, Germany) by exposing the membrane to UV light (UV Transilluminator UVP_{INC.}) for 5 min.

PCR labelling of probe

The probe was constructed by PCR amplification of the dysfunctional GLRaV-3 HSP-70h fragment (1650bp) with the ClosF1 and ClosR2 primers (Table 4) (Freeborough 2003). The PCR 25 μ l reaction consisted of 1 x KAPA Taq buffer A (105mM Mg), 1 x cresol, 0.4 μ M forward and reverse primers, 0.2mM dNTPs, and 0.5U of *Taq* Polymerase. The standard PCR reaction cycle was performed with annealing temperature as indicated in Table 4. This PCR product was diluted 1:100 for re-amplification with 10 x DIG labelling mix (Roche Ref 11277065910, lot 11967222). The 50 μ l PCR reaction consisted of 1 x Ex Taq buffer (Takara), 0.4 μ M forward and reverse primers (ClosF1 and ClosR2), 0.5 x DIG DNA labelling mix, 0.2mM dNTPs (Takara), 3.75U Ex Taq (Takara). The above mentioned PCR cycle was repeated. Two of these 50 μ l PCR reactions were performed and the products were denatured at 95°C for 5min and placed on ice. These PCR products were added to 10ml of prehybridization solution (DIG Easy Hyb Granules Roche) and this mixture was incubated at 68°C for 10min.

Prehybridization and hybridization

Prehybridization was performed with prehybridization solution (DIG Easy Hyb Granules Roche) for 2 hours. Overnight hybridization with the hybridisation solution (containing the DIG labelled probe) followed thereafter. Both of these reactions were performed at 37°C in a rolling tube (Techne Hybridiser HB-1D). After hybridisation,

stringency washes were performed with 2 x wash solution and 0.5 x wash solution. Each wash step was performed at 68°C for 30min and was repeated 3 times.

Chemiluminescent detection

Chemiluminescent detection was performed according to the DIG system user's guide for filter hybridization (1995) by Roche Molecular Biochemicals. CDP-Star, ready-to-use (Roche) was used for chemiluminescent detection. The Anti-Digoxigenin-AP Fab fragments (Roche) was diluted 1: 20 000 in blocking solution. The filter-batch method was used for the application of diluted substrate. Finally the membrane was exposed to X-ray high performance chemiluminescence film (Amersham Hyperfilm™ ECL, GE Healthcare) for approximately 6 hours before development.

3.2.6 RNA extraction

Transgene expression levels were also determined for the transgenic lines. A small scale CTAB RNA isolation procedure was followed as described by White et al. (2008). Leaf material (0.3g) was frozen with liquid nitrogen and finely ground in a 1.5ml eppendorf tube. One millilitre of 2% CTAB buffer (2% CTAB, 2% (w/v) PVP, 100mM Tris, 25mM EDTA, 2M NaCl and 0.5g/l spermidine) preheated to 65 °C and 3% (v/v) B-Merchптоethanol was added to the ground material. The mixture was vortexed and incubated at 65°C for 30min. After incubation the samples were centrifuged for 10min at 13 000rpm where after the supernatant was transferred to a clean tube. Two chloroform extractions were then performed by adding an equal volume of chloroform to the supernatant and vortexing for 30sec, followed by centrifugation at 13 000rpm for 15min. Eight molar LiCl was added to the supernatant to a final concentration of 2M and incubated at 4°C overnight. The samples were then centrifuged at 13 000rpm for 60min at 4°C. The pellet was washed in 500µl 70% EtOH and resuspended in 20µl dH₂O. A DNase treatment was performed on the samples to ensure elimination of any DNA still present. The samples were filled to 179µl with dH₂O and 1µl RNase free DNase I (Fermentas) and 20µl 10 x DNase buffer (Fermentas) was added to the samples and placed at 37°C for 30min. To precipitate the RNA, 70µl dH₂O, 100µl phenol (pH4) and 100µl chloroform was added to the samples and vortexed. Samples were then centrifuged at maximum rpm for 5 min. About 200µl of supernatant was transferred to a clean tube. 20µl NaOAc (3M) and 500µl ethanol (EtOH) was added to the supernatant and

centrifuged at 4°C for 10min at 13 000 rpm. The supernatant was removed and the pellet resuspended in 20µl dH₂O.

3.2.7 Estimation of relative transgene mRNA expression levels

3.2.7.1 Real time RT-PCR (qRT-PCR)

Initial RT-PCR optimisation

The RNA extracted from the transgenic plants was diluted to 100ng/ul. These samples were initially amplified in a normal RT-PCR reaction with the HSP-70h primers and the different reference gene primers (β -Tubulin, Cyclophilin and GAPDH) to evaluate the primers and PCR cycle before further optimisation with qRT-PCR. The standard 25µl RT-PCR reaction mix was prepared (Appendix A). The standard PCR cycles were used for amplification for the various primer pairs (Appendix A) with all annealing temperatures set at 55°C. To ensure that false amplification with genomic DNA was eliminated, the samples were amplified with conventional PCR methods and no amplification was present.

qRT-PCR

For quantification by qRT-PCR, a one step qRT-PCR protocol was followed. For the construction of a standard curve, serial 5 fold dilutions of the RNA of a specific sample were made (from 500ng to 0.8ng) and subsequently amplified, in duplicate, with the primers for the gene of interest (HSP-70h) and reference genes (β -Tubulin, Cyclophilin and GAPDH). Approximately 100ng of RNA was used for duplicate amplification of each of the transgenic samples. We chose sample 8 as calibrator sample as it had a high Ct value compared to the rest of the samples during amplification with HSP-70h primers, indicating relatively low transgene mRNA expression levels (thus a good sample to enable relative expression levels to). The standard 25µl qRT-PCR reaction mix was prepared (Appendix A) with standard qRT-PCR amplification cycles (Appendix A) with the annealing temperatures for HSP-70h at 57°C and 60°C for GAPDH. The other reference genes weren't used for transgene mRNA expression level determination as they showed poor amplification with the RNA samples. REST was used for the estimation of the level of transgene expression for each transgenic plant as described previously in 3.2.5.2 (Pfaffl et al. 2001).

3.3 Results

3.3.1 DNA extraction from transgenic grapevine

DNA was extracted from transgenic grapevine plants for molecular characterisation. Extracted DNA was visualised on a 1.2% agarose gel to evaluate quality. High molecular weight bands were visible for most DNA samples, RNA contamination was not observed (Figure 21).

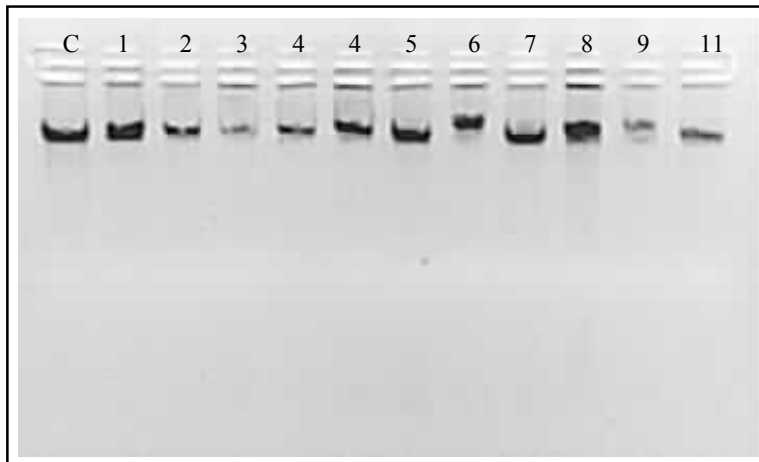


Figure 21: DNA extracted from transgenic plants visualised on a 1.2% agarose gel. Lane 1: untransformed control, lane 2: Transgenic Grapevine plant line Δ HSP-Mut1, lane 3: Δ HSP-Mut2, lane 4: Δ HSP-Mut3, lane 5: Δ HSP-Mut4, lane 6: Δ HSP-Mut 4, lane 7: Δ HSP-Mut5, lane 8: Δ HSP-Mut6, lane 9: Δ HSP-Mut7, lane 10: Δ HSP-Mut8, lane 11: Δ HSP-Mut9, lane 12: Δ HSP-Mut11

The extracted DNA was subjected to spectrophotometry using a NanoDrop®ND-1000 Spectrophotometer to determine the concentration and purity of the nucleic acid. Concentrations of between 94 ng/ μ l – 294 ng/ μ l were measured and the 260 nm/280 nm and 260nm/230nm wavelength ratios were within the expected range, indicating DNA of sufficient quality for downstream application.

3.3.2 Detection and quantification of the transgene

3.3.2.1 Amplification of a fragment of the transgene

The antiviral Δ HSP-Mut construct that was used to create the transgenic plant lines, contains a disrupted GLRaV-3 HSP-70 homologue (HSP-70h) fragment. HSP-70h primers were designed (Table 4) for the detection of the HSP-70h transgene (consisting of a disrupted GLRaV-3 HSP-70h region) and estimation of the copy numbers in the transgenic plant lines. The optimised PCR amplification resulted in a

470 bp fragment being visible as a clear band after agarose gel electrophoresis (Figure 22). The negative control plant (C in lane 2) and the non- template control (lane 13) did not amplify with the HSP primers. Samples 6 and 7 also showed no amplification.

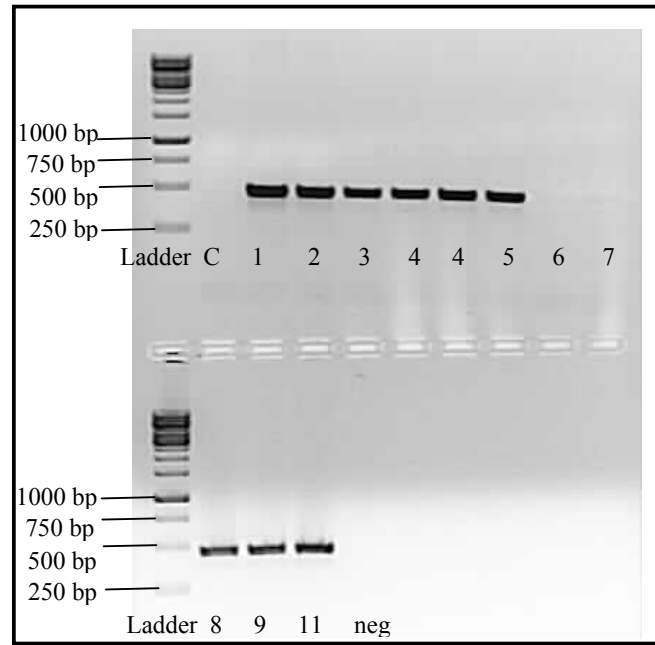


Figure 22: DNA from transgenic plants amplified with HSP primers visualised on a 1.2% agarose gel to confirm transformation with the antiviral construct. At the top lane 1: 1kb DNA ladder, lane 2: untransformed control, lane 3: Δ HSP-Mut1, lane 4: Δ HSP-Mut2, lane 5: Δ HSP-Mut3, lane 6: Δ HSP-Mut4, lane 7: Δ HSP-Mut4, lane 8: Δ HSP-Mut5, lane 9: Δ HSP-Mut6, lane 10: Δ HSP-Mut7. At the bottom row lane 1: 1kb DNA ladder, lane 2: Δ HSP-Mut8, lane 3: Δ HSP-Mut9, lane 4: Δ HSP-Mut11, lane 5: no template control

3.3.2.2 qPCR detection of the Δ HSP-Mut transgene construct

Amplification of the HSP-70h fragment was further optimised using the RotorGene 6000 real time thermal cycler. Serial dilutions were prepared of sample 9 and were amplified in duplicate with the primers for the Δ HSP-Mut construct or gene of interest, HSP-70h. This data was used for the construction of a standard curve (Figure 23). The standard curve was constructed by correlating the Ct values and the log of the specified concentrations for each sample.

For the HSP-70h standard curve, an amplification efficiency of 0.98 was obtained, indicating an efficient doubling of PCR product during each PCR cycle. The standard curve also had a high R^2 value of 0.99, indicating a good correlation coefficient, implying that the data is consistent with the hypothesis (thus the given standards are easily fit onto the graph).

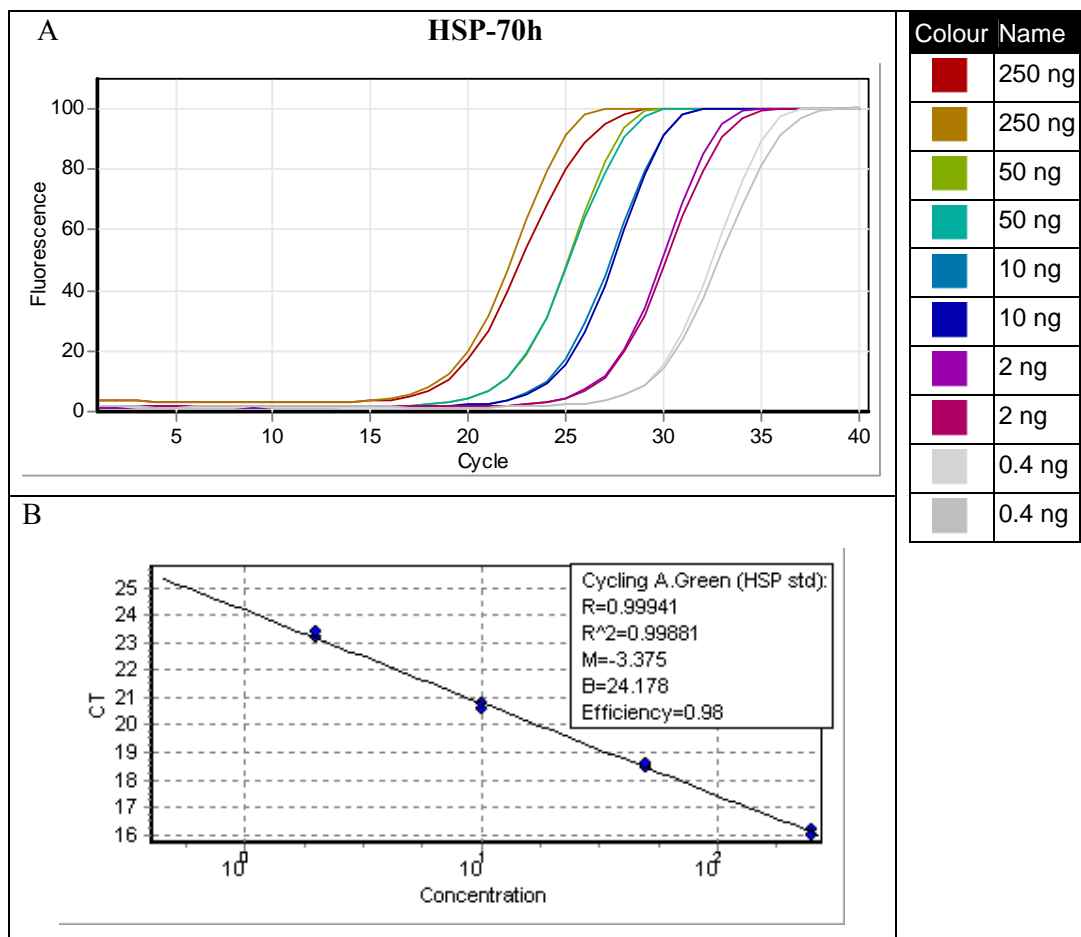


Figure 23: (A) Amplification curves of five fold DNA serial dilutions from sample 9 (from 250ng/reaction to 0.4ng/reaction as indicated in the legend) of a specific transgenic plant, amplified with HSP-70h primers to produce (B) a standard curve (Ct vs log of concentration) for the gene of interest (Δ HSP-Mut). R: square root of correlation coefficient, R²: correlation coefficient, M: slope of the standard curve, B: intercept of the standard curve and efficiency (effective doubling of PCR product during each PCR cycle) as indicated on the standard curve

Equal amounts of DNA (50ng) of the remaining samples were amplified in duplicate with the gene of interest primers. Using the same amount of starting material facilitated further data analysis. Samples containing the transgene were identified via melting curve analysis of the amplified qPCR product and showed melting temperatures between 83.5°C and 83.8°C. The Ct values of the amplified samples fell within the Ct range of the standard curve and were thus well aligned with the standard curve (Figure 24).

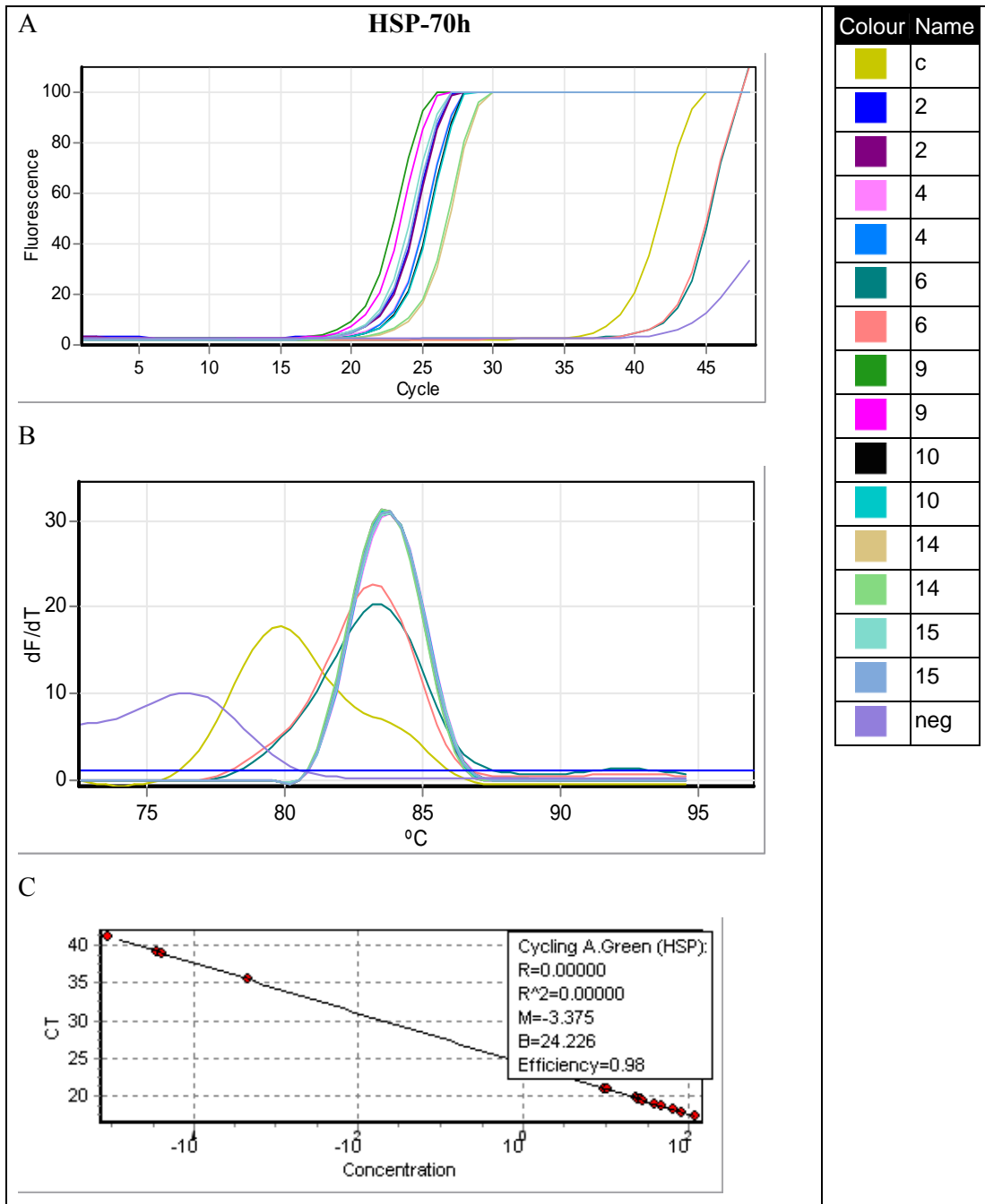


Figure 24: (A) Amplification curves for transgenic Δ HSP-Mut grapevine samples amplified via qPCR with HSP-70h primers (see different Δ HSP-Mut samples in legend). (B) Melting curve analysis to confirm amplification of correct amplicon. Samples containing the HSP fragment had a melting peak between 83.5°C and 83.8°C. (C) Ct values of amplified samples imported onto HSP-70h standard curve

3.3.2.3 qPCR amplification of reference genes

In order to obtain a relative quantification of the transgene copy numbers and for accurate normalisation of the data, it was necessary to also amplify a reference gene. This would be an endogenous gene with a single or known copy number in the specific organism studied. Three different reference genes were used in this analysis,

β -tubulin, Cyclophilin and GAPDH (Figure 25 – Figure 30). Analysis indicated that these genes were present in a single copy in the *V.vinifera* genome¹. Standard curves were constructed from serial dilutions, the remainder of the samples were amplified with the primers for the different reference genes as described for HSP-70h (3.3.2.2).

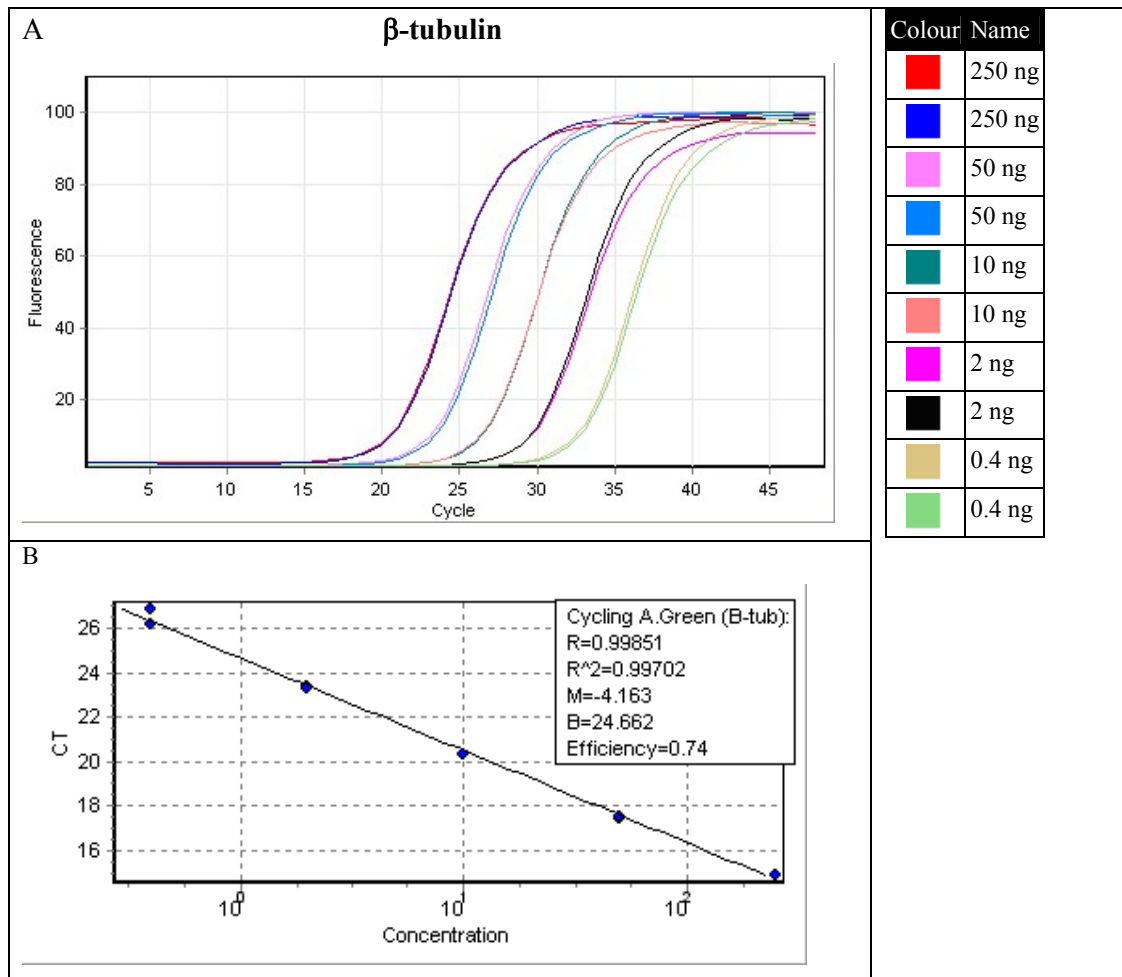


Figure 25: (A) Amplification curves of five fold DNA serial dilutions from sample 9 (from 250ng/reaction to 0.4ng/reaction as indicated in the legend) of a specific transgenic plant, amplified with β -tubulin primers to produce (B) a standard curve (Ct vs log of concentration) for the β -tubulin reference gene. R, R², M, B and efficiency values as indicated on the standard curve (as explained in Figure 23)

¹ http://www.ncbi.nlm.nih.gov/projects/mapview/map_search.cgi?taxid=29760&query=beta-tubulin&qchr,
http://www.ncbi.nlm.nih.gov/projects/mapview/map_search.cgi?taxid=29760&query=cyclophilin&qchr,
http://www.ncbi.nlm.nih.gov/projects/mapview/map_search.cgi?taxid=29760&query=GAPDH&qchr

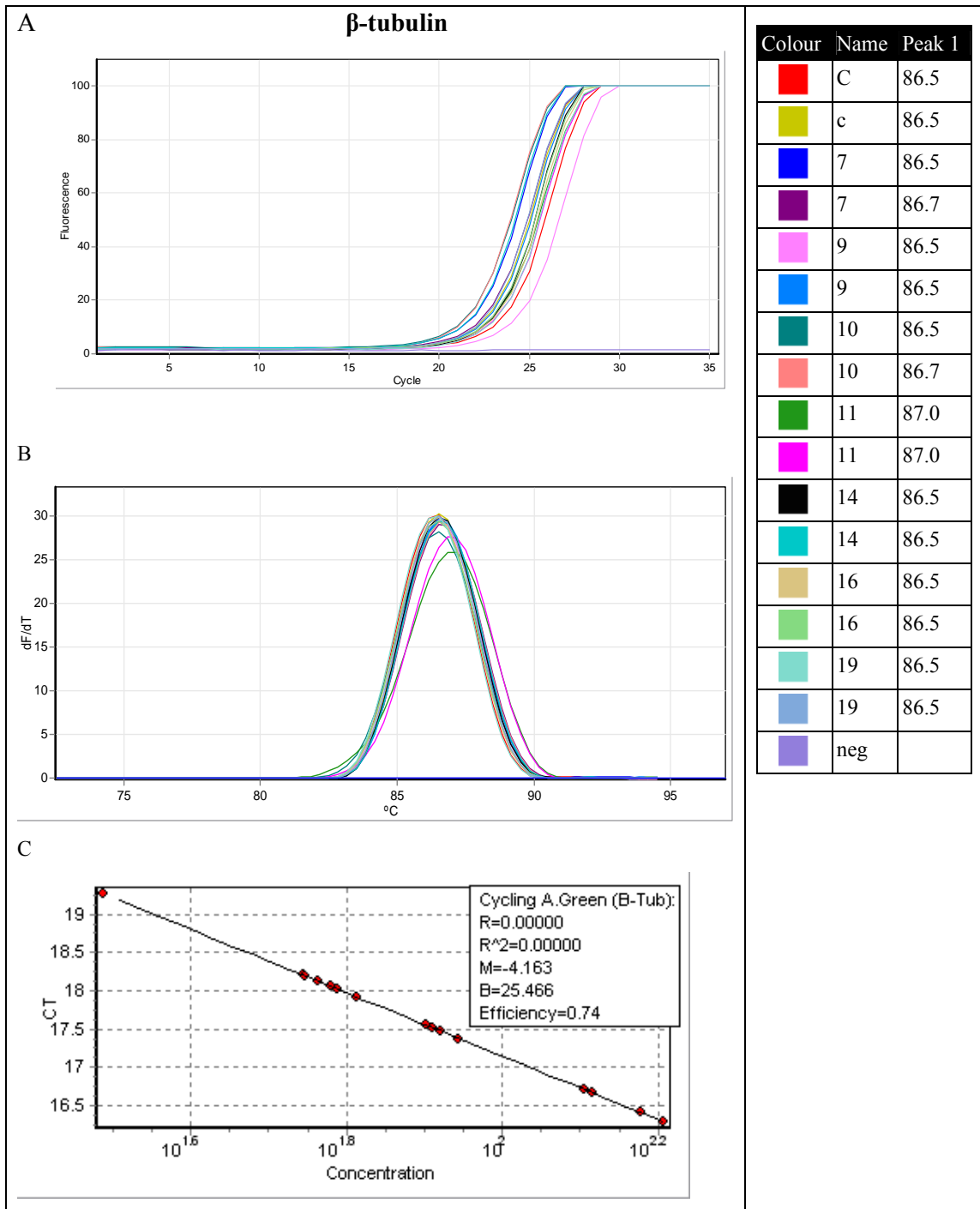


Figure 26: (A) Amplification curves for transgenic Δ HSP-Mut grapevine samples amplified via qPCR with β -tubulin primers (see different Δ HSP-Mut samples in legend). (B) Melting curve analysis to confirm amplification of correct amplicon, shown as melting peaks between 86.5°C and 87°C. (C) Ct values of amplified samples imported onto β -tubulin standard curve

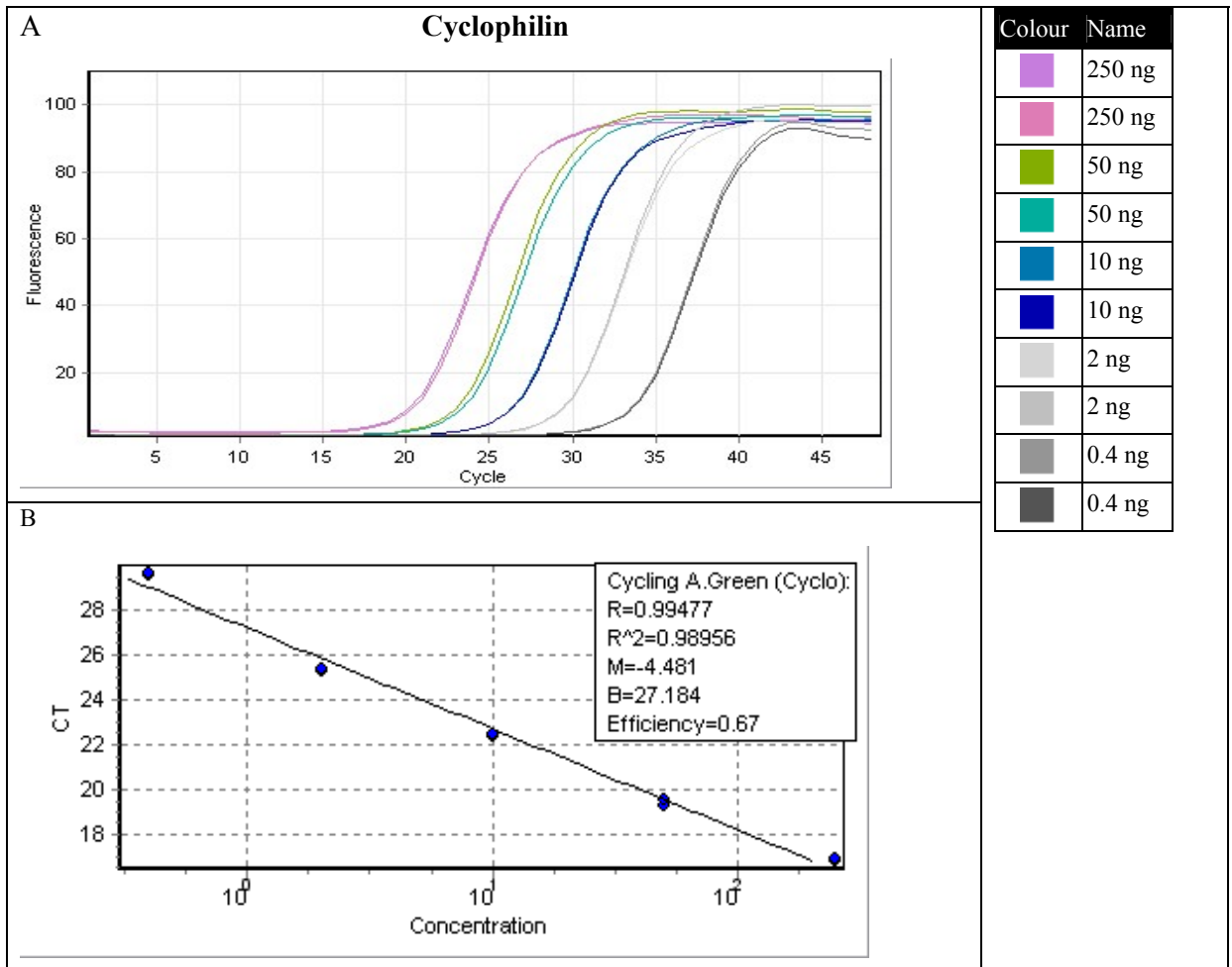


Figure 27: (A) Amplification curves of five fold DNA serial dilutions from sample 9 (from 250ng/reaction to 0.4ng/reaction as indicated in the legend) of a specific transgenic plant, amplified with cyclophilin primers to produce (B) a standard curve (Ct vs log of concentration) for the cyclophilin reference gene. R, R², M, B and efficiency values as indicated on the standard curve (as explained in Figure 23)

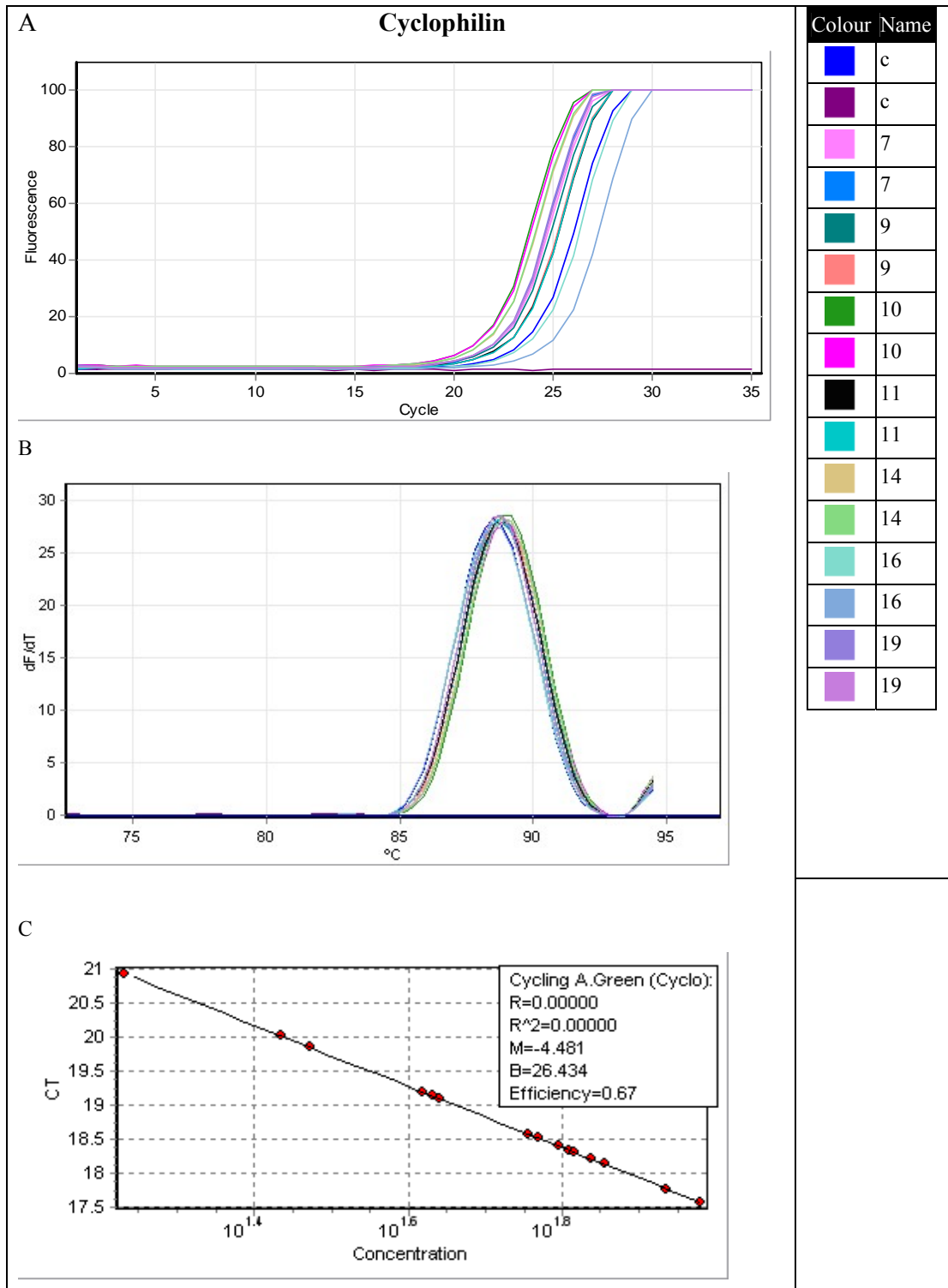


Figure 28: (A) Amplification curves for transgenic Δ HSP-Mut grapevine samples amplified via qPCR with cyclophilin primers (see different Δ HSP-Mut samples in legend). (B) Melting curve analysis to confirm amplification of correct amplicon, shown as melting peaks between 88.5 °C-89°C. (C) Ct values of amplified samples imported onto Cyclophilin standard curve

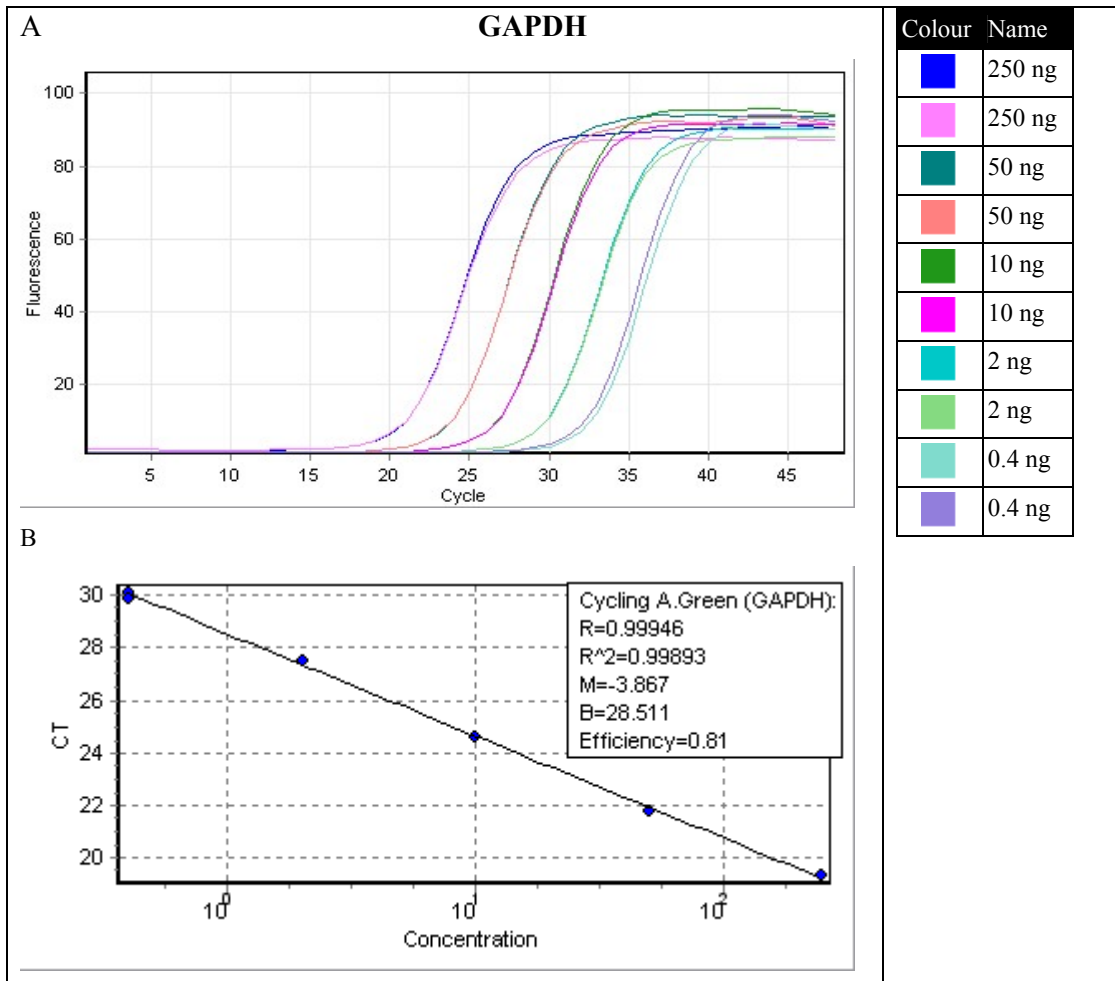


Figure 29: (A) Amplification curves of five fold DNA serial dilutions from sample 9 (from 250ng/reaction to 0.4ng/reaction as indicated in the legend) of a specific transgenic plant, amplified with GAPDH primers to produce (B) a standard curve (Ct vs log of concentration) for the GAPDH reference gene. R, R², M, B and efficiency values as indicated on the standard curve (as explained in Figure 23)

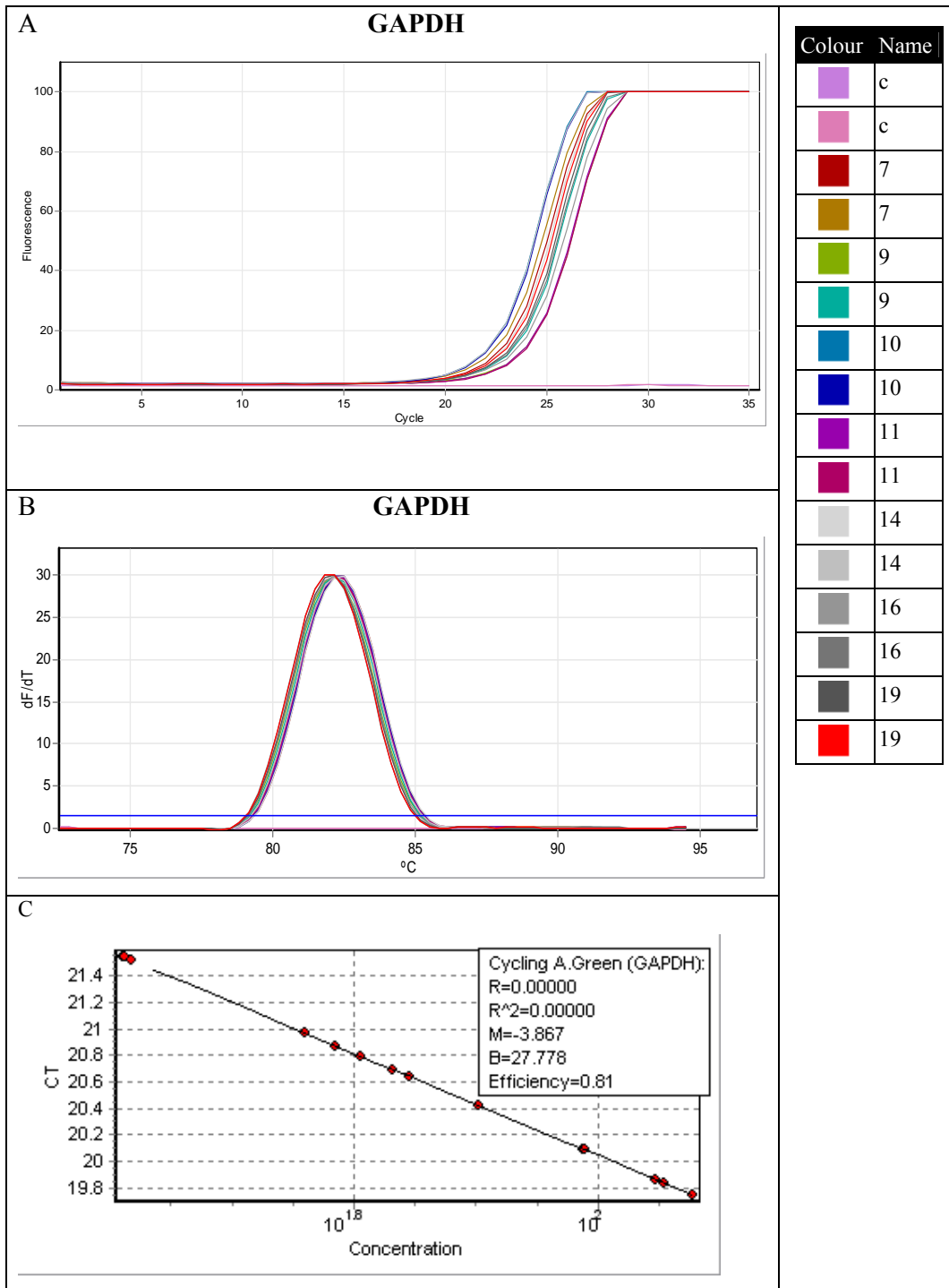


Figure 30: (A) Amplification curves for transgenic Δ HSP-Mut grapevine samples amplified via qPCR with GAPDH primers (see different Δ HSP-Mut samples in legend). (B) Melting curve analysis to confirm amplification of correct amplicon, shown as melting peaks between 82.0°C and 82.3°C. (C) Ct values of amplified samples imported onto GAPDH standard curve

The efficiencies for β -tubulin and cyclophilin was lower than that of GAPDH and therefore the doubling of PCR product was less successful with those two primer sets. The R^2 values for the β -tubulin and GAPDH standard curves were 0.99, which indicated a good correlation coefficient and the given standards were thus easily fitted

onto the graph. The R^2 value of cyclophilin was 0.98, a relatively good correlation coefficient value (close to ideal 0.99). The standards were amplified in duplicate to ensure accuracy. Comparable amplification curves were produced for duplicate samples. The standards were therefore accurately and efficiently amplified with the reference gene primers.

3.3.2.4 Estimation of transgene copy numbers with qPCR using REST

REST (relative expression software tool) was used to generate a reliable copy number estimation of the Δ HSP-Mut transgene in each of the transgenic lines. The REST algorithm uses the C_t values for the sample in question amplified with both the gene of interest and reference gene primers; as well as the calibrator sample amplified with both these primer sets. The copy number of a particular sample was then calculated relative to the calibrator sample (copy number determined by Southern blot analysis) and the reference gene. The efficiency of the reactions is incorporated in the equation to enable an accurate and reliable estimation (Equation 3). These calculated values were then compared to the copy number results of the Southern blot (Table 5)

3.3.2.5 Southern Blot Analyses for transgene copy number estimation

The DNA extracted from the transgenic plants was subjected to further purification with DEAE sepharose. This removed the polyphenolic compounds in the extract which interferes with efficient transfer of the DNA from the gel to the membrane. Three of the transgenic lines did not survive and Southern blot results for lines 3, 5 and 19 are therefore not available. Various controls were included to ensure accurate interpretation of the results. An undigested, untransformed genomic DNA sample was included (Figure 31, lane 2) in order to identify any undigested DNA in any of the samples. A plasmid containing the Δ HSP-Mut construct was digested with *HindIII*, an enzyme that has recognition sites at either side of the construct and thus digests the construct out of the plasmid. This control was included as a verification that the enzyme used to digest the samples, did not digest the construct out of the plasmid. This also indicates the smallest fragment detectable by the probe. A summary of the copy number results are shown in Table 5.

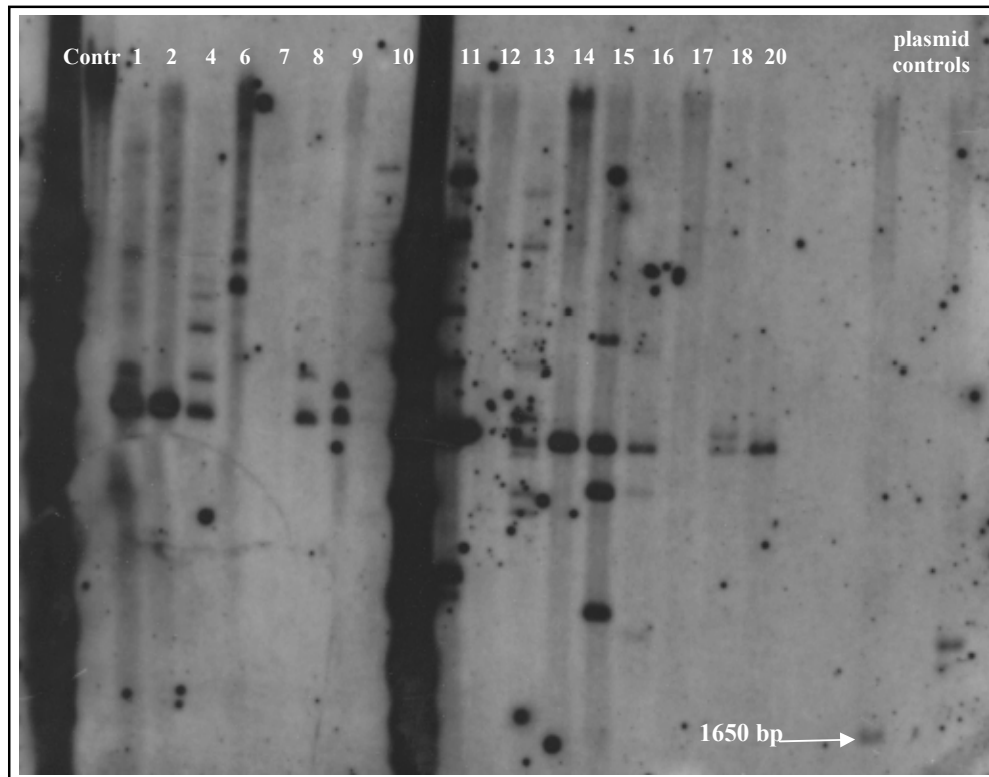


Figure 31: Southern blot of transgenic samples containing the Δ HSP-Mut construct (approximately 1500bp). Lane 1: DIG molecular weight marker VII, lane 2: untransformed, undigested genomic DNA control, lane 3: Δ HSP-Mut1, lane 4: Δ HSP-Mut2, lane 5: Δ HSP-Mut4, lane 6: Δ HSP-Mut6, lane 7: Δ HSP-Mut7, lane 8: Δ HSP-Mut8, lane 9: Δ HSP-Mut9, lane 10: Δ HSP-Mut10, lane 11: DIG molecular weight marker VII, lane 12: Δ HSP-Mut11, lane 13: Δ HSP-Mut12, lane 14: Δ HSP-Mut13, lane 15: Δ HSP-Mut14, lane 16: Δ HSP-Mut15, lane 17: Δ HSP-Mut16, lane 18: Δ HSP-Mut17, lane 19: Δ HSP-Mut18, lane 20: Δ HSP-Mut20, lane 23: plasmid, containing Δ HSP-Mut construct, digested with *Hind*III, lane 24: undigested plasmid (containing Δ HSP-Mut construct)

3.3.3 Estimation of relative transgene mRNA expression levels with qRT-PCR and REST

Total RNA extracted from the transgenic plants was used for relative quantification of mRNA expression levels of the transgene. The mRNA expression levels were calculated relative to the GAPDH reference gene. Amplification with reference genes, β -tubulin and cyclophilin, yielded poor amplification and were not included in the estimation.

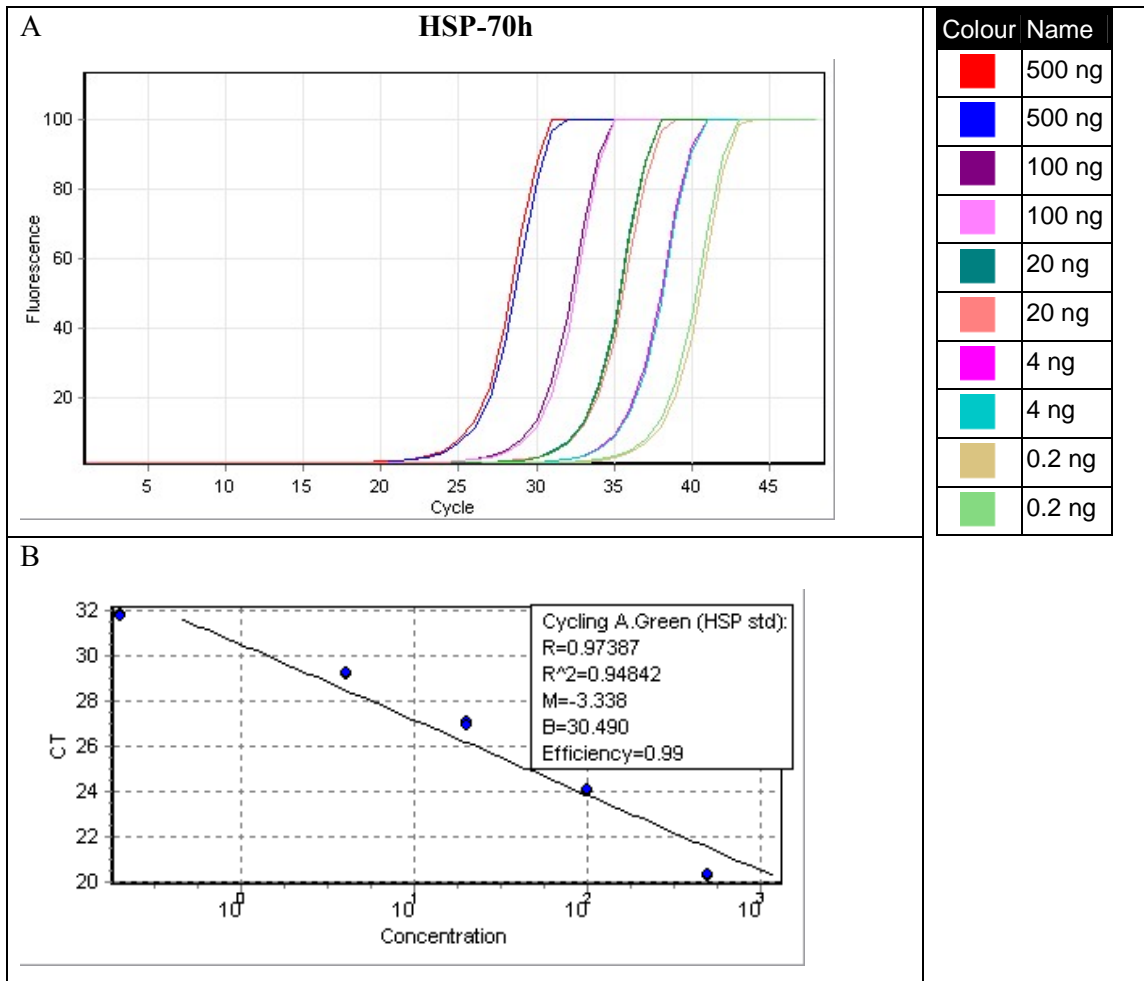


Figure 32: (A) Amplification curves of five fold RNA serial dilutions from sample 8 (from 500ng/reaction to 0.2ng/reaction as indicated in the legend) of a transgenic plant, amplified with HSP-70h primers to produce (B) a standard curve (Ct vs log of concentration) for the gene of interest. R, R², M, B and efficiency values as indicated on the standard curve (as explained in Figure 23).

The efficiency of the qRT-PCR amplification reaction with the gene of interest primers (HSP-70h) was high with a value of 0.99 (Figure 32 B). However the R²-value of the curve was lower than the ideal value of 0.99, indicative of a lower correlation coefficient. Standards were amplified in duplicate and the duplicates delivered comparable amplification curves. The standards were therefore accurately amplified with the gene of interest primers with high amplification efficiency. The Ct values of the remainder of the samples were imported onto the gene of interest standard curve (Figure 33 C).

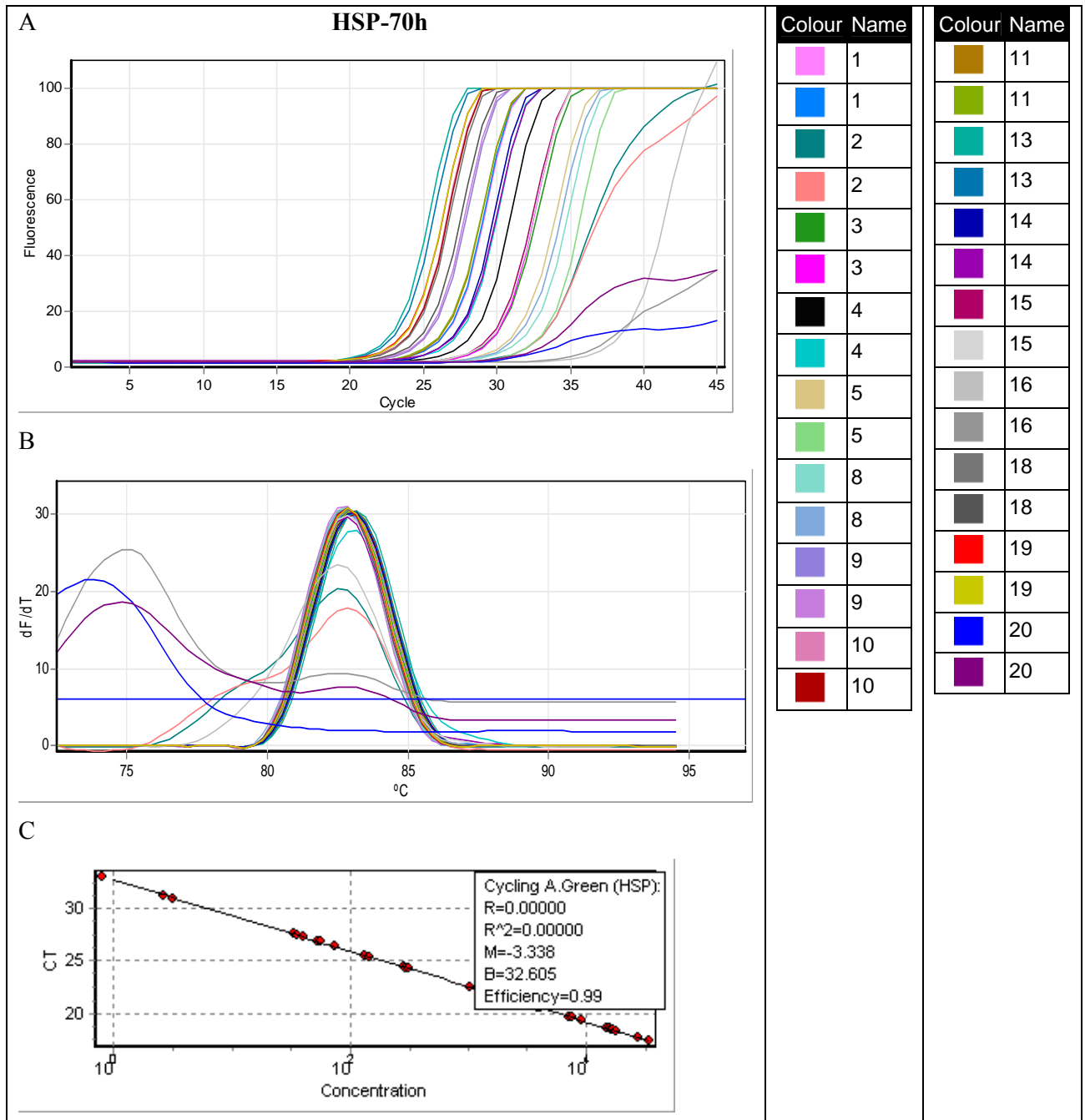


Figure 33: (A) Amplification curves for transgenic Δ HSP-Mut grapevine samples (as indicated in the legend) amplified via qRT-PCR with HSP-70h primers for transgene expression level determination (see different Δ HSP-Mut samples in legend). (B) Melting curve analysis to verify amplification of correct amplicon, shown as melting peaks between 82.5°C and 83.0°C. (C) Ct values of the amplified samples imported onto the gene of interest (HSP) standard curve

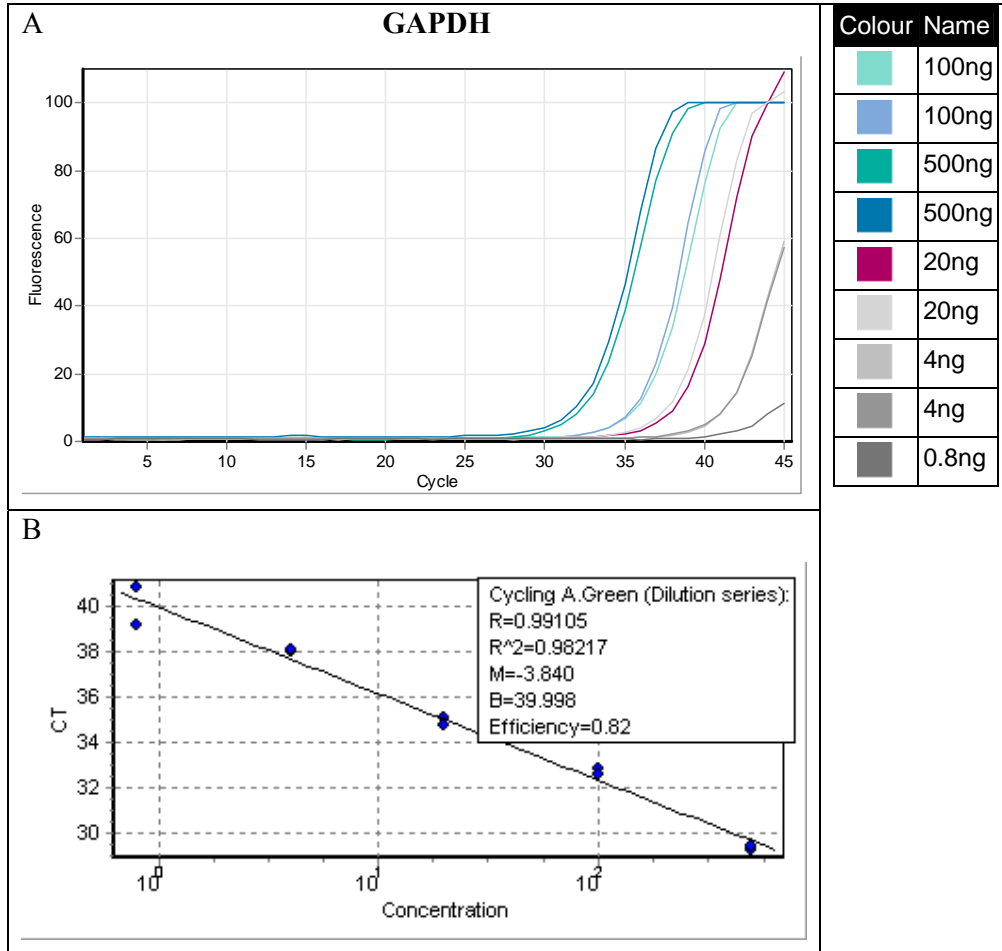


Figure 34: (A) Amplification curves of five fold RNA serial dilutions from sample 8 (from 500ng/reaction to 0.2ng/reaction as indicated in the legend) of a transgenic plant, amplified with GAPDH primers to produce (B) a standard curve (Ct vs log of concentration) for the gene of interest. R, R², M, B and efficiency values as indicated on the standard curve (as explained in Figure 23)

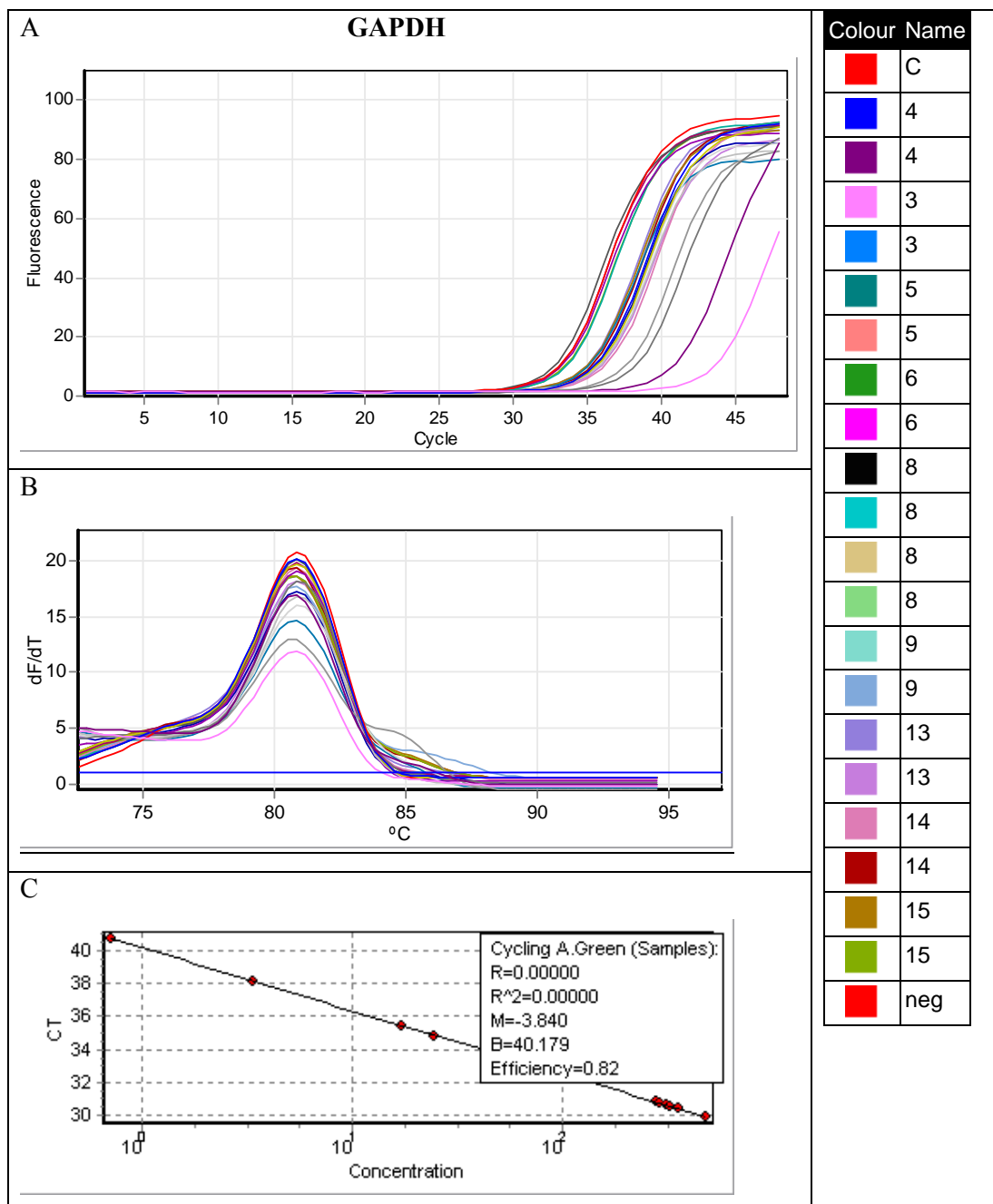


Figure 35: (A) Amplification curves for transgenic grapevine samples amplified via qRT-PCR with GAPDH primers for transgene expression level determination. (B) Melting curve analysis to verify amplification of correct amplicon, as shown in melting peaks between 80.7°C and 81.0°C. (C) Ct values of the amplified samples imported onto the reference gene (GAPDH) standard curve

The efficiency of the qRT-PCR amplification reaction with the reference gene primer (GAPDH) was relatively high with a value of 0.82 (Figure 34). The R^2 -value of the curve (0.98) was close to that of the ideal value of 0.99, indicating a good fit of the standards on the standard curve. The standards were thus accurately and efficiently amplified with the GAPDH reference gene primer pair. The Ct values of the

remainder of the samples were imported onto the reference gene standard curve (Figure 35 C).

The Δ HSP-Mut transgene expression levels were estimated relative to the GAPDH reference gene with the REST software and are shown in Table 5.

Table 5: Δ HSP-Mut copy numbers for the transgenic samples relatively quantified to each of the reference genes as well as determined by the Southern blot analysis. Δ HSP-Mut expression levels for the transgenic samples relatively quantified to GAPDH

Sample	Copy numbers				Expression levels
	B-tub	Cyclophilin	GAPDH	Southern	GAPDH
1	>4	>4	>4	>4	3
2	1	1	1	1	1
3	1	1	2	-	1
4	1	1	2	>4	7
5	1	1	1	-	4
6	0	0	0	0	0
7	0	0	0	0	0
8	4	4	4	2	1
9	2	2	2	2	>30
10	1	2	2	3	>30
11	>4	>4	>4	>4	>30
12	0	0	0	0	0
13	>4	>4	>4	>4	>30
14	1	1	1	1	>20
15	2	3	3	4	12
16	4	>4	2	3	0
17	0	0	0	0	0
18	2	2	2	2	>20
19	1	1	1	-	>50
20	2	2	2	2	1

3.4 Discussion

After initial PCR confirmation of transgene integration and evaluation of the primers, we proceeded to obtain more quantitative results for relative copy number and mRNA expression level estimation of the transgenic grapevine plant lines via SYBR Green qPCR and qRT-PCR. Most studies prefer to utilise TaqMan probes for quantification as these reactions require less optimisation since only specific products will be detected. However, numerous studies have demonstrated that, once thoroughly optimised, SYBR Green can effectively be used for accurate quantification of transgene copy numbers and expression levels.

Some of the amplification efficiencies obtained during this study were lower than ideally expected. Various factors can influence the efficiency of a PCR cycle, including the primer sets, starting material or contamination with salts, phenol, chloroform or ethanol (Ramakers et al. 2003). Nevertheless, as we didn't utilise a quantification technique that assumed 100% or equal efficiencies for the different genes, it was incorporated in the relative copy number estimation with REST.

REST estimated the copy number of each sample relatively to the reference gene and the calibrator sample. The REST results for copy number determination were compared to the results obtained by Southern blot (Figure 31 and Table 5). The results from qPCR and Southern blot revealed that most of the transformation events were successful and that the transgene was present at different levels in the different plant samples. Most of the plants had between one and four copies of the Δ HSP-Mut transgene inserted into their genome. The Southern blot and qPCR data correlated for most of the transgenic samples. However there were a few discrepancies. The Southern blot detected more than 4 Δ HSP-Mut copies in sample 4, whereas qPCR detected between 1 and 2 copies depending on the reference gene.

A possible explanation for the higher copy numbers detected by the Southern blot than the qPCR, is the DEAE sepharose clean-up. The cleanup was only performed on the samples used for the Southern blot due to the fact that it is a laborious technique and it was an essential step to obtain clear signal in the Southern blot. It could be that the DNA of this sample (sample 4) used for qPCR, contained contaminants (proteins or polyphenols) that inhibited the qPCR reaction and led to an underestimated copy

number result. The DEAE sepharose cleanup could have removed these contaminants, and explain why the Southern blot was able to detect more copies.

qPCR detected 4 transgene copies in sample 8, but the Southern blot indicated only 2. One explanation could be that the exposure time of the film to the membrane wasn't sufficient enough for all the bands in sample 8 to become visible. It is also possible that the transgene integrated into an area in the genome with a high mutation rate, which could have lead to rearrangements or alterations of the transgene. Mason et al. (2002) showed that rearrangement of transgenic DNA is not an exception, but happens more often than usually recognised. Such changes could still be detected by qPCR but would not always be detected by performing a single Southern blot analysis (Mason et al. 2002).

These results suggest that an accurate result is not guaranteed with either the qPCR or Southern blot techniques. What is important is that 76.5% of the samples' estimated copy numbers correlated between the two techniques. This validates the use of qPCR for copy number estimation. With such high correlation, the only determining factors for choosing a quantification technique are time, cost, and simplicity of the technique. Advantages of qPCR include time and cost effectiveness and a relatively simple technique. The technique is also statistically validated to support the data as samples are amplified in duplicate and REST performs 50 000 mathematical iterations to generate an estimated copy number value. The Southern blot analysis, on the other hand, is laborious and time consuming. Additionally, Southern blots are routinely only performed once or twice and repeats might even further complicate results.

The same procedure, as explained for copy number determination, was used to construct a standard curve with the RNA extracted from the transgenic plants. The dilution series however started with a higher RNA concentration (500ng/reaction – 0.8ng/reaction) than the DNA series. mRNA is present at variable levels and higher concentrations starting material were required to produce amplification curves within the cycle range where the samples would amplify. For the remainder of the samples, 100ng of RNA was used as for amplification with the HSP-70h and GAPDH primers. GAPDH was used as a reference gene for normalisation. The other reference genes, β -tubulin and cyclophilin, yielded poor amplification with the RNA and were not included in the relative expression determination. GAPDH has been shown to be a

reliable reference gene in other studies and was shown to be stably expressed in the leaves of grapevine (Ma et al. 2009).

The Ct and efficiency values were imported into REST for relative transgene mRNA expression level estimation. As qRT-PCR is routinely used for the determination of transgene expression level, no northern blot analysis was performed for validation of the technique. As indicated in Table 5, no expression of the transgene was detected in samples 6, 7, 12, 16 and 17. This correlates with the copy numbers estimated with qPCR that indicated that these samples didn't contain the transgene (except for sample 16). Relatively high expression levels of the transgene were detected in several of the transgenic samples (9, 10, 11, 13, 14, 18 and 19). These samples would be good candidates for further GLRaV-3 anti viral resistance studies.

Silencing effects regularly occur with the integration of multiple copies of transgenic DNA into the genome of another organism. A correlation could thus be made between low copy numbers and high expression levels of transgenic DNA. This was true for samples 9, 14, 18 and 19 (no Southern blot data, but qPCR indicated 1 transgene copy). However for the rest of the samples no such correlation could be made.

To conclude, the qPCR and Southern blot data correlated for most of the transgenic samples. qPCR together with REST thus provides a tool for accurate transgene copy number estimation. With the qRT-PCR relative mRNA expression level estimation, several samples were identified that had high expression levels of the transgene and that could be utilised in further studies to verify and further develop GLRaV-3 resistant grapevines. In conclusion, the results demonstrated the utility of qPCR and qRT-PCR for molecular characterisation of transgenic grapevine plants.

Chapter 4

4. Conclusion

GLRaV-3 and GVA are two of the most important viruses globally which pose a significant threat to the South African grapevine industry. Sensitive and accurate virus detection, in both grapevine rootstock and scion material, is of the utmost importance in order to prevent further spread. The aim of this study was to optimise a sensitive qRT-PCR detection system for GLRaV-3 and GVA in grapevine rootstock material; to determine optimum sampling time for sensitive and accurate detection of the viruses and to compare qRT-PCR and DAS-ELISA for GLRaV-3 detection in both a severely infected vineyard and propagation material from nurseries.

The protocol for GLRaV-3 was optimised for sensitive detection in grapevine rootstock material. After initial screening (September 2008) of the severely infected vineyard, fortnightly screenings were conducted (January 2009 – April 2009 and July 2009). Those results indicated an increased ability to detect GLRaV-3 as the season progressed towards winter. The best time for sensitive GLRaV-3 detection would be from the end of July to September as the highest number of GLRaV-3 infected samples were detected during these periods. The qRT-PCR also proved to be more sensitive than DAS-ELISA throughout the season up to the end of July. During July the DAS-ELISA detected several false positive samples. This presents a problem for accurate GLRaV-3 detection. qRT-PCR delivered reproducible results throughout the screening period. Exactly the same samples tested positive for two consecutive years which demonstrates the accuracy of the qRT-PCR technique. qRT-PCR thus proved to be the more accurate and sensitive detection system for GLRaV-3 in rootstock material for the screening of a severely infected vineyard.

qRT-PCR detection of GVA in the severely infected vineyard didn't show any specific correlation between the ability to detect GVA and the time of growth season. Variable percentages of GVA infected samples were detected throughout the season. GVA detection also lacked consistency as different samples were found to be infected at different screening periods. The published universal primer pair used for the GVA

detection in this study therefore needs to be questioned. Various factors could further contribute to the poor results for qRT-PCR GVA detection, including the heterogeneous nature of the GVA genome. Future studies could focus on improved strategies for more accurate and reproducible GVA detection with qRT-PCR. Recent findings suggest that certain variants of GVA are more prevalent in the Stellenbosch area than others. This information, together with any new findings on sequence variation, could aid in the design of more suitable diagnostic primers for detection of GVA via qRT-PCR in grapevine rootstocks.

Finally, during the nursery rootstock screenings, we concluded that none of the samples tested were infected with GLRaV-3. The qRT-PCR and DAS-ELISA results correlated for all the samples confirming that the samples we received were free of any GLRaV-3 infection. We can thus conclude that qRT-PCR is an effective system for accurate, sensitive and high throughput detection of GLRaV-3 in grapevine rootstock material.

Molecular characterisation of genetically transformed grapevine with resistance to GLRaV-3 was also performed in this study. In addition to detecting and identifying infected grapevine and the removal of these plants, plants can also be genetically engineered to provide resistance to pathogens as an additional strategy for eradicating disease. qPCR with REST analysis was used to estimate the transgene (Δ HSP-Mut) copy numbers relative to three reference genes (β -tubulin, cyclophilin and GAPDH). Southern blot analysis was also performed and the results of the two techniques were compared. The results for both techniques showed some discrepancies, nonetheless 76.5% of samples correlated for the copy number estimations by both techniques. This indicates that both techniques were able to produce accurate results; however techniques that are less time consuming and labour intensive are more suitable to high through-put analysis. qPCR is able to deliver results within one day, whereas a Southern blot requires several days without any apparent advantage in accuracy. Thus qPCR can effectively be utilized for copy number estimation in transformed plants. qRT-PCR has been utilized in various studies for the estimation of RNA expression levels in transformed plants. The transformed grapevines were subjected to qRT-PCR analysis to determine transgenic mRNA expression levels relative to the GAPDH reference gene. Hereby suitable candidates for further GLRaV-3 resistance studies were identified. Several plant lines showed high levels of Δ HSP-Mut

expression (9, 10, 11, 13 14 18 and 19) and would be utilized in further GLRaV-3 resistance trials. Future studies for this aspect of the project would entail exposing these transformed plants to insect vectors carrying GLRaV-3. The qRT-PCR detection system developed in this study can then be used to detect these low titres of GLRaV-3 and confirm resistance of the plant to the virus.

Real time PCR is highly sensitive, reproducible, reliable and is efficient over a large dynamic range, making it a powerful tool for the detection and quantification of nucleic acids. The system is easily implemented in the laboratory and enables a simple transfer of conventional PCR procedures to real time PCR thus eliminating additional training. This study illustrated the versatility of real time PCR for multiple applications in the vast research field of molecular biology.

References

- Alkowni R, Digiario M, Savino V. 1998. Viruses and virus diseases of grapevine in Palestine. EPPO Bulletin 28, 189-195.
- Altschul SF, Gish W, Miller W, Myers EW, Lipman DJ. 1990. Basic local alignment search tool. J. Mol. Biol 215, 403-410.
- Andersen CB, Holst-Jensen A, Berdal KG, Thorstensen T, Tengs T. 2006. Equal performance of TaqMan, MGB, molecular beacon, and SYBR green-based detection assays in detection and quantification of roundup ready soybean. Journal of Agricultural and Food Chemistry 54, 9658-9663.
- Assem SK, Hassan OS. 2008. Real Time quantitative PCR Analysis of Transgenic Maize Plants Produced by Agrobacterium-mediated Transformation and Particle Bombardment. Journal of Applied Sciences Research 4, 408-414.
- Basic Local Allignment search Tool (BLAST). Available at <http://ncbi.nlm.nih.gov/Blast.cgi>. (Accessed on 20 January)
- Beuve M, Semp'e L, Lemaire O. 2007. A sensitive one-step real-time RT-PCR method for detecting *Grapevine leafroll-associated virus 2* variants in grapevine. Journal of Virological Methods 141, 117-124.
- Borgo M, Angelini E. 2002. Influence of grapevine leafroll (GLRaV3) on Merlot cv. grape production. Bulletin OIV 75, 611-622.
- Bottalico G, Savino V, Campanale A. 2000. Improvements in grapevine sanitation protocols. Extended Abstracts, 13th Meeting of ICVG, Adelaide, Australia , 165-166.
- British Columbia, Ministry of Agriculture and lands. Pest management, Grape virus diseases website. Available at: <http://www.agf.gov.bc.ca/cropprot/grapeipm/virus.htm> (Accessed on 30 April 2009)

Brown T. 1999. Analysis of DNA Sequences by Blotting and hybridization. *Current Protocols in Molecular Biology*, 2.9.1-2.9.20 Supplement 68 Copyright © 2004 by John Wiley & Sons, Inc.

Bustin SA, Nolan T. 2004. Pitfalls of quantitative real-time reverse-transcription polymerase chain reaction. *Journal of Biomolecular Techniques* 15, 155-166.

Charles JG, Cohen D, Walker JTS, Forgie SA, Bell VA, Breen KC. 2006. A review of Grapevine Leafroll associated Virus type 3 (GLRaV-3) for the New Zealand wine industry. Hort Research Client Report 18447.

Chevalier S, Greif C, Clauzel JM, Walter B, Fritsch C. 1995. Use of an immunocapture-polymerase chain reaction procedure for the detection of grapevine virus A in Kober stem grooving-infected grapevines. *Journal of Phytopathology* 143, 369–373.

Czechowski T, Bari RP, Stitt M, Scheible WR, and Udvardi MK. 2004. Real-time RT-PCR profiling of over 1400 Arabidopsis transcription factors: unprecedented sensitivity reveals novel root- and shoot-specific genes. *The Plant Journal* 38, 366-379.

Dianese E, Ramalho ED, Cerqueira DM, Lopes DB, Fajardo TVM, Ferreira MASV, Martins CRF. 2005. Variability of the 3' Terminal of the Polymerase Gene of Grapevine leafroll-associated virus 3 Isolates from Vale do São Francisco, Brazil. *Fitopatologia Brasileira* 30, 173-176.

Dorak MT. 2006. Real-Time PCR (Advanced Methods Series). <http://www.dorak.info/genetics/realtime.html>.

Dovas CI, Katis NI. 2003. A spot multiplex nested RT-PCR for the simultaneous and generic detection of viruses involved in the aetiology of grapevine leafroll and rugose wood of grapevine. *Journal of Virological Methods* 109, 217-226.

Efron B, Tibshirani RJ. 1993. An Introduction to the Bootstrap. Chapman & Hall/CRC. Boca Raton, FL, USA.

Engel EA, Girardi C, Escobar PF, Arredondo V, Domínguez C, Pe´rez-Acle T , Valenzuela PDT. 2008. Genome analysis and detection of a Chilean isolate of Grapevine leafroll associated virus-3. *Virus Genes* DOI 10.1007/s11262-008-0241-1.

Espinoza C, Vega A, Medina C, Schlauch K, Cramer G, Arce-Johnson P. 2007. Gene expression associated with compatible viral diseases in grapevine cultivars. *Functional & Integrative Genomics* 7, 95–110.

Fajardo TVM, Eiras M, Scheiato PG, Nickil O, Kuhn GB. 2004. Evaluation of Grapevine leafroll-associated virus 1 and 3 variability by nucleotide sequence analysis and single-strand conformation polymorphism. *Fitopatologia Brasileira* 70, 177-182.

FAO Corporate Document Repository, Graft-transmissible diseases of grapevines Handbook for detection and diagnosis (Edited by GP Martelli). Available at: <http://www.fao.org/docrep/t0675e/T0675E09.htm> (Accessed on 29 September 2008).

Feng J, Zeng R, Chen J. 2008. Accurate and efficient data processing for quantitative real-time PCR using a tripartite plant virus as a model. *BioTechniques* 44, 901-912.

Fleige S, Walf V, Huch S, Prgomet C, Sehm J, Pfaffl MW. 2006. Comparison of relative mRNA quantification models and the impact of RNA integrity in quantitative real-time RT-PCR. *Biotechnology Letters* 28, 1601–1613.

Freeborough M-J. 2003. A pathogen-derived resistance strategy for the broad-spectrum control of Grapevine leafroll-associated virus infection. PhD thesis. Stellenbosch University.

Freeborough M-J, Burger JT. 2008. Leafroll: Economic implications. Wynboer.

Ginzinger DG. 2002. Gene quantification using real-time quantitative PCR: An emerging technology hits the mainstream. *Experimental Hematology* 30, 503–512.

Goszczynski DE, Kasdorf GGF, Pietersen G. 1996. Western blots reveal that grapevine virus A and grapevine virus B are serologically related. *Journal of Phytopathology* 144, 581- 583.

Goszczynski DE, Jooste AEC. 2003. Identification of grapevines infected with divergent variants of Grapevine virus A using variant-specific RT-PCR. *Journal of Virological Methods* 112, 157-164.

GENBANK database of the National Centre for Biotechnology Information. Available at: www.ncbi.nlm.nih.gov (Accessed on 20 January 2008).

Goszczynski DE. 2007. Single-strand conformation polymorphism (SSCP), cloning and sequencing reveal a close association between related molecular variants of Grapevine virus A (GVA) and Shiraz disease in South Africa. *Plant Pathology* 56, 755–762.

Goszczynski DE, Du Preez J, Burger JT. 2008. Molecular divergence of Grapevine virus A (GVA) variants associated with Shiraz disease in South Africa. *Virus Research* 138, 105–110.

Gugerli P, Gehrig W. 1980. Enzyme-linked immunosorbent assay (ELISA) for the detection of potato leafroll virus and potato virus Y in potato tubers after artificial break of dormancy. *Potato Research* 23, 353–359.

Herna'ndez M, Esteve T, Prat S, Pla M. 2004. Development of real-time PCR systems based on SYBR Green I, Amplifluore and TaqMan technologies for specific quantitative detection of the transgenic maize event GA21. *Journal of Cereal Science* 39, 99–107.

Integrated DNA Technologies (IDT) website. Available at: <http://www.idtdna.com/Home/Home.aspx> (Accessed on 19 January 2008).

Köhler G, Milstein C. 1975. Continuous cultures of fused cells secreting antibody of predetermined specificity. *Nature* 256, 495–497.

Ling K-S, Zhu H-Y, Petrovic N, Gonsalves D. 2001. Comparative effectiveness of ELISA and RT-PCR for detecting Grapevine Leafroll-Associated Closterovirus-3 in field Samples. *American Journal of Enology and Viticulture* 52, 21-27.

Ling K, Zhu H, Gonsalves D. 2004. Complete nucleotide sequence and genome organization of Grapevine leafroll-associated virus 3, type member of the genus *Ampelovirus*. *Journal of General Virology* 85, 2099–2102.

Livak KJ, Schmittgen TD. 2001. Analysis of relative gene expression data using Real-Time Quantitative PCR and the 2^{-ΔΔCT} method. *Methods* 25, 402–408.

Ma Y, Slewinski TL, Baker RF, Braun DM. 2009. Tie-dyed1 encodes a novel, phloem-expressed transmembrane protein that functions in carbohydrate partitioning. *Plant Physiology* 149, 181–194.

MacKenzie, DJ. 1997. A standard protocol for the detection of viruses and viroids using a reverse transcription-polymerase chain reaction technique. The Canadian Food Inspection Agency Document CPHBT-RT-PCR1.00.

Map Viewer, NCBI.

http://www.ncbi.nlm.nih.gov/projects/mapview/map_search.cgi?taxid=29760&query=beta-tubulin&qchr=

http://www.ncbi.nlm.nih.gov/projects/mapview/map_search.cgi?taxid=29760&query=cyclophilin&qchr=

http://www.ncbi.nlm.nih.gov/projects/mapview/map_search.cgi?taxid=29760&query=GAPDH&qchr=

Maree HJ, Freeborough MJ, Burger JT. 2008. Complete nucleotide sequence of a South African isolate of grapevine leafroll-associated virus 3 reveals a 5'UTR of 737 nucleotides. *Archives of Virology*, 153(4): 755-757.

Martelli GP (1993) Rugose wood complex. In: Martelli GP (ed) Graft-transmissible disease of grapevines, handbook for detection and diagnosis. FAO, Rome, pp 45–53.

Martelli GP, Agranovsky AA, Bar-Joseph M, Boscia D, Candresse T, Coutts RHA, Dolja VV, Falk BW, Gonsalves D, Jelkmann W, Karasev AV, Minafra A, Namba S, Vetten HJ, Wisler GC, Yoshikawa N. 2002. The family Closteroviridae revised. *Archives of Virology* 147, 2039-2044.

Martelli GP, Boudon-Padieu E. 2006. Directory of infectious diseases of grapevines and viroses and virus-like diseases of grapevine: Bibliographic report 1998-2004. ISSN: 1016-1228, 279.

Mason G, Provero P, Vaira AM, Accotto GP. 2002. Estimating the number of integrations in transformed plants by quantitative real-time PCR. *BioMed Central Biotechnology*, doi: 10.1186/1472-6750-2-20.

Minafra A, Saldarelli P, Martelli GP. 1997. Grapevine virus A: nucleotide sequence, genome organization, and relationship in the Trichovirus genus. *Archives of Virology* 142, 417–423.

Murolo S, Romanazzi G, Rowhani A, Minafra A, La Notte P, Branzanti MB, Savino V. 2008. Genetic variability and population structure of Grapevine virus A coat protein gene from naturally infected Italian vines. *European Journal of Plant Pathology* 120, 137–145.

Nakaune R, Toda S, Mochizuki M, Nakano M. 2008. Identification and characterization of a new vitivirus from grapevine. *Archives of Virology* 153, 1827–1832.

Nel AC, Engelbrecht DJ. 1972. Grapevine virus diseases in South Africa and the influence of latent viruses in the nursery. *Annual Phytopathology n' horsésrie* , 67-74.

Nicholas P. 2006. Selection of Clones for the Australian National Nuclear Grapevine Collection. *The Australian & New Zealand Grapegrower & Winemaker*, 31-33.

O'Donnell KJ. 1999. Plant pathogen diagnostics: present status and future developments. *Potato Research* 42, 437-447.

Osman F, Rowhani A. 2006. Application of a spotting sample preparation technique for the detection of pathogens in woody plants by RT-PCR and real-time PCR (TaqMan). *Journal of Virological Methods* 133, 130–136

Osman F, Leutenegger C, Golino D, Rowhani A. 2007. Real-time RT-PCR (TaqMan®) assays for the detection of Grapevine Leafroll associated viruses 1–5 and 9. *Journal of Virological Methods* 141, 22–29.

Osman F, Leutenegger C, Golino D, Rowhani A. 2008. Comparison of low-density arrays, RT-PCR and real-time TaqMan® RT-PCR in detection of grapevine viruses. *Journal of Virological Methods* 149, 292–299.

Osman F, Rowhani A. 2008. Real-time RT-PCR (TaqMan®) assays for the detection of viruses associated with Rugose wood complex of grapevine. *Journal of Virological Methods* 154, 69–75.

Papin JF, Vahrson W, Dittmer DP. 2004. SYBR Green-based Real-Time Quantitative PCR assay for detection of West Nile virus circumvents false-negative results due to strain variability. *Journal of Clinical Microbiology* 42, 1511–1518.

Pfaffl MW. 2001. A new mathematical model for relative quantification in real-time RT-PCR. *Nucleic Acids Research* 29, 2001-2007.

Pietersen G. 2002. Analysis of spatial distribution patterns indicative of spread of grapevine leafroll disease. Annual Winetech Report.

Pietersen G. 2004. Spread of Grapevine Leafroll Disease in South Africa - a difficult, but not insurmountable problem. Wynboer.

Ramakers C, Ruijter JM, Lekanne Depreza RH, Moorman AFM. 2003. Assumption-free analysis of quantitative real-time polymerase chain reaction (PCR) data. *Neuroscience Letters* 339, 62–66.

Reid KE, Olsson N, Schlosser J, Peng F, Lund ST. 2006. An optimized grapevine RNA isolation procedure and statistical determination of reference genes for real-time RT-PCR during berry development. *BMC Plant Biology*, doi:10.1186/1471-2229-6-27 .

Richards GP, Watson MA, Kingsley DH. 2004. A SYBR green, real-time RT-PCR method to detect and quantitate Norwalk virus in stools. *Journal of Virological Methods* 116, 63–70.

Saldarelli P, Minafra A, Martelli GP. 1996. The nucleotide sequence and genomic organization of Grapevine virus B. *Journal of General Virology* 77, 2645–2652.

Sambrook J, Fritsch EF, Maniatis T. 1989. *Molecular cloning: a laboratory manual*, 2nd edition. Cold Spring Harbour Laboratory Press, New York.

Sanford JC, Johnston SA. 1985. The concept of parasite-derived resistance – deriving resistance genes from the parasite's own genome. *Journal of Theoretical Biology* 115, 395-405.

Savazzini F, Dalla Costa L, Martinelli L. 2005. Evaluation of Exogenous DNA by Quantitative Real-time PCR in Transgenic Grape. Proc. VIIth IS on Grapevine. *Acta Hort.* 689 ISHS, 499-504.

Schena L, Nigro F, Ippolito A, Gallitelli D. 2004. Real-time quantitative PCR: a new technology to detect and study phytopathogenic and antagonistic fungi. *European Journal of Plant Pathology* 110, 893–908.

Sforza R, Boudon-Padiou E, Greif C. 2003. New mealybug species vectoring Grapevine leafroll-associated viruses-1 and -3 (GLRaV-1 and -3). *European Journal of Plant Pathology* 109, 975–981.

Sharma KK, Lavanya M, Anjaiah V. 2000. A method for isolation and purification of peanut genomic DNA suitable for analytical applications. *Plant Molecular Biology Reporter* 18, 393a–393h.

Škulj M, Okršlar V, Jalen Š, Jevševar S, Petra Slanc, Štrukelj B, Menart V. 2008. Improved determination of plasmid copy number using quantitative real-time PCR for monitoring fermentation processes. *Microbial Cell Factories* 7, 1475-2859.

Song P, Cai CQ, Skokut M, Kosegi BD, Petolino JF. 2002. Quantitative real-time PCR as a screening tool for estimating transgene copy number in WHISKERS™-derived transgenic maize. *Plant Cell Reports* 20, 948–954.

South African Wine, SA Wine Industry Information & Systems. Available at: (http://www.wine.co.za/Misc/Page_Detail.aspx?PAGEID=304) (Accessed on 12 May 2009).

The DIG Systems User's Guide for filter hybridization. 1995. Roche Molecular Biochemicals. Boehringer Mannheim GmbH, Biochemica.

Toplak N, Okršlar V, Stanic-Racman D, Gruden K, Zel J. 2004. A high-throughput method for quantifying transgene expression in transformed plants with Real-Time PCR Analysis. *Plant Molecular Biology Reporter* 22, 237-250.

Tsai CW, Chau J, Fernandez L, Bosco D, Daane KM, Almeida RPP. 2008. Transmission of Grapevine leafroll-associated virus 3 by the Vine Mealybug

(*Planococcus ficus*). *Phytopathology* 98, 1093-1098.

Turturo C, Saldarelli P, Yafeng D, Digiario M, Minafra A, Savino V, Martelli GP. 2005. Genetic variability and population structure of Grapevine leafroll-associated virus 3 isolates. *Journal of General Virology* 86, 217–224.

Tzanetakakis IE, Postman JD, Martin RR. 2005. Mint virus X: a novel potexvirus associated with symptoms in ‘Variegata’ mint. *Archives of Virology* 151, 143–153.

Varga A, James D. 2006. Real-time RT-PCR and SYBR Green I melting curve analysis for the identification of Plum pox virus strains C, E, A, and W: Effect of amplicon size, melt rate, and dye translocation. *Journal of Virological Methods* 132, 146–153.

Viviers MA, Pretorius IS. 2000. Genetic improvement of grapevine: tailoring grape varieties for the third millennium. *South African Journal of Enology and viticulture*, 5–26.

Waite diagnostics, University of Adelaide, Australia. Available at: <http://www.agwine.adelaide.edu.au/facilities/wdiag.html> (Accessed on 9 February 2009).

Wang T, Brown MJ. 1999. mRNA quantification by real time TaqMan polymerase chain reaction: validation and comparison with RNase protection. *Analytical Biochemistry* 269, 198–201.

Ward E, Foster SJ, Fraaje BA, McCartney HA. 2004. Plant pathogen diagnostics: immunological and nucleic acid-based approaches. *Annals of Applied Biology* 145, 1-16.

Weng H, Pan A, Yang L, Zhang C, Liu Z, Zhang D. 2004. Estimating Number of Transgene Copies in Transgenic Rapeseed by Real-Time PCR Assay With HMG I/Y as an Endogenous Reference Gene. *Plant Molecular Biology Reporter* 22, 289–300.

White EJ, Venter M, Hiten NF, Burger JT. 2008. Modified Cetyltrimethylammonium bromide method improves robustness and versatility: The benchmark for plant RNA extraction. *Biotechnology Journal* 3, 1424-1428.

Wynboer website, Recent articles, Characterisation of grapevines visually infected with Shiraz disease associated viruses. Available at:
(<http://www.wynboer.co.za/recentarticles/200612shiraz.php3>) (Accessed on 4 March 2008).

Yun JJ, Heisler LE, Hwang IIL, Wilkins O, Lau SK, Hycza M, Jayabalasingham B, Jin J, McLaurin J, Tsao M-S, Der SD. 2006. Genomic DNA functions as a universal external standard in quantitative real-time PCR. *Nucleic Acids Research* 34, doi:10.1093/nar/gkl400.

Appendix A

PCR and real time PCR constituents and cycles

Standard 25µl PCR reaction mix

1 x KapaTaq buffer A (1.5mM Mg) (Kapa Biosystems), 1 x cresol, 0.4µM forward and reverse primers, 0.2mM dNTPs and 1U of KapaTaq (Kapa Biosystems)

Standard 25µl RT-PCR reaction mix

1 x KapaTaq buffer A (1.5mM Mg) (Kapa Biosystems), 1 x cresol, 5mM dithiothreitol (DTT), 0.4µM forward and reverse primers, 0.2mM dNTPs, 1U AMV reverse transcriptase (Fermentas) and 1U of KapaTaq (Kapa Biosystems)

Standard 25µl qPCR reaction mix

1 x SensiMix, 0.2 x SYBR® Green I solution and 0.2µM forward and reverse primers

Standard 25µl qRT-PCR reaction mix

1 x One step SensiMix One-Step, 0.2 x SYBR® Green I solution, 5U RNase Inhibitor and 0.2µM forward and reverse primers

Standard PCR amplification cycle

1 cycle of 5 min at 94°C, 30 cycles of 30 sec at 94°C, 30 sec at specific annealing temperature and 30 sec at 72°C respectively, 1 cycle of 7 min at 72°C

Standard RT-PCR amplification cycle

1 cycle of 45 min at 45°C, 1 cycle of 5 min at 94°C, 30 cycles of 30 sec at 94°C, 30 sec at specific annealing temperature and 30 sec at 72°C respectively, 1 cycle of 7 min at 72°C

Standard qPCR amplification cycle

1 cycle of 10 min at 95°C, 45 cycles of 20 sec at 95°C, 20 sec at specific annealing temperature and 30 sec at 72°C respectively, followed by a melting cycle from 72°C - 95°C (5 sec per step)

Standard qRT-PCR amplification cycle

1 cycle of 45 min at 42°C, 1 cycle of 10 min at 95°C, 45 cycles of 20 sec at 95°C, 20 sec at specific annealing temperature and 30 sec at 72°C respectively, followed by a melting cycle from 72°C - 95°C (5 sec per step)

Appendix B

Protocols

Chemically competent cells

A single *E. coli* DH5 α colony was inoculated into 5ml of Luria Bertani (LB) broth and incubated overnight at 37°C shaking at 225rpm. The overnight culture was used to inoculate 500ml LB broth (1:100 dilution) and was incubated at 37°C and 225rpm shaking until the optical density was between 0.5 - 0.6 at an absorption value of 600 (OD₆₀₀). The culture was centrifuged (5 000 xg, 10 min, 4°C) and the pelleted cells were resuspended in 100ml ice cold 100mM MgCl₂ and incubated on ice for 30min. The cells were pelleted by centrifugation (4 000g, 10min, 4°C) and resuspended in 10ml filter sterilised (0.2 μ m) CaCl₂ (100mM, with 15% glycerol). One hundred microlitres of the cells were aliquoted into 1.5ml prechilled tubes, flash frozen in ice-cold 96% (v/v) ethanol and stored at -80°C for later use.

Transformation with the pDrive cloning vector

Transformation procedures were performed according to the protocol of Sambrook et al. (1989). One hundred microlitres of the chemically competent *E. coli* DH5 α cells were added to the ligation reaction, gently mixed and incubated for 10min on ice. The cells were heat shocked (45sec, 42°C) and incubated on ice for 5min. Nine hundred microlitres of LB broth (Merck) was added to the transformation reaction and incubated for an hour shaking at 155rpm at 37°C. One hundred microlitres was plated out onto LB bacteriological agar (Merck) plates containing 100 μ g/ml Ampicillin (Amp), for pDrive selection and 40 μ g/ml 5-bromo-4-chloro-3-indolyl- β -D-galactoside (X-Gal, Fermentas) and 0.2mM Isopropyl- β -D-thiogalactoside (IPTG, Fermentas), for blue-white colony selection. The remaining 900 μ l of the transformation reaction was centrifuged (2 000 xg, 60sec), the cells resuspended in 100 μ l of LB broth and plated out (in case low transformation efficiencies were expected). The plates were incubated overnight at 37°C.

White colonies were selected and screened via colony PCR with insert specific primers (GLRaV-3 CP forward and reverse primers as in Table 1). The standard PCR

mix was prepared (Appendix A) with GLRaV-3 coat protein forward and reverse primers. The standard PCR amplification cycle conditions were used (Appendix A) with the specific annealing temperature as indicated in Table 1. The confirmed positive white colonies were inoculated in 5ml LB broth containing 100µg/ml Amp and incubated (225rpm, overnight, 37°C).

Virus detection via DAS-ELISA

The crude virus extracts of the plant samples were clarified by low speed centrifugation and added to the microtitre plate pre-coated with polyclonal antiserum. The plate was incubated overnight at 4°C. The plate was washed five times for 3min each with TBS-T to remove unbound antibodies. GLRaV-3 specific antisera was prepared (1:10 000) and 100µl was added to each well and the plate was incubated at 37°C for 2h. The previous washing step was repeated. One hundred microlitres of goat anti-rabbit immunoglobulins conjugated to alkaline phosphatase (GAR-AP) (1:30 000) was added to each well and the plate was incubated at 37°C for 2h. The wash step was repeated and 100µl of substrate buffer with 0.01g/ml p-nitrophenyl phosphate was added to the wells and the plate incubated at room temperature until colour developed. The enzymatic reaction was stopped by adding 3M NaOH and the absorbance values were measured at 405nm.

Appendix C

Sequence Alignments

GLRaV-3 variants for CP primer design

```
gi|53987039      TCTTTACATCGTCTTCGACGGAGTTCAAAGAGTTCGACTACATAGAAACG 50
gi|115203853    .....T.....C 50
gi|110564204    .....T.....C 50
gi|110564202    .....T.....C 50
gi|71564275     .....T.....T 50
gi|67005448     .....T.....C 50
gi|29366687:NY-1 .....T.....C 50
GP18            ..... 50
623 CP         ..... 50
621 CP         .TC..TACATCGTC.TCGAC.GAG.TC..AGAG.TTGACTACATAG..AC 50
EU344893.1     .....T.....C 50
EU344895.1     .....T.....C 50
EU344894.1     .....T.....T.....C 50
EF445655.1     .....G.....G..AG.T.....T.....A.....T..TG.G.....C 50
EU259806.1     .TC..TACATCGTC.TCGAC.GAG.TC..AGAG.TCGACTACATAG..AC 50
Consensus      .TC..TACRTCGTCKTCRRCKGAG.TY..AGAR.TYGAYTAYRTRG..AC 50
CP F primer    ~~~~~ACATCGTC.TCGAC.GAG.T~~~~~ 20
CP Primer     ~~~~~ 1

gi|53987039      GACGATGGAAGAAGATATATGCGGTGTGGATATACGATTGCATTAAACA 100
gi|115203853    ..T.....G.....T..... 100
gi|110564204    ..T.....G.....T..... 100
gi|110564202    ..T.....G.....T..... 100
gi|71564275     ..T.....G.....T..... 100
gi|67005448     ..T.....G.....T..... 100
gi|29366687:NY-1 ..T.....G.....T..... 100
GP18            .....G..... 100
623 CP         .....G..... 100
621 CP         CGATGAT.G..AG.AGATATATGC.GTGT.GGTATATGA.TGCA.T..AC 100
EU344893.1     ..T.....G.....T..... 100
EU344895.1     ..T.....G.....T..... 100
EU344894.1     ..T.....G.....T..C.....C..... 100
EF445655.1     .....A.....TC.....G.G.....C..T.....G.. 100
EU259806.1     .GACGAT.G..AG.AGATATATGC.GTGT.GGTATACGA.TGCA.T..AC 100
Consensus      BGAYGAT.G..AG.ARATATWYGC.GTGT.GRTRTAYGAYTYA.Y..RC 100
CP F primer    ~~~~~ 20
CP Primer     ~~~~~ 1

gi|53987039      AGCTGCCGCTTCAACGGGTTACGAAACCCGGTAAGGCAGTATCTAGCAT 150
gi|115203853    .....T.....G.....T.....G..... 150
gi|110564204    .....T.....G.....T.....G..... 150
gi|110564202    .....T.....G.....T.....G..... 150
gi|71564275     .....T.....G.....T.....G..... 150
gi|67005448     .....T.....G.....T.....G..... 150
gi|29366687:NY-1 .....T.....G.....T.....G..... 150
GP18            ..... 150
623 CP         ..... 150
621 CP         .AGCTG.TGC.TCGAC..G.TATG...A..C.GT.A.GCAGTATCTAGCG 150
EU344893.1     .....T.....G.....T.....G..... 150
EU344895.1     .....T.....G.....T.....G..... 150
EU344894.1     ...C..T.....G.....T..... 150
EF445655.1     .....G..G..T.....G.....A.....A..A..CT...T... 150
EU259806.1     .AGCTG.CGC.TC.AC..G.TACG...A..C.GT.A.GCAGTATCTAGCA 150
Consensus      .AGCYG.BGCKTCDAC..G.TAYG.R.A..CRGT.A.RCARTAYYTAGCD 150
CP F primer    ~~~~~ 20
CP Primer     ~~~~~ 1

gi|53987039      ACTTCACGCCAACCTTGATCAGGCGACCCCTGAATGGTAAACTGGTGATG 200
gi|115203853    .....A.....C.....A.C..... 200
gi|110564204    .....A.....C.....A..... 200
gi|110564202    .....A.....C.....A..... 200
gi|71564275     .....A.....C.....A..... 200
```

```

gi|67005448          .....A.....C..T.....A..... 200
gi|29366687:NY-1    .....A.....C.....A..... 200
GP18                 .....A..... 200
623 CP               ..... 200
621 CP               TAC.TCACAC.C.A.C.TCATCAC.GCGA..CTG.AT.GT..ACTAGTGAT 200
EU344893.1          .....A.....C.....A..... 200
EU344895.1          .....A.....C.....A..... 200
EU344894.1          .....T..A.....C.....T.....A..... 200
EF445655.1          .....A..G..G..T..A.....T..GT.....A..C... 200
EU259806.1          TAC.TCACG.C.A.A.TGATCAC.GCGA..CTG.AT.GT..ACT.GTGAT 200
Consensus           TAC.TYACR.CRA.V.TBATHAC.GCKA.SYTG.AT.GT..ACTRGYSAT 200
CP F primer         20
CP Primer           ~~~~~ 1

gi|53987039          AATGAAAAGGTCATGGCACAGCATGGAGTACCACCGAAATTCCTTCCGTA 250
gi|115203853        ..C..G.....T..... 250
gi|110564204        ..C..G.....T..... 250
gi|110564202        ..C..G.....T..... 250
gi|71564275         ..C..G.....T.....G..... 250
gi|67005448         ..C..G.....T..... 250
gi|29366687:NY-1    ..C..G.....T..... 250
GP18                 .....A..... 250
623 CP               ..... 250
621 CP               G.ACG.G.A.GTTAT.GCACAGCAT.GAGTA.CA.CG..A.TC..T.CGT 250
EU344893.1          ..C..G.....T..... 250
EU344895.1          ..C..G.....T..... 250
EU344894.1          .....G.....T.....T..... 250
EF445655.1          ..C..G..A..T.....C..A..C..C..T..G.....G..T..C..A.. 250
EU259806.1          G.ATG...AAGTCAT.GCACAGCAT.GAGTA.CA.CG..A.TC..T.CGT 250
Consensus           G..AYG..R..ARGTYAT.GCHCARCAY.GMGTW.CR.CG..R.TY...Y.CRT 250
CP F primer         20
CP Primer           ~~~~~ 1

gi|53987039          CGCGATTGACTGCGTTCGTCGACGTACGATCTGTTCAATAACGACGCAA 300
gi|115203853        .....A.....C..... 300
gi|110564204        .A...A.....C..... 300
gi|110564202        .A...A.....C..... 300
gi|71564275         .A...A.....C..... 300
gi|67005448         .A...A.....C..... 300
gi|29366687:NY-1    .A...A.....C..... 300
GP18                 ..... 300
623 CP               ..... 300
621 CP               ACACGA.AGACTGCG.TCGT.CGACGTACGATCTG.TC.AC.ACGACGC. 300
EU344893.1          .A...A.....C..... 300
EU344895.1          .A...A.....C..... 300
EU344894.1          .A...A.....T..... 300
EF445655.1          .A...C..T..T..A.....TT.....T.A..T..... 291
EU259806.1          ACGCGA.TGACTGCG.TCGT.CGACGTACGATCTG.TC.AT.ACGACGC. 300
Consensus           ACRCGA.HGAYTGYG.WCGT.CKWCGTAYGATYTR.TY.AY.ACGACGC. 300
CP F primer         20
CP Primer           ~~~~~ 1

gi|53987039          TACTAGCATGGAATTTAGCTAGACAGCAGGCGTTTAGAAATAA 343
gi|115203853        .....G.....C... 343
gi|110564204        .....C... 343
gi|110564202        .....C... 343
gi|71564275         .....C... 343
gi|67005448         .....C... 343
gi|29366687:NY-1    ..T.....C... 343
GP18                 ..... 343
623 CP               ..... 343
621 CP               ATACTAGCAT.G.A..TAGCTAGACAGCA.GCG..TAG..AC. 343
EU344893.1          .....C... 343
EU344895.1          .....C... 343
EU344894.1          .....G.....CG. 343
EF445655.1          ----- 291
EU259806.1          ATACTAGCAT.G.A..TAGCTAGACAGCA.GCG..TAG..AT. 343
Consensus           ATAYTAGCRT.G.A..TAGCTAGACAGCA.GCG..TAG..AYR 343
CP F primer         20
CP Primer           ~~~~~GCTAGACAGCA.GCG..TAG 20

```

GVA variants and published universal primers

```

          10      20      30      40      50
DQ787959.1  ....|....|....|....|....|....|....|....|....|....|
DQ855088.1  TCACGGGTAGGTCTACTTATGCTAAACGTAGGAGGGCCAGGCGTATGAAT
DQ855087.2  ..G.....C..G.....G.....C..C..T.....C.....
GVA F       ~~~~~~.C..G.....G
GVA R       ~~~~~~

          60      70      80      90      100
DQ787959.1  ....|....|....|....|....|....|....|....|....|....|
DQ855088.1  GTGTGTAAGTGTGGTGCATATTTGCACAATAATAAGATTGTAGGTCTAG
DQ855087.2  .....A.....G.....C..AA..C..
GVA F       ~~~~~~
GVA R       ~~~~~~

          110     120     130     140     150
DQ787959.1  ....|....|....|....|....|....|....|....|....|....|
DQ855088.1  TACAATCTCGGGTCATAAACCTTGATCGACTCCGGTTCGTAAAAGAGGGAA
DQ855087.2  ..GT.....A.....C.....C..CA..T..GA.....G.....
GVA F       ~~~~~~
GVA R       ~~~~~~

          160     170     180     190     200
DQ787959.1  ....|....|....|....|....|....|....|....|....|....|
DQ855088.1  GAGTAGCCCTAGAGGGCGAGACTCCTGTTTATCGAACTTGGGTCAAGTGG
DQ855087.2  .....T..ACA.....C.....A...
GVA F       ~~~~~~
GVA R       ~~~~~~

          210     220     230     240
DQ787959.1  ..G.....
DQ855088.1  GTAGAGACCGAGTATCATATAAATATATTAGAACTCAGATGATGAGG
DQ855087.2  ..G.....T.....C.....C.....
GVA F       ~~~~~~
GVA R       ~~~~~~.C.....C.....

```

Appendix D

Amplification curves for all 34 Nietvoorbij samples

GLRaV-3 screening in January 2009

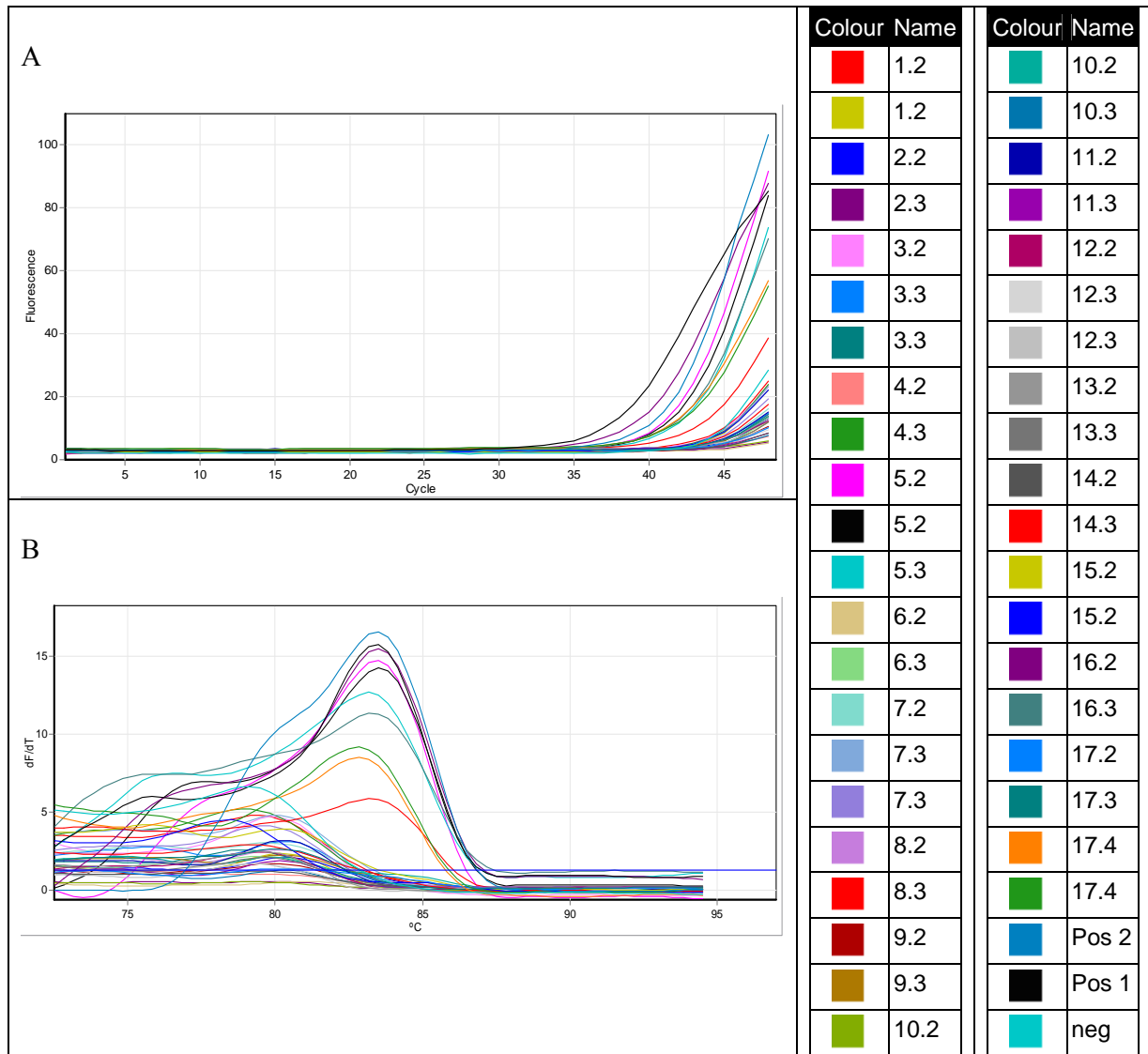


Figure 36: (A) Amplification curves for all 34 Nietvoorbij rootstock samples tested via qRT-PCR for GLRaV-3 infection during January 2009. (B) Melting curves for the amplified samples to identify samples infected with GLRaV-3.

GLRaV-3 screening in July 2009

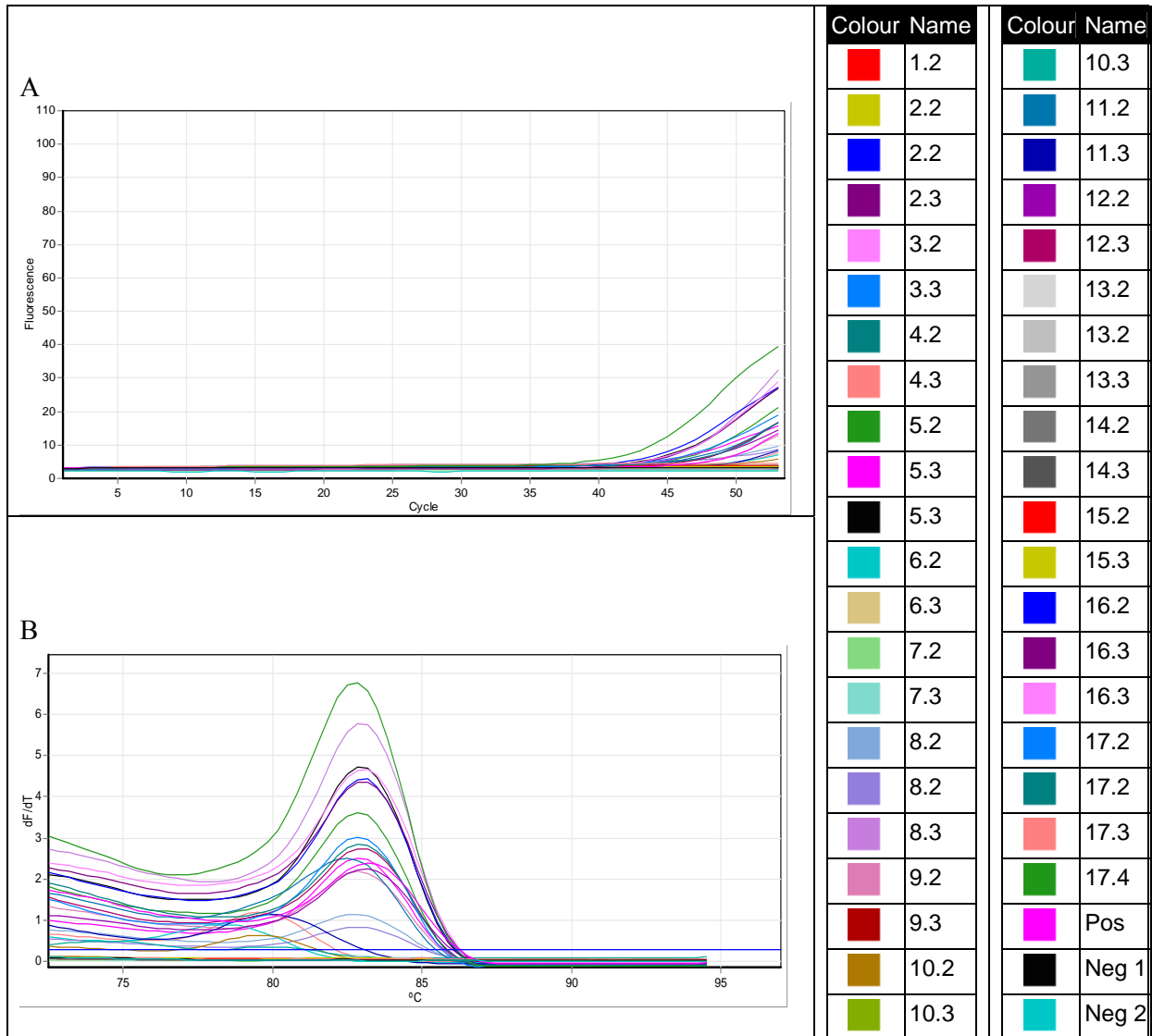


Figure 37: (A) Amplification curves for all 34 Nietvoorbij rootstock samples tested via qRT-PCR for GLRaV-3 infection during July 2009. (B) Melting curves for the amplified samples to identify samples infected with GLRaV-3.

GVA screening in July 2009

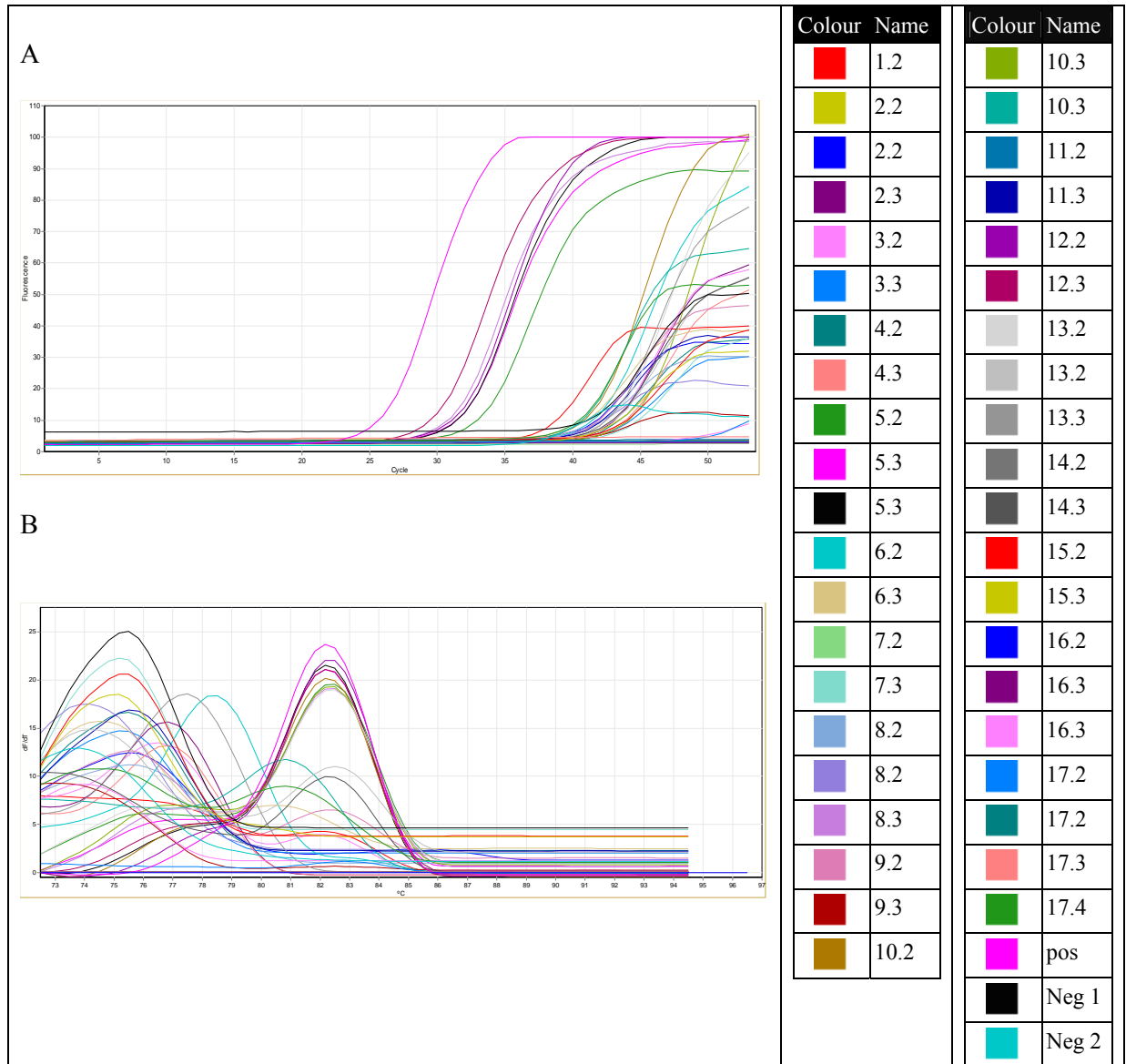


Figure 38: (A) Amplification curves for all 34 Nietvoorbij rootstock samples tested via qRT-PCR for GVA infection during July 2009. (B) Melting curves for the amplified samples to identify samples infected with GLRaV-3.